Moistening processes before the convective initiation of Madden-Julian Oscillation events during the CINDY2011/DYNAMO period

Tomoe Nasuno [1], Tim Li [2], Kazuyoshi Kikuchi [2], Hiroaki Miura [1,3], Tomoki Miyakawa [1], and Masaki Satoh [1,4]

1.RIGC, Japan Agency for Marine-Earth Science and Technology

2.International Pacific Research Center, University of Hawaii

3.Department of Earth and Planetary Physics, the University of Tokyo

4.AORI, the University of Tokyo

Workshop on Tropical Dynamics and the MJO

January 14-16, 2014

East-West Center, University of Hawaii, Honolulu Hawaii

Backgrounds

- **Convection initiation** of MJO over the western **Indian Ocean (IO)** is one of most difficult tasks in understanding and prediction of MJO. Major target of **CINDY2011/DYNAMO** field program [October 2011-March 2012 (Yoneyama et al. 2013)].
- **moist static energy (MSE)/moisture** is a key variable that controls the MJO initiation, development, eastward propagation [e.g., Blade and Hartmann 1993; Kemball-Cook and Weare 2001; Maloney 2009] . Observational studies evidenced the **buildup of moisture** associated with MJO (Kikuchi and Takayabu 2004; Kiladis et al. 2005; Yoneyama et al. 2008, 2013; Johnson and Ciesielski 2013)
- Triggering of MJO convection initiation vary with cases

Circumnavigation (tropical dynamics)

Knutson and Weickmann 1987; Wang and Li 2004; Matthews 2008; Straub 2013

Extratropical forcing (e.g., Rossby wave activity in the upper troposphere, cold surge event) Lau and Peng 1987; Hsu et al. 1990; Ray et al.2009; Ray and Li 2013; Zhao et al. 2013; Wang et al. 2012)

Moistening??

Goal:

- Gain insight into MJO convection initiation processes over the IO by case studies; MJO events during the CINDY2011/DYNAMO period
- A case study has an advantage in examining the roles of transient/local scale processes which tend to be smoothed out in statistical analysis of a large number of samples.
- Similarities and differences in the two MJO events (MJO-1 and MJO-2) will help understand the key processes.

Precursor signals prior to MJO initiation

Zhao et al. 2013

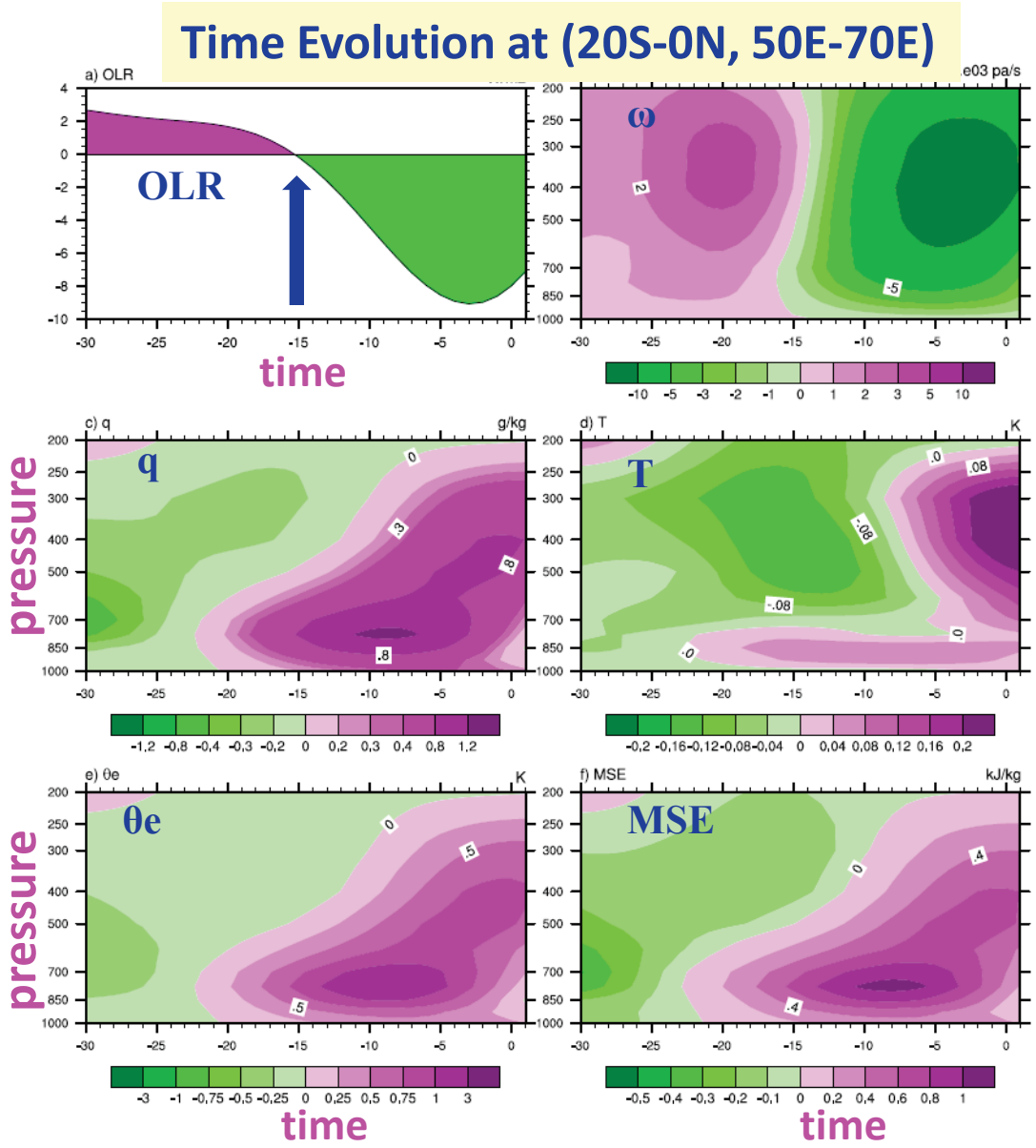

ERA-40, NOAA OLR (2.5deg)

Boreal winter **1982-2001**

MJO Initiation Region

(20ºS – 0N , 50ºE - 70ºE)

day -15 is regarded as the initiation date

Major precursor features:

Positive specific humidity & temperature anomalies in lower troposphere prior to the MJO initiation

↓

Increase of equivalent potential temperature θe & moist static energy MSE

↓

Atmosphere becomes convectively more unstable

Data and methods

- **ERA-Interim** (1.0 x 1.0) and NOAA daily interpolated Outgoing Long-wave Radiation (OLR) (2.5 x 2.5) for the period of August 2011–January 2012 were used.
- Daily-mean variables were separated into low-frequency basic state (>80 day), intraseasonal (20–80 day), and high-frequency (<20 day) components by Lanczos filtering.
- **<u>Moisture and temperature budgets</u>** for the intraseaonal tendencies were diagnosed following Zhao et al. (2013).

$$\left(\frac{\partial q}{\partial t}\right)' = -(V\nabla q)' + -\omega\frac{\partial q}{\partial p}' + -\frac{Q_2}{L}'$$

prime: 20-80 day (ISO)

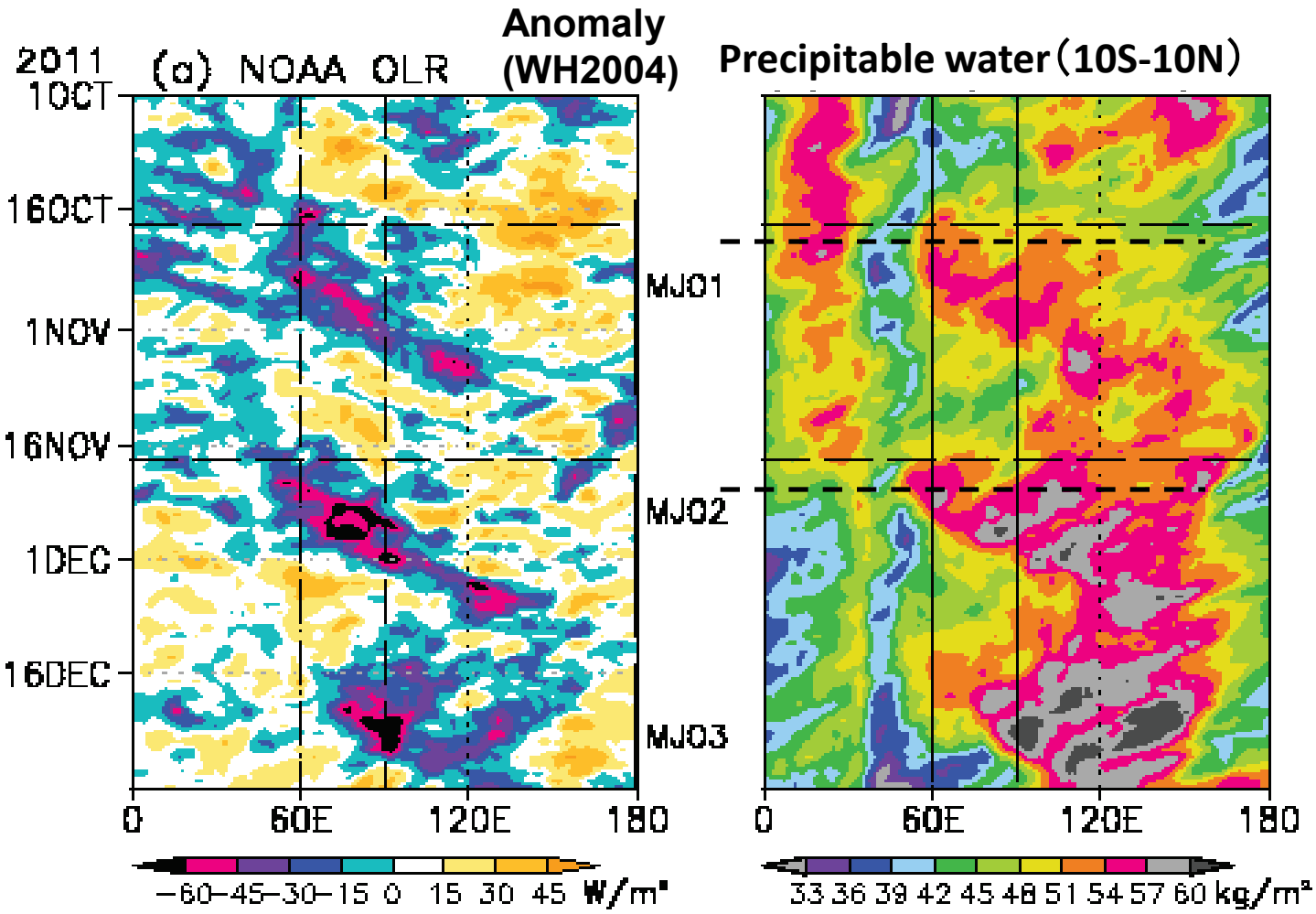

MSE start Increasing 7-10 days before OLR<0

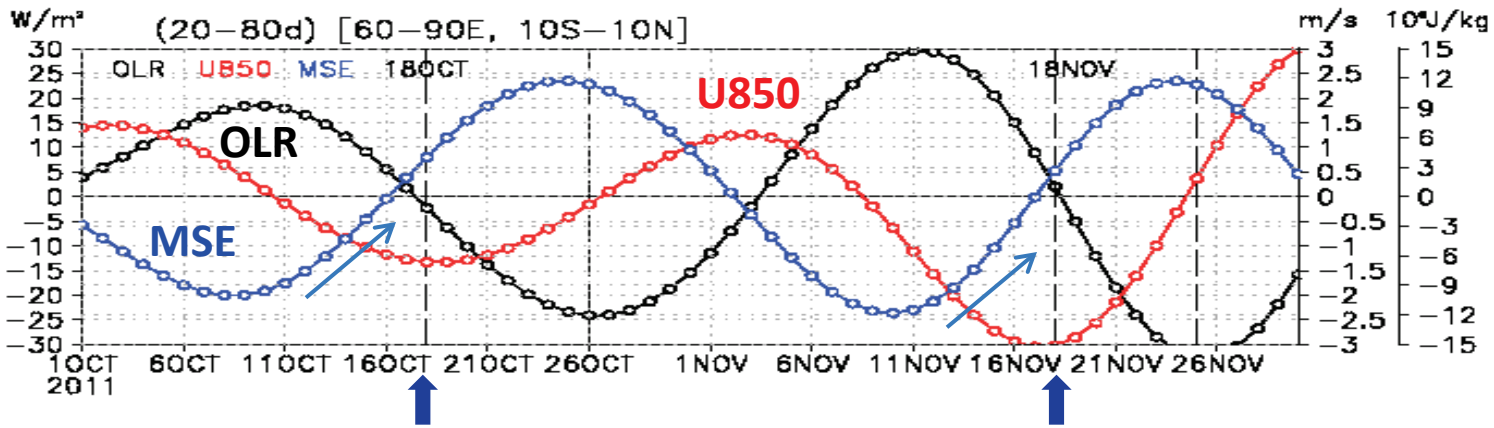

ERA-Interim
20-80d filtered
60-90E, 10S-10N

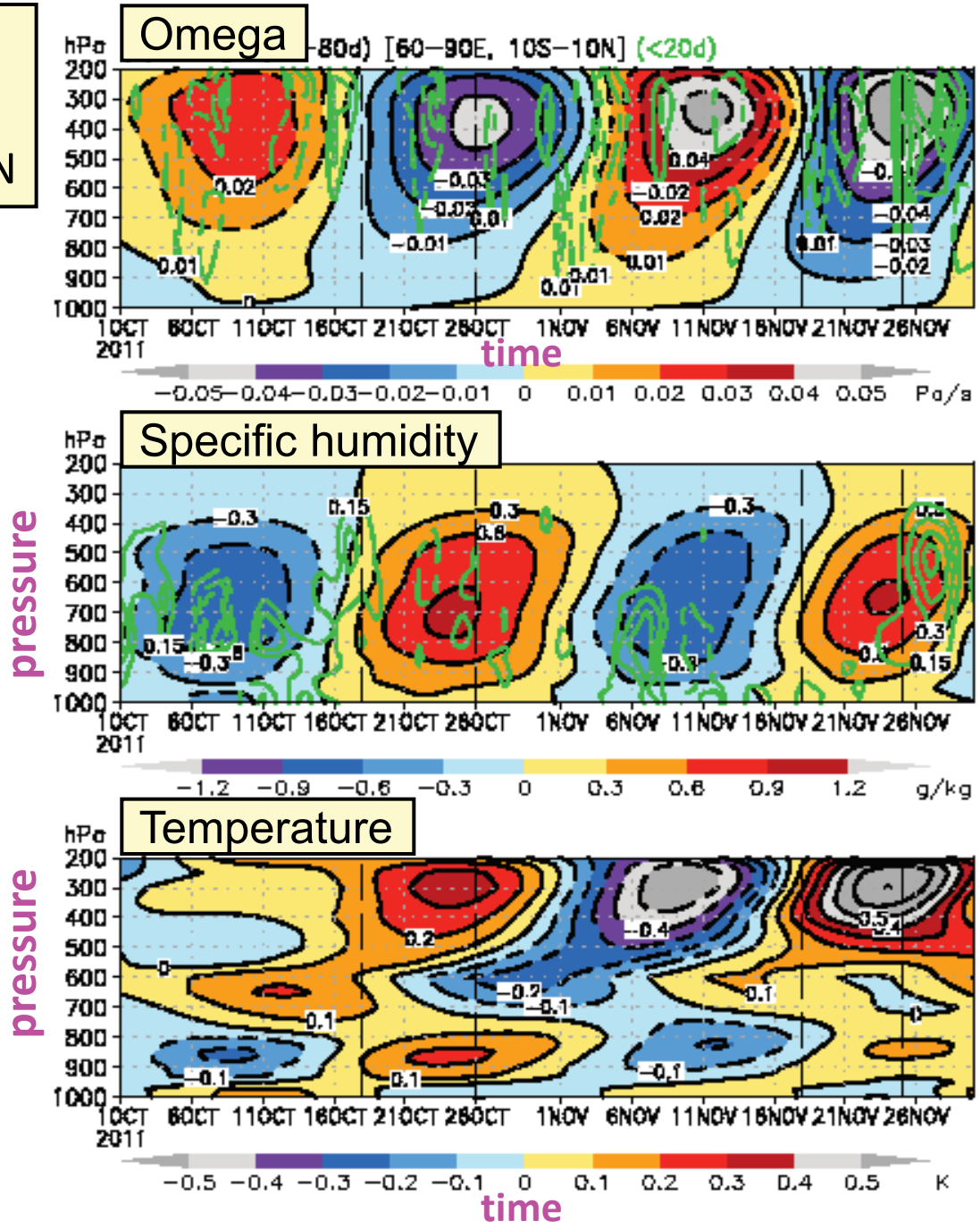

ERA-Interim
Moisture advection
20-80d filtered
60-90E, 10S-10N

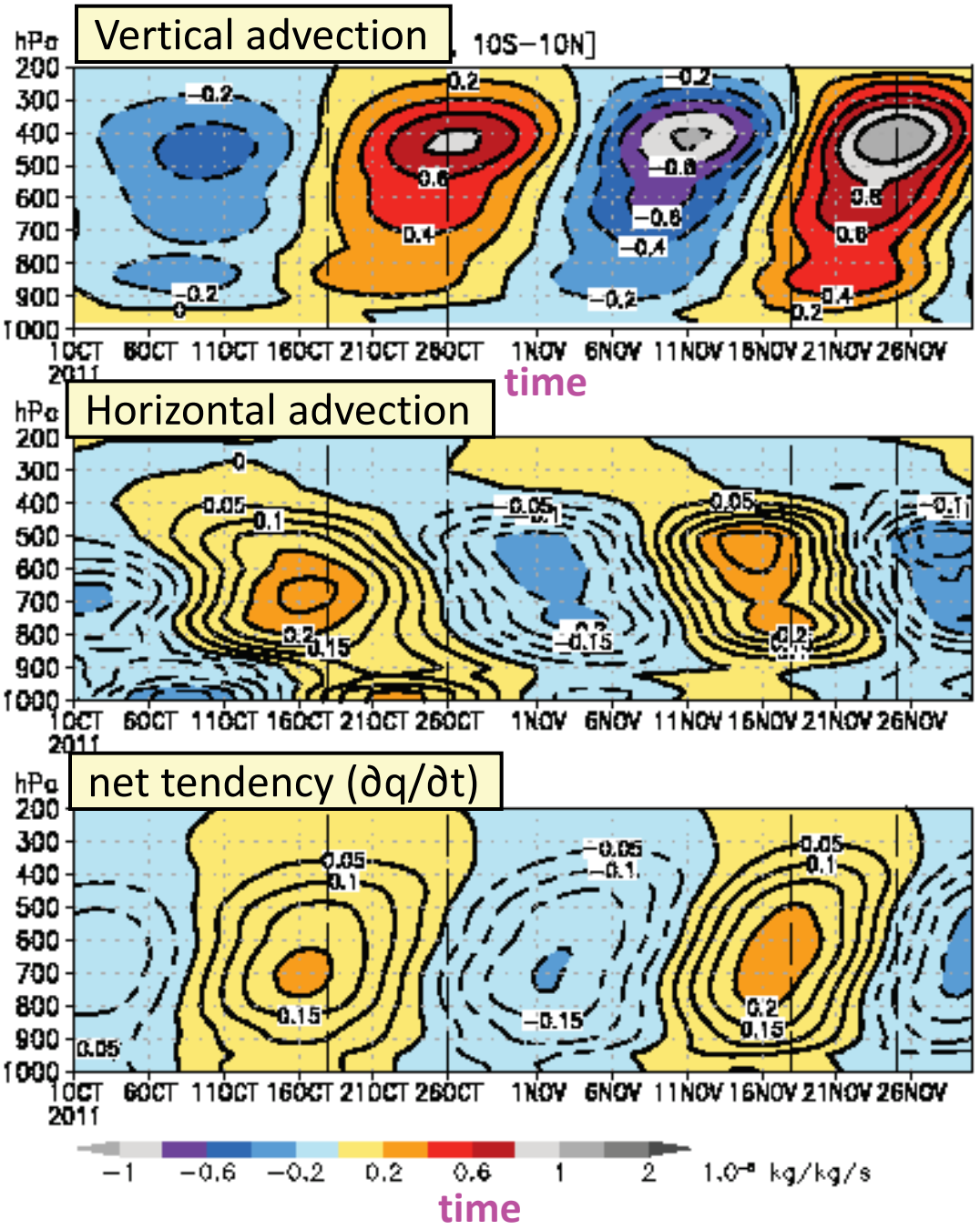

Horizontal advection Preceded major Moistening by Vertical advection

Magnitude comparable to net tendency

ERA-Interim
Moisture advection
20-80d filtered
60-90E, 10S-10N

Horizontal advection Preceded major Moistening by Vertical advection

Magnitude comparable to net tendency

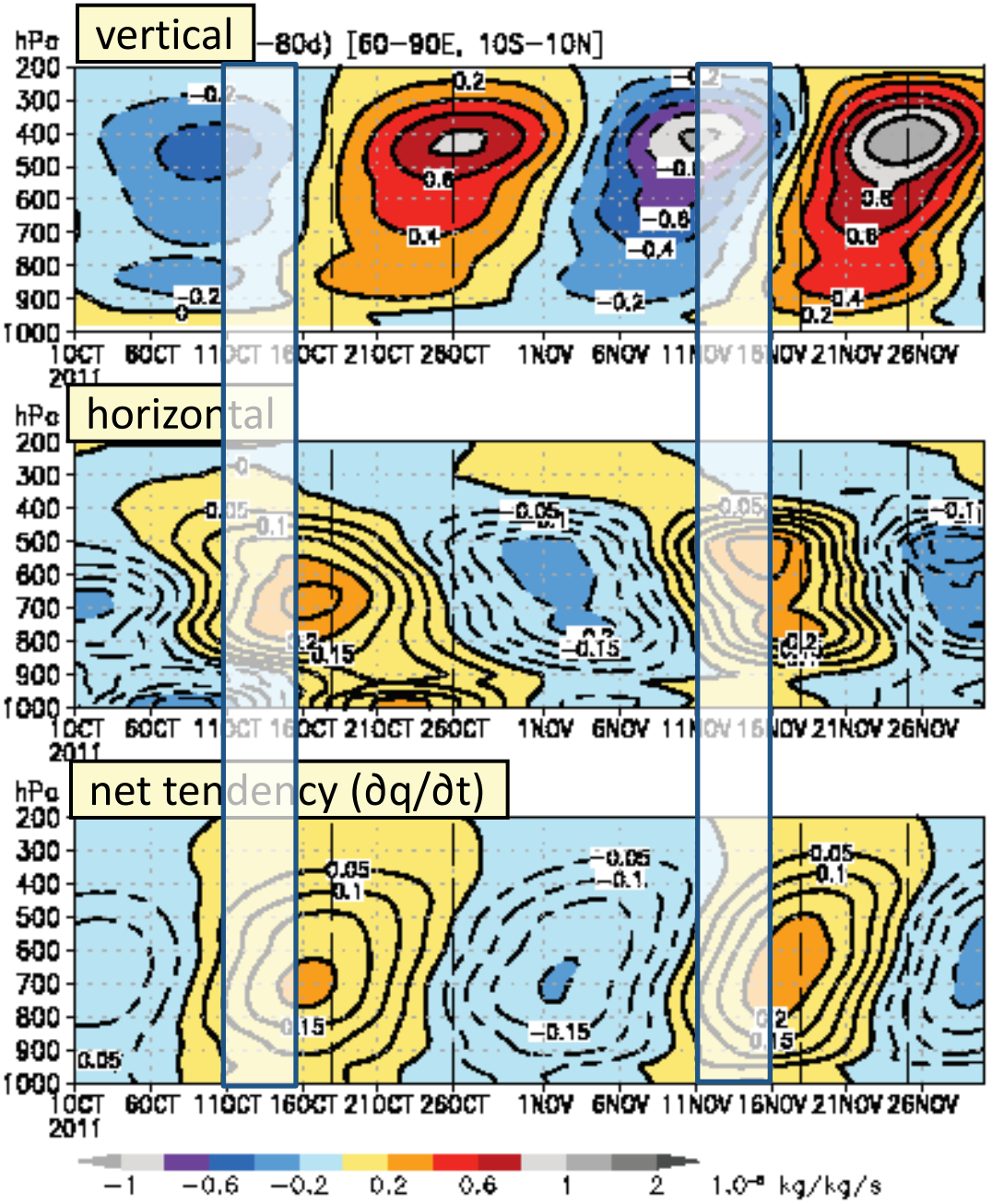

Moisture budgets

60-90E
10S-10N

MJO1
11-14 Oct

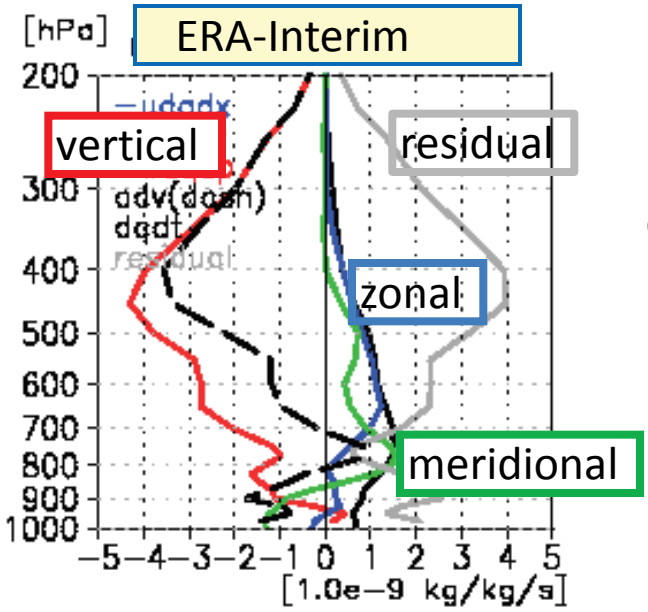

$$\left(\frac{\partial q}{\partial t}\right)' = (-V\nabla q)' + \left(-\omega\frac{\partial q}{\partial p}\right)' + \left(-\frac{Q_2}{L}\right)'$$

MJO2
11-16 Nov

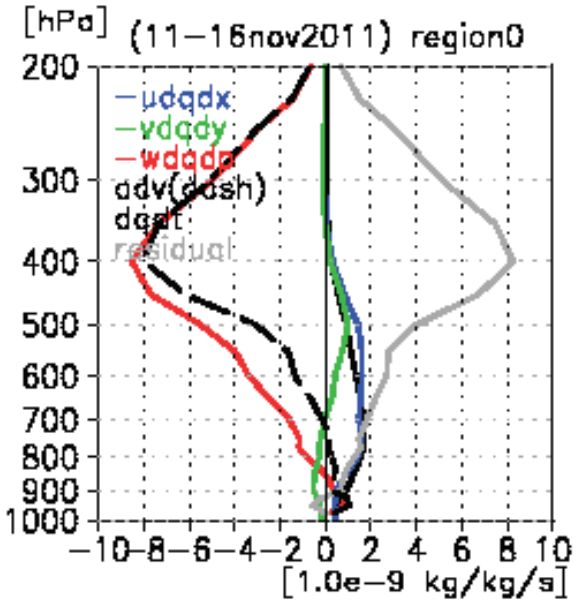

NICAM CINDY2011 simulations

- Realtime forecasts
- 14～56 km mesh
- 40L
- 7-days (daily updated)
  2011/7/27-2012/1/31

SST: nudged to initial value

Nasuno (2013), SOLA

(previous talks in this workshop)

- Hindcasts
- 14 km, 7 km, 3.5km mesh
- 40L
- 60 (30) days
  init: 2011/10/16
  (init: 2011/11/17)

SST: fixed to observation etc.

NICAM simulation (real-time forecasts)

Nasuno (2013, SOLA, 9, 69-73)

Nonhydrostatic ICosahedral Atmospheric Model
Satoh et al. (2008)

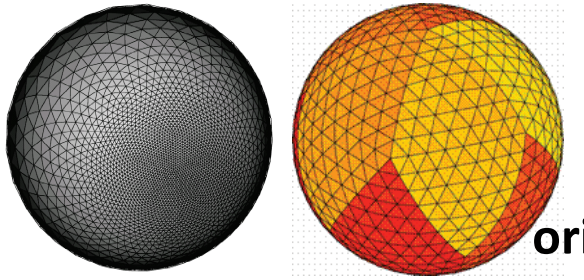

stretched grid
Tomita (2008)

original grid

Model: regionally stretched NICAM

Resolution: 14~56 km mesh (center: 80E, 8S), 40 levels

Domain of output data: 20-140E, 53S-37N

Length of forecasts: 7-days (6.5-days useful)

Period: 1 Oct. 2011-31 Jan. 2012

Frequency: daily

initialization: NCEP_FNL, interpolation

SST: slab ocean model (1-layer)

Data access (CINDY2011 JAMSTEC web site):

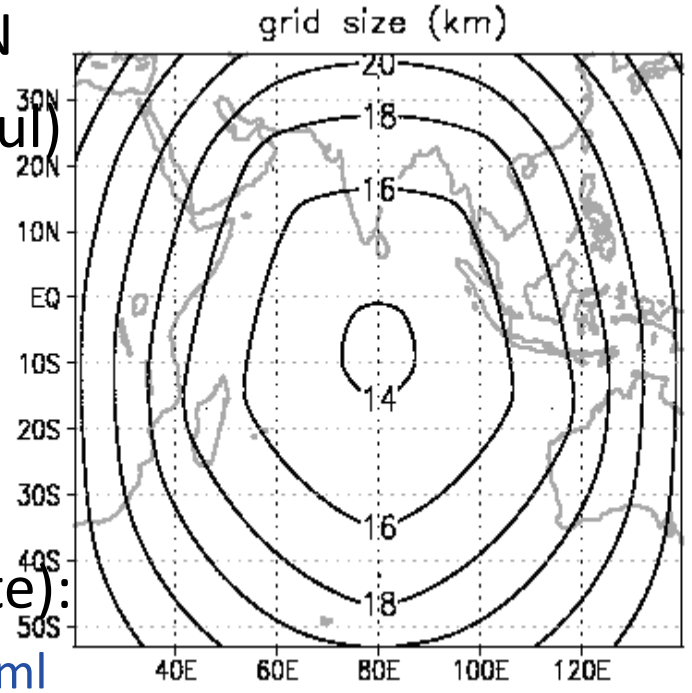

http://www.jamstec.go.jp/iorgc/cindy/obs/obs.html

link from DYNAMO page
(http://data.eol.ucar.edu/master_list/?project=DYNAMO)

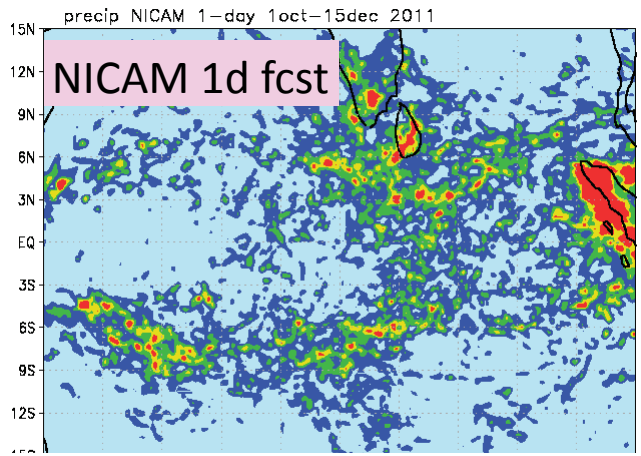

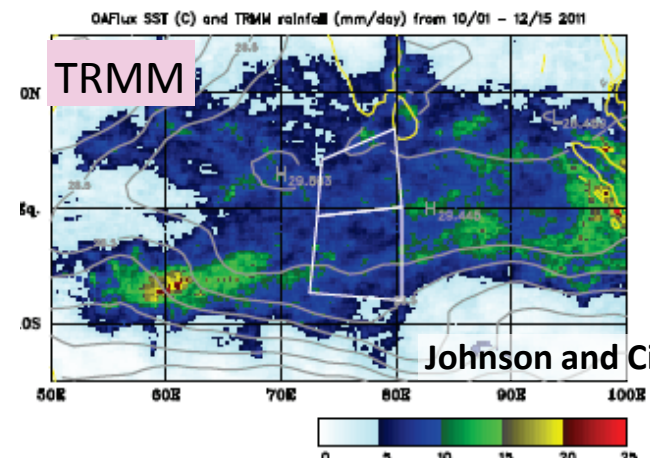

IOP mean (10/01-12/15 2011)
Daily precipitation
in stretch NICAM and TRMM

Johnson and Ciesielski (2013)

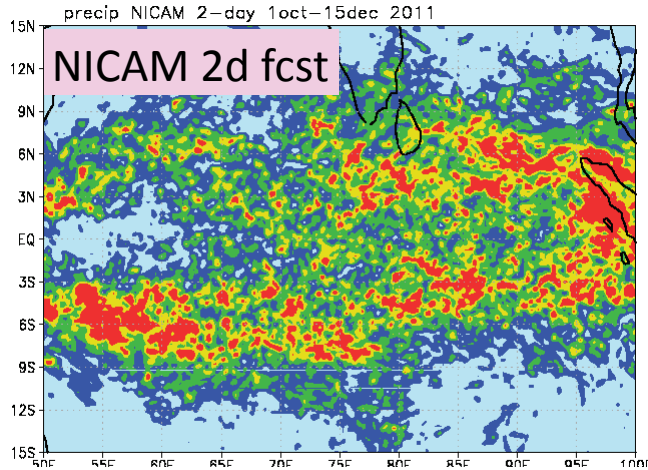

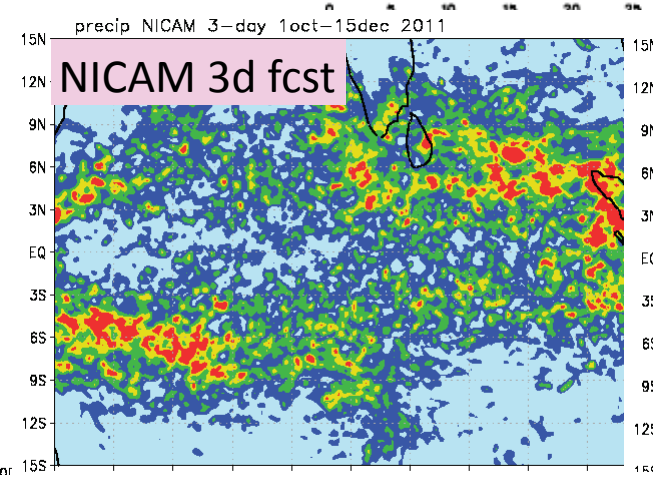

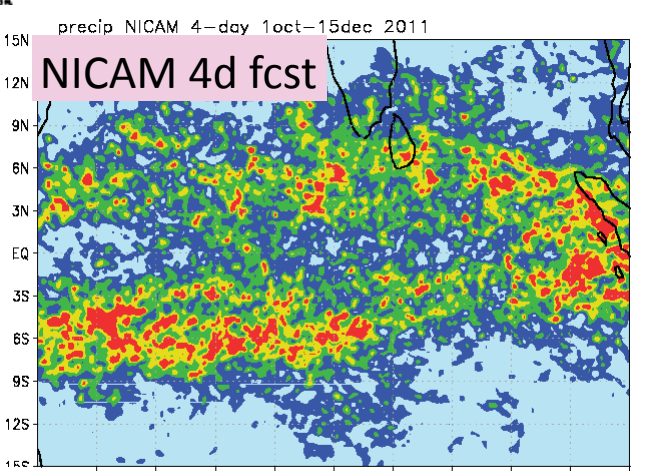

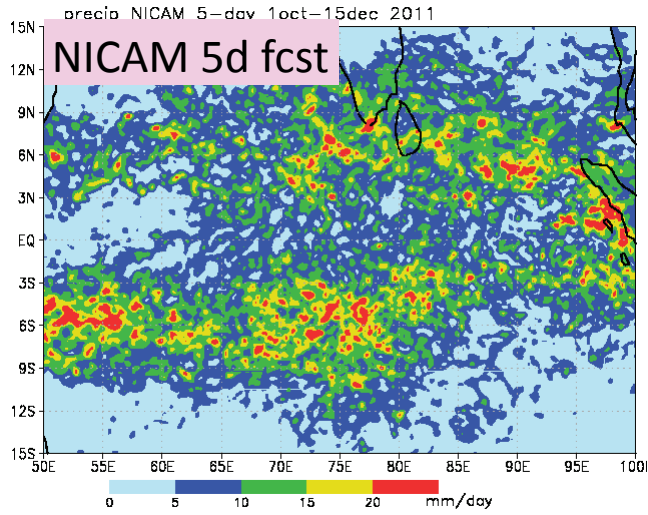

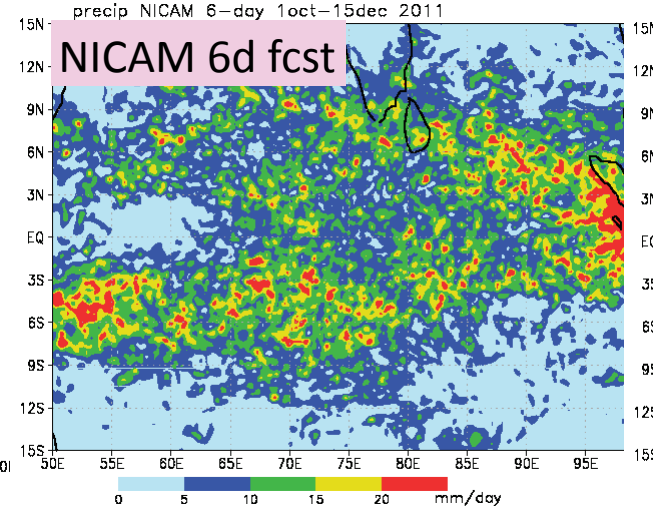

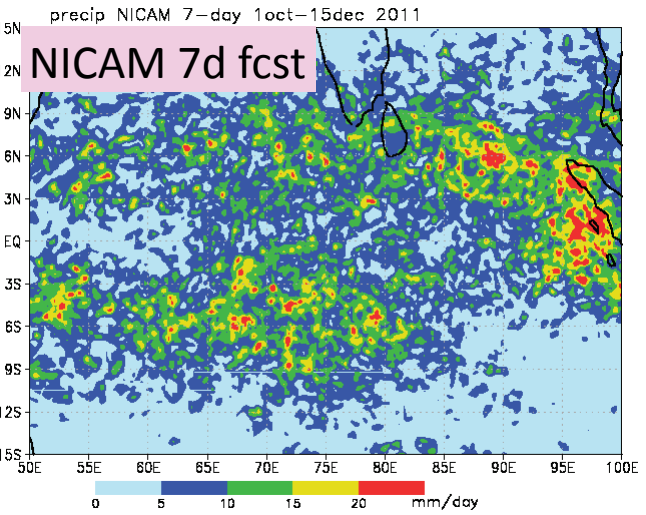

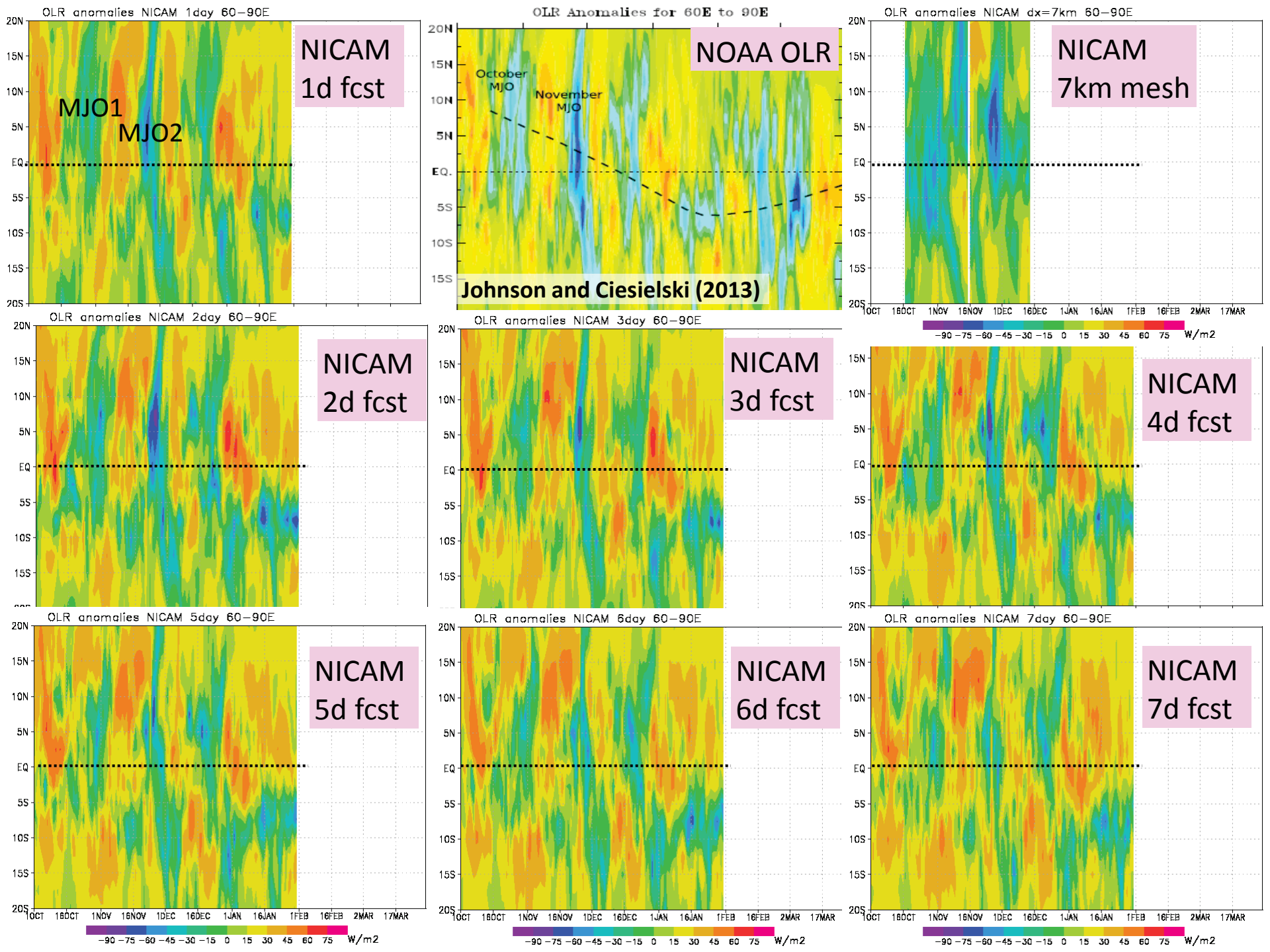
OLR anomalies NICAM 1day 60–90E
NICAM 1d fcst
MJO1
MJO2
OLR Anomalies for 60E to 90E
NOAA OLR
October MJO
November MJO
Johnson and Ciesielski (2013)
OLR anomalies NICAM dx=7km 60–90E
NICAM 7km mesh
OLR anomalies NICAM 2day 60–90E
NICAM 2d fcst
OLR anomalies NICAM 3day 60–90E
NICAM 3d fcst
NICAM 4d fcst
OLR anomalies NICAM 5day 60–90E
NICAM 5d fcst
OLR anomalies NICAM 6day 60–90E
NICAM 6d fcst
OLR anomalies NICAM 7day 60–90E
NICAM 7d fcst
20N 15N 10N 5N EQ 5S 10S 15S 20S
1OCT 16OCT 1NOV 16NOV 1DEC 16DEC 1JAN 16JAN 1FEB 16FEB 2MAR 17MAR
−90 −75 −60 −45 −30 −15 0 15 30 45 60 75 W/m2

Moisture buildup in CINDY2011/DYNAMO Array and Stretch NICAM (1d forecast)

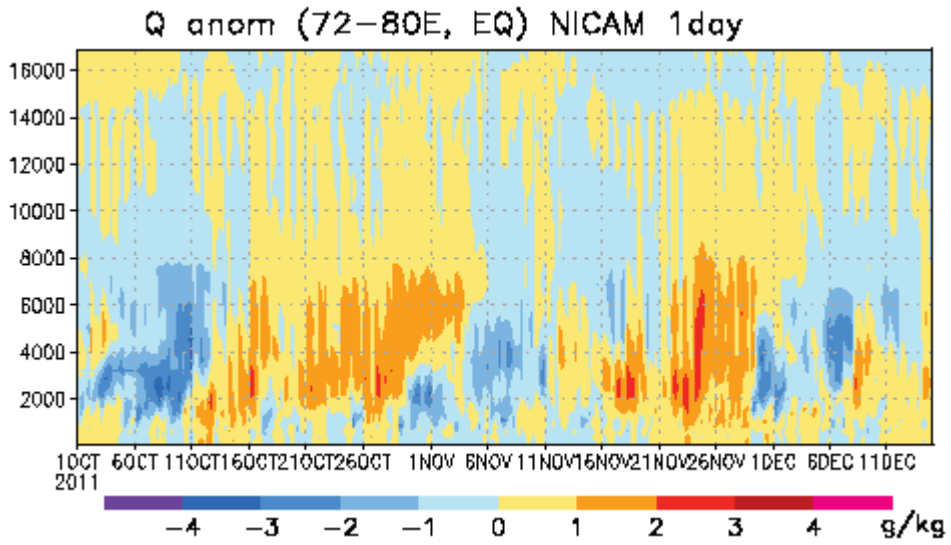

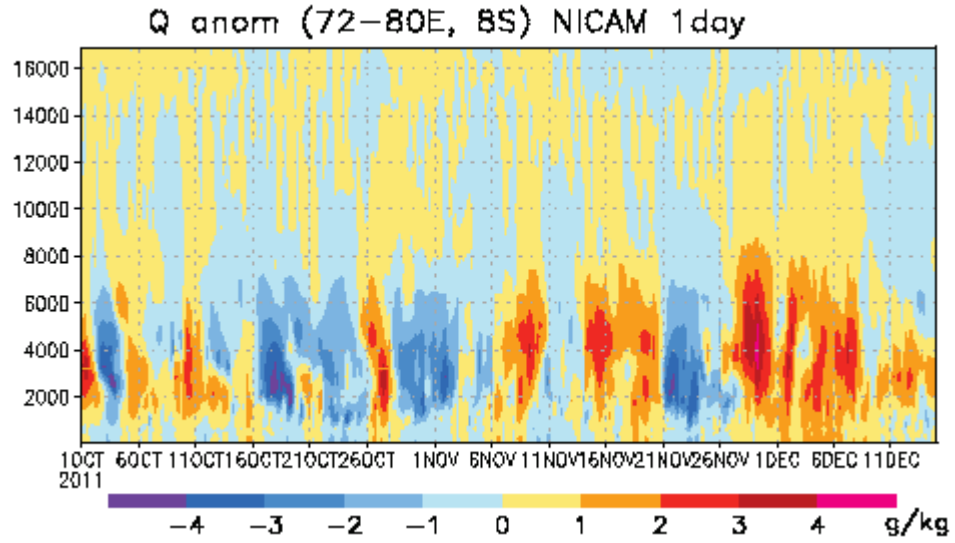

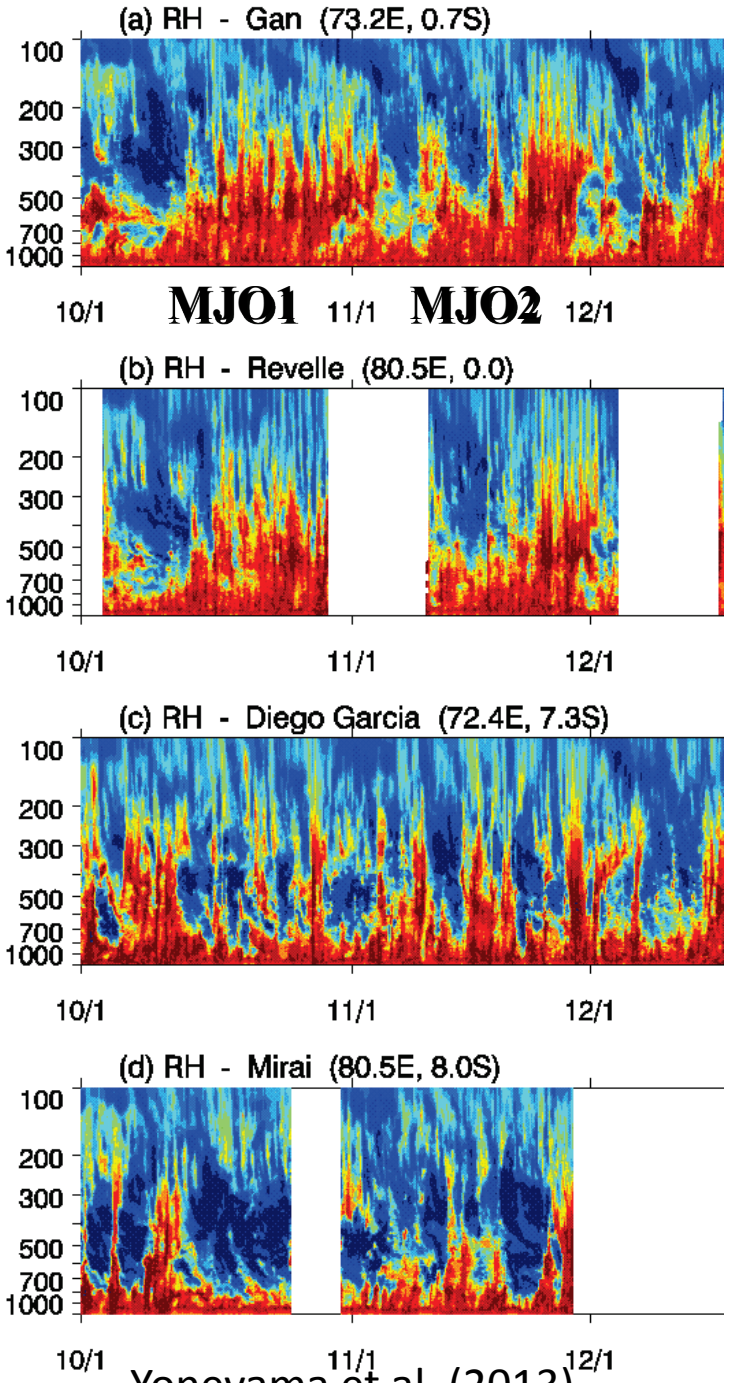

Yoneyama et al. (2013)

Moisture budgets

60-90E
10S-10N

MJO1
11-14 Oct

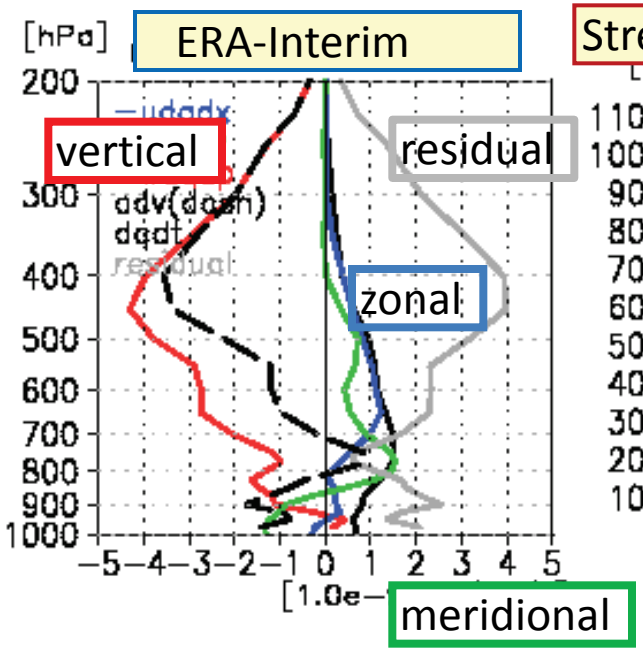

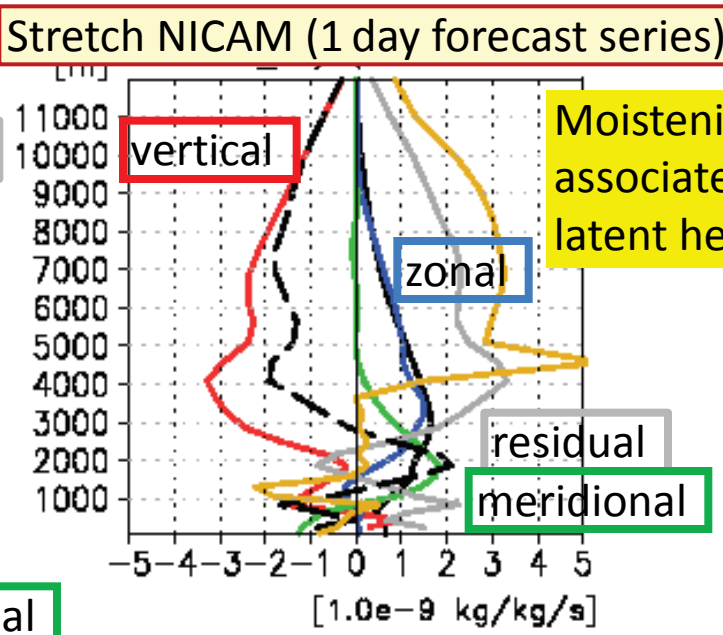

Moistening associated with latent heating

MJO2
11-16 Nov

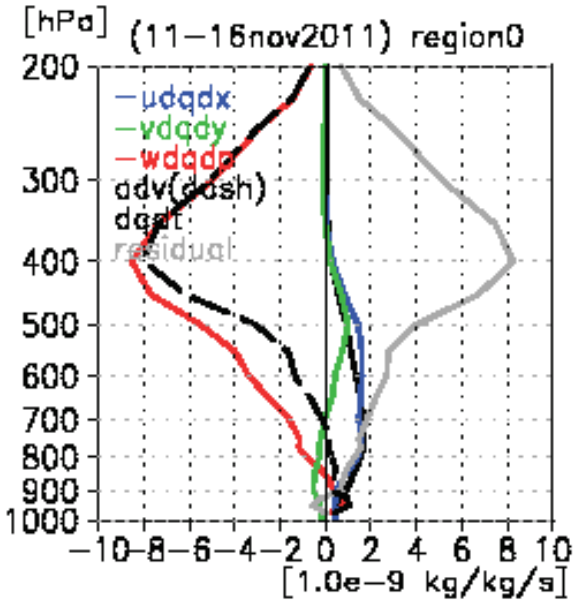

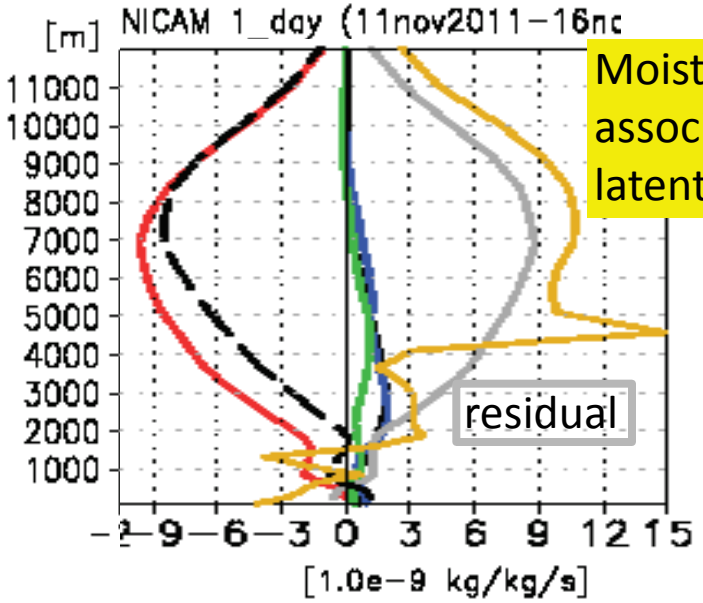

Moistening associated with latent heating

Latent heating
20-80d filtered
60-90E, 10S-10N

Evaporation
of preexisting
Water condensates

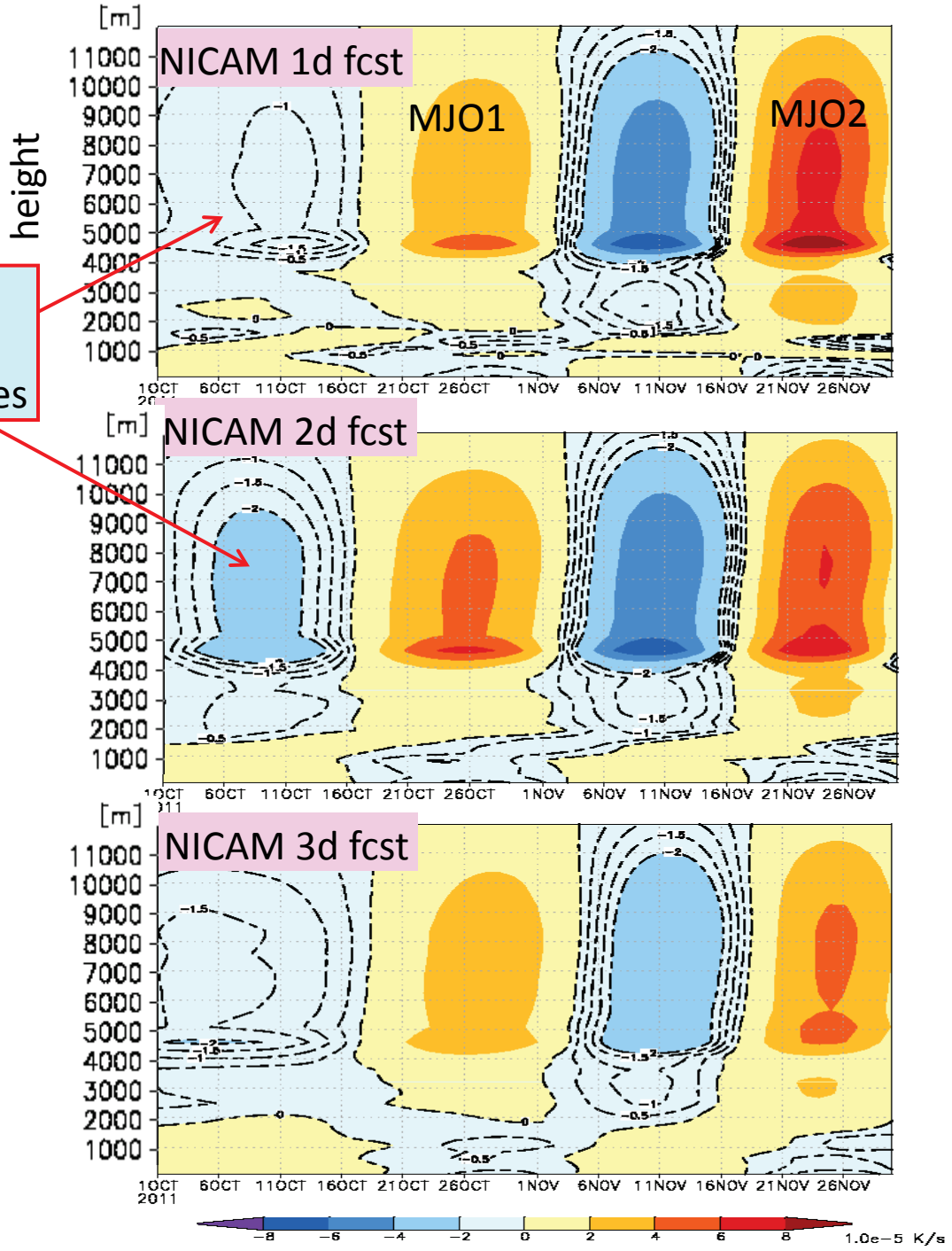

Decomposition of horizontal moisture advection

Zhao et al. 2013

$$\left(\frac{\partial q}{\partial t}\right)' = \left(-V\nabla q\right)' + \left(-\omega\frac{\partial q}{\partial p}\right)' + \left(-\frac{Q_2}{L}\right)'$$

60-90E, 10S-10N

$$u=\bar{u}+u'+u^* \quad , \quad v=\bar{v}+v'+v^* \quad q=\bar{q}+q'+q^*$$

overbar: >80 day (basic state) prime: 20-80 day (ISO) asterisk: < 20 day (high-freq)

$(-\bar{V}\cdot\nabla\bar{q})'$ 1 $(-\bar{V}\cdot\nabla q')'$ 2 $(-\bar{V}\cdot\nabla q^*)'$ 3 $(-V'\cdot\nabla\bar{q})'$ 4 $(-V'\cdot\nabla q')'$ 5 $(-V'\cdot\nabla q^*)'$ 6 $(-V^*\cdot\nabla\bar{q})'$ 7 $(-V^*\cdot\nabla q')'$ 8 $(-V^*\cdot\nabla q^*)'$ 9

400-750hPa MJO1 750-1000hPa 400-750hPa MJO2 750-1000hPa

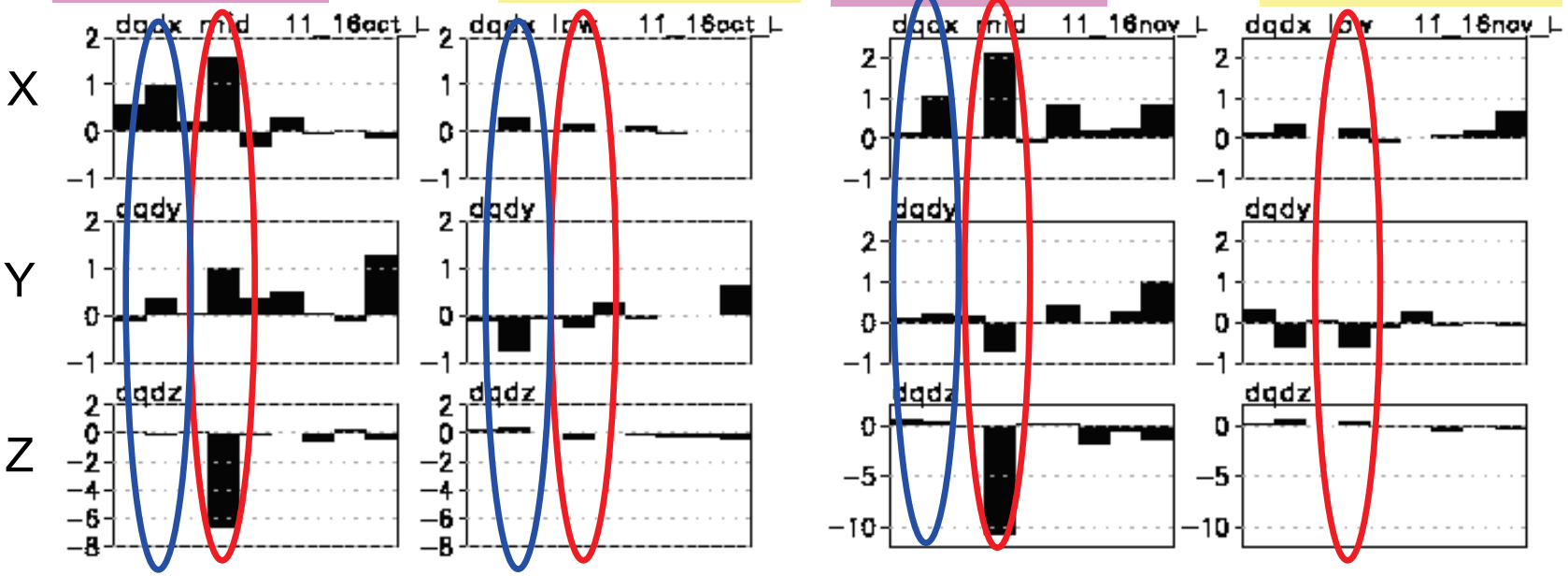

Advection of ISO moisture by basic winds Basic moisture by ISO winds

Era-Interim

600 hPa
Basic wind
(> 80d)
ISO moisture
(20-80 d)

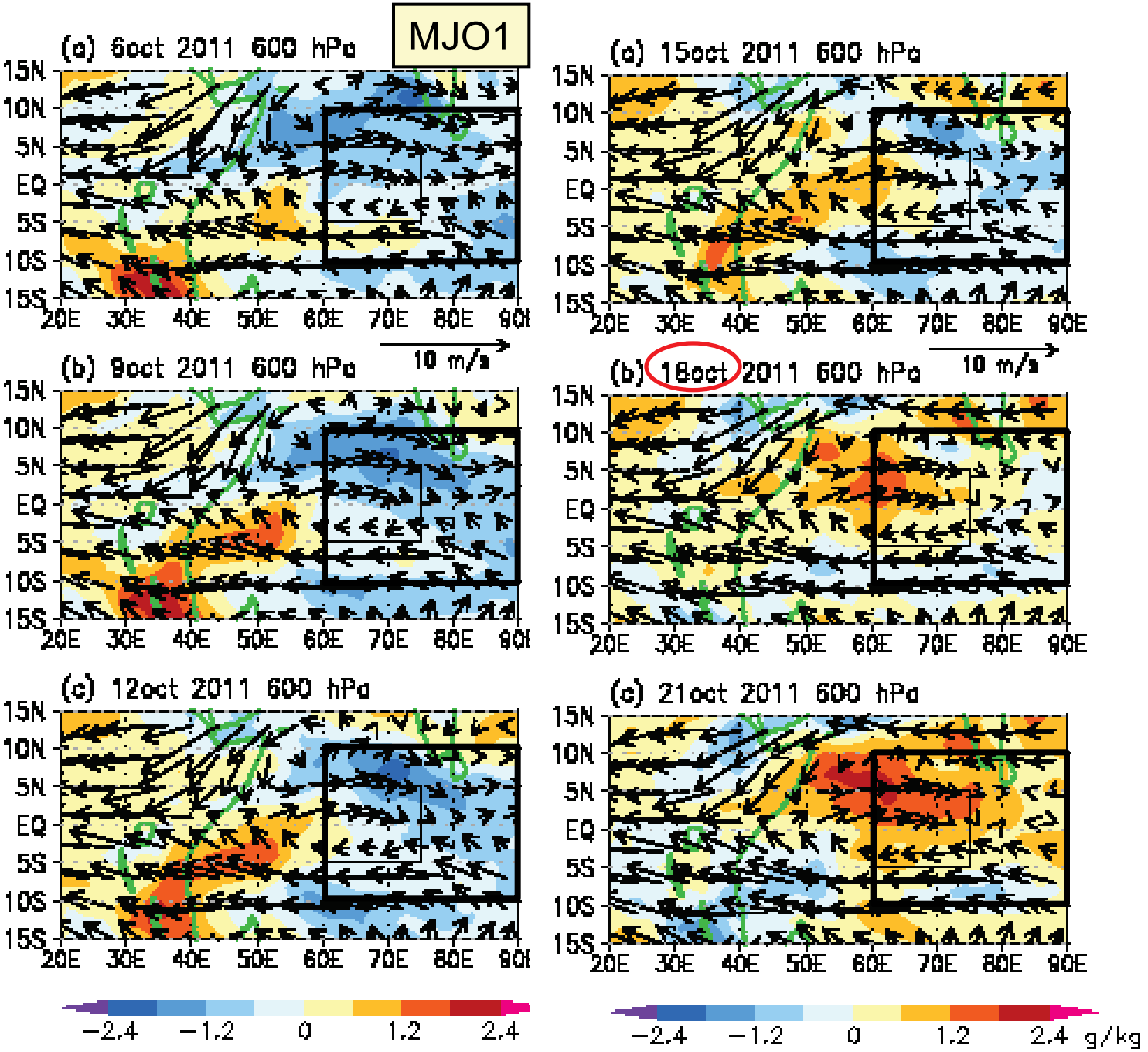

Era-Interim

600 hPa
Basic wind
(> 80d)
ISO moisture
(20-80 d)

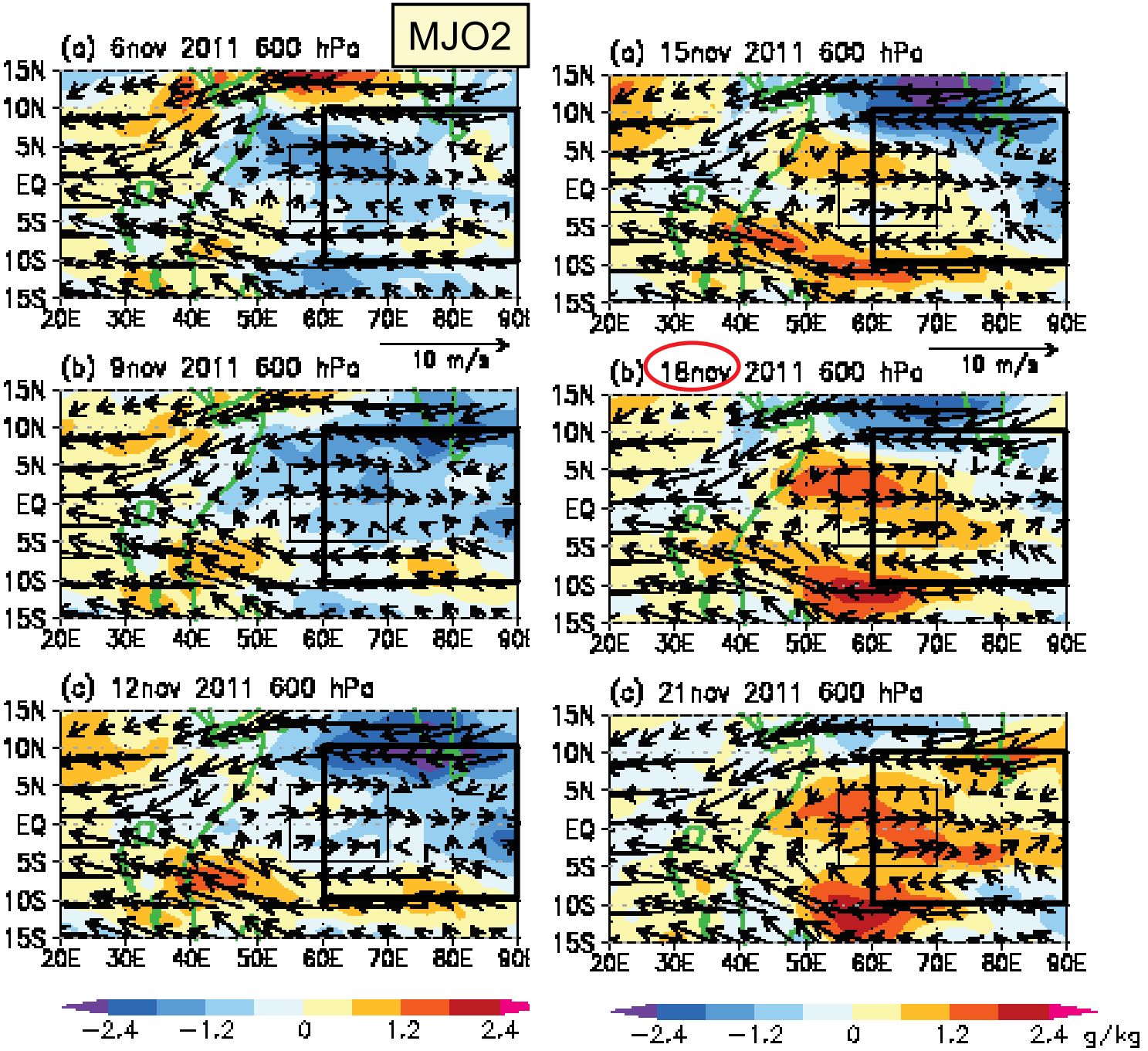

OLR (20-80 day) 850hPa wind

MJO1

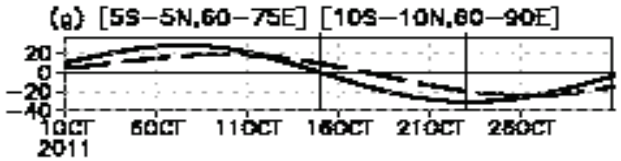

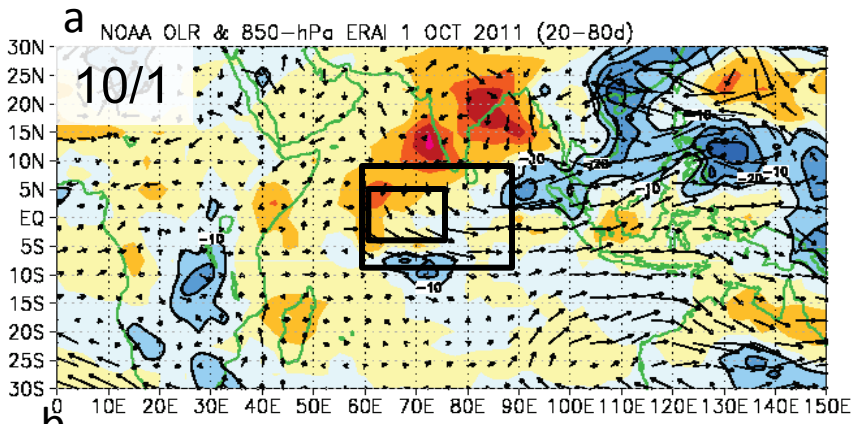

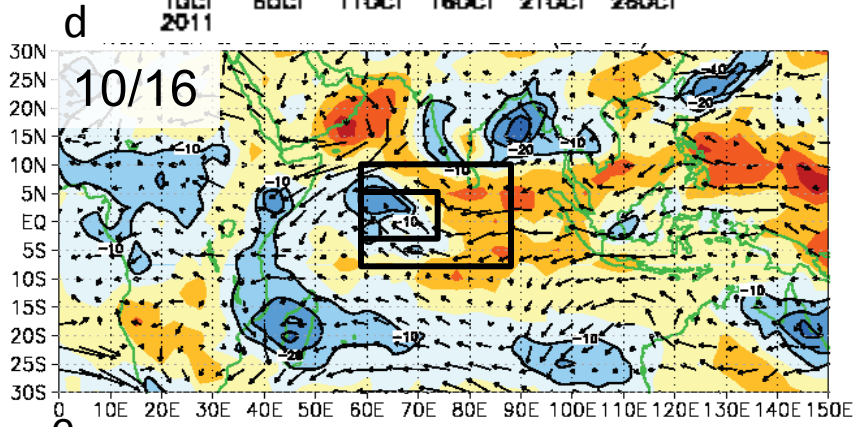

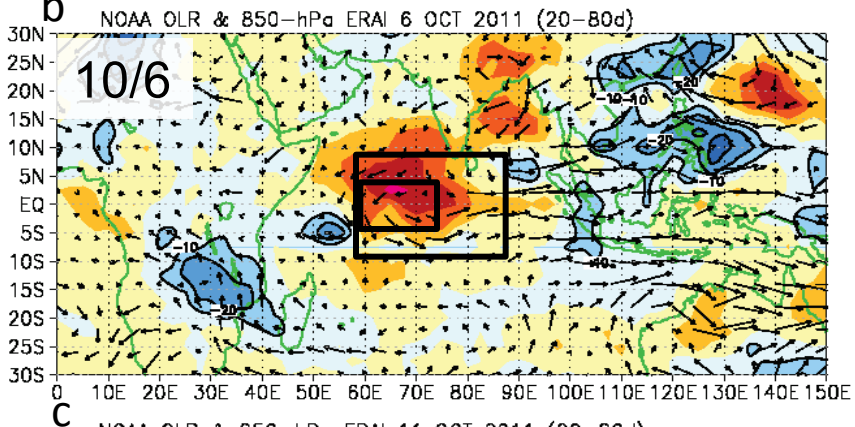

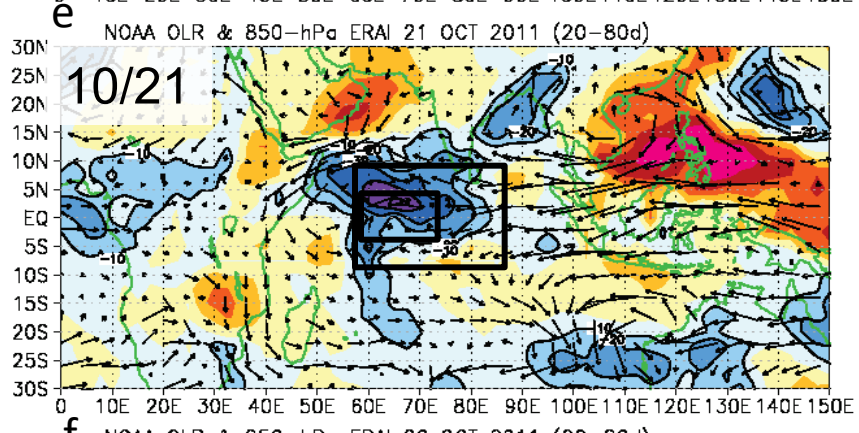

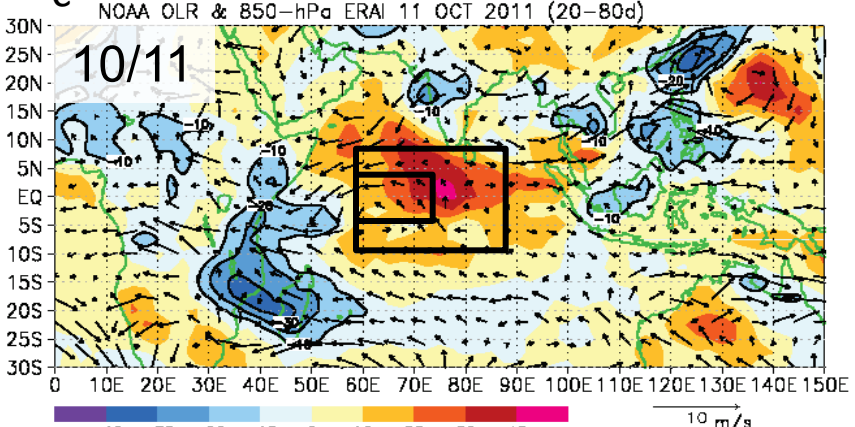

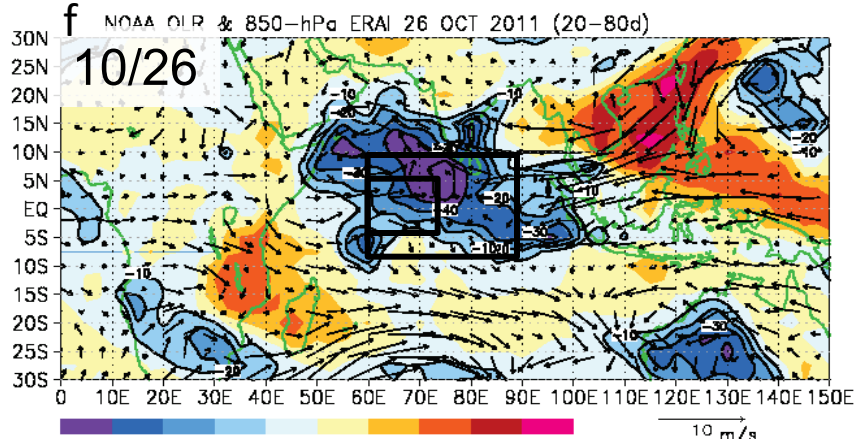

-40 -30 -20 -10 0 10 20 30 40 W/m2

10 m/s

OLR (20-80 day) 850hPa wind

MJO2

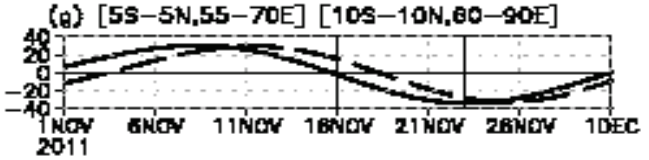

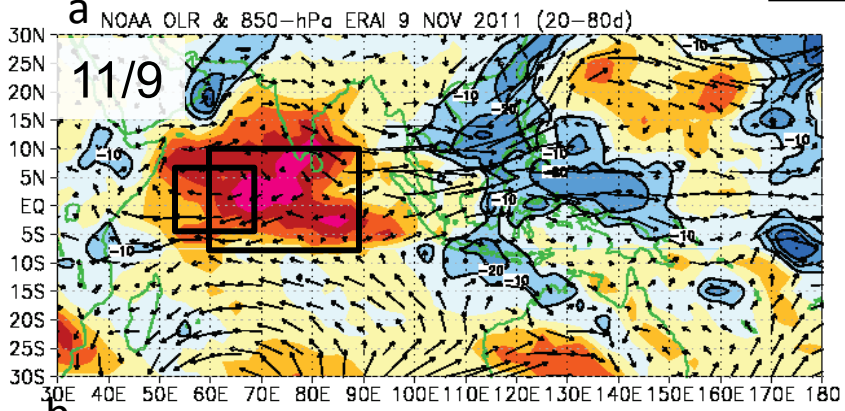

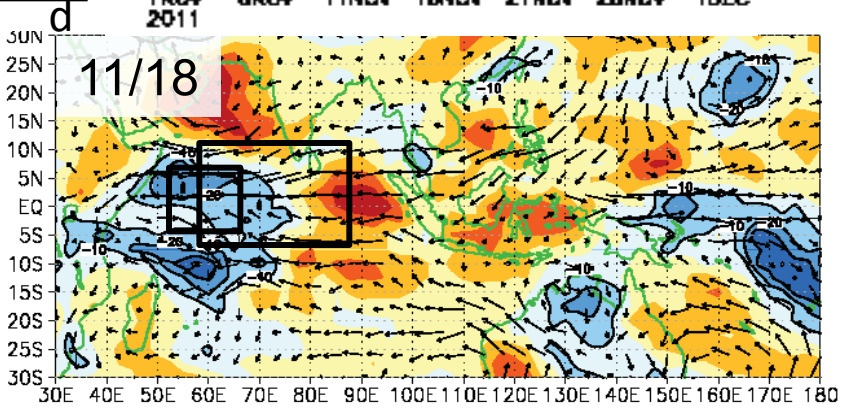

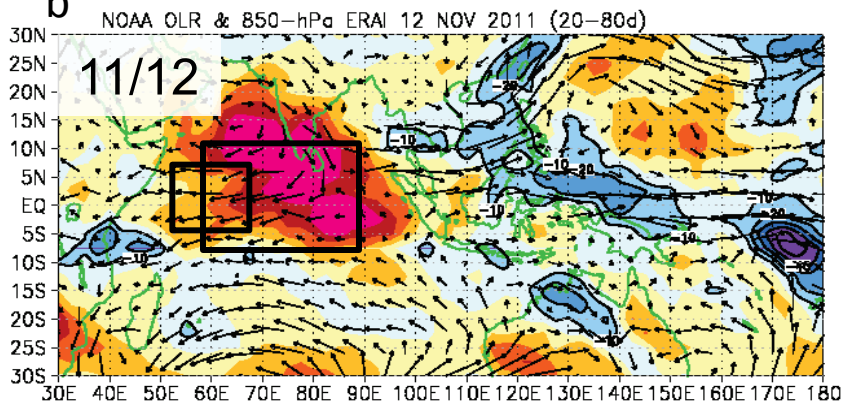

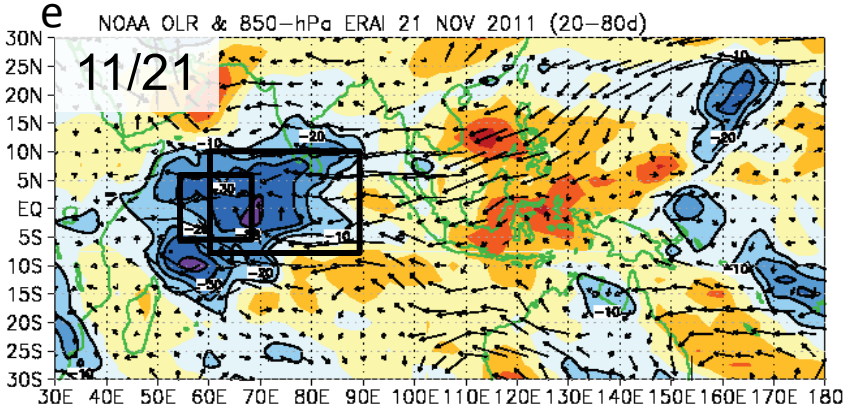

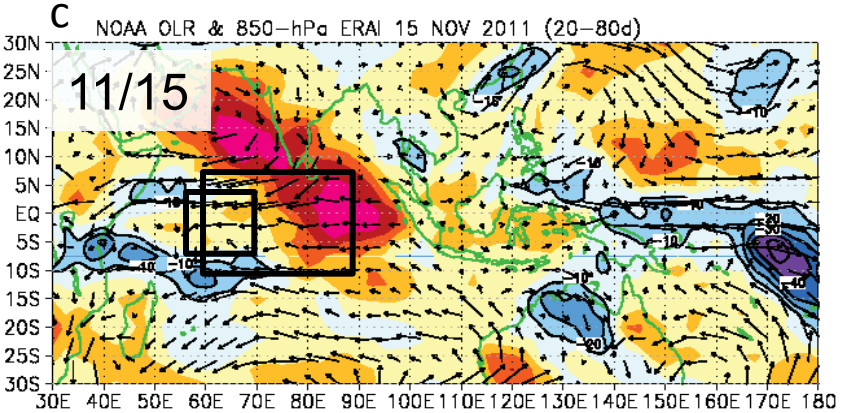

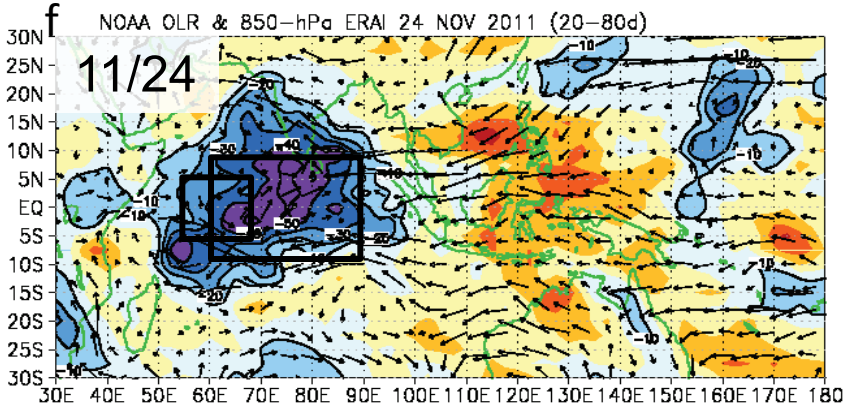

Era-Interim

MJO1
600 hPa

Basic moisture (> 80d)
ISO wind (20-80 d)

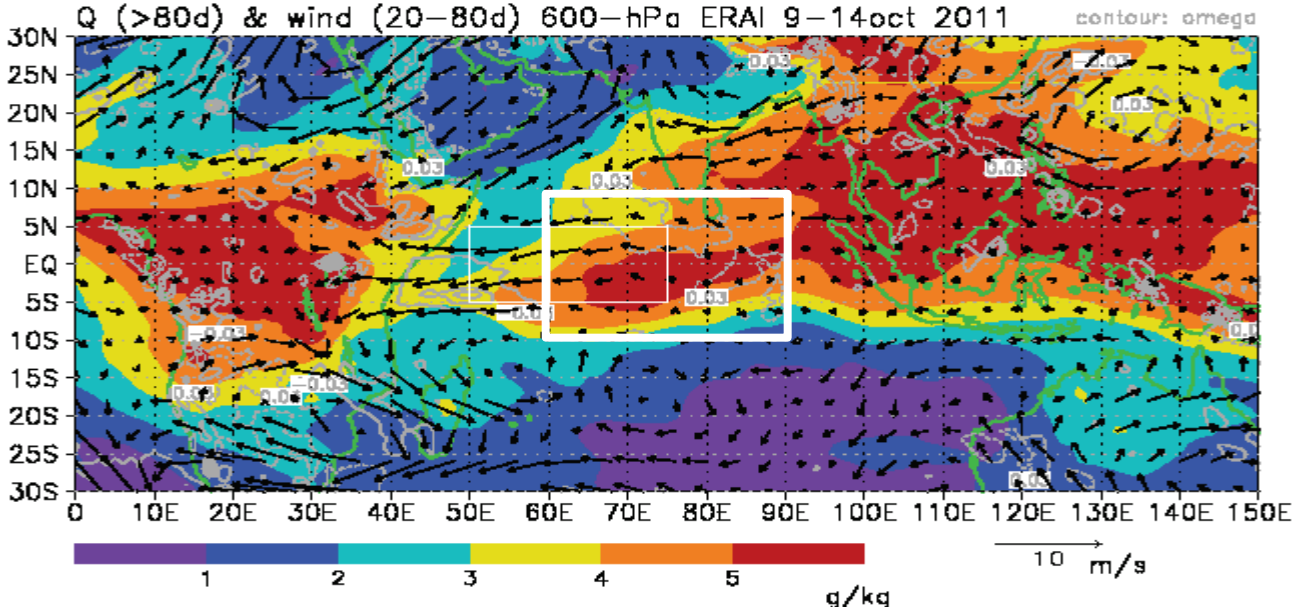

V (20-80d)

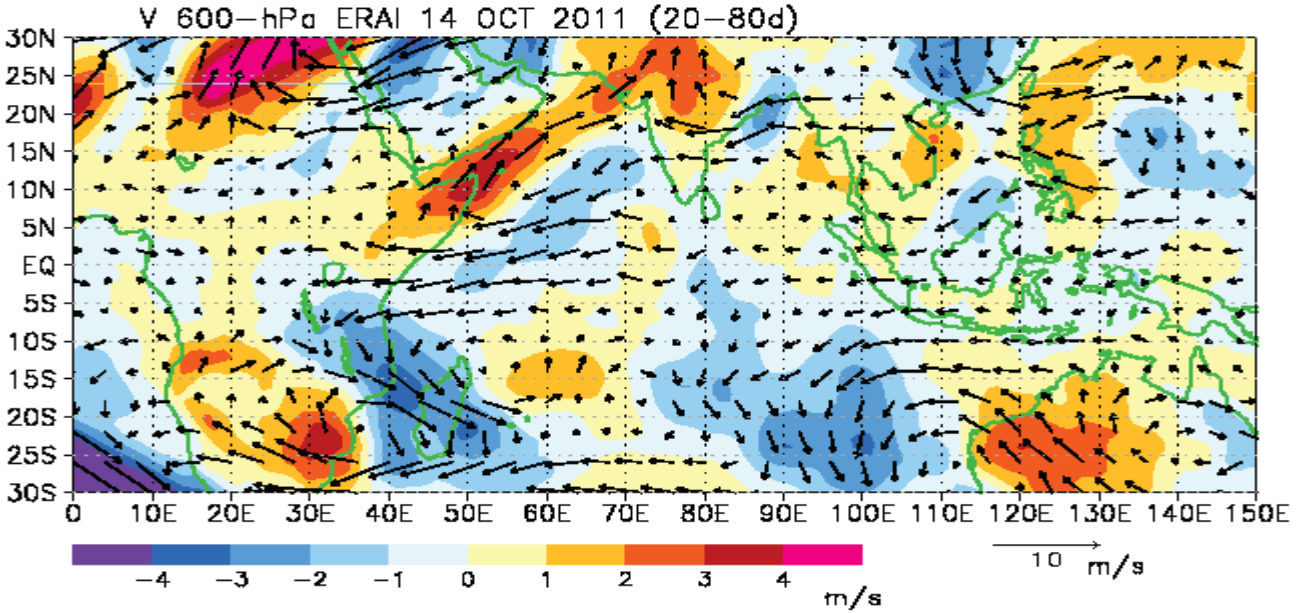

Era-Interim

MJO2

500 hPa
U(20-80d)

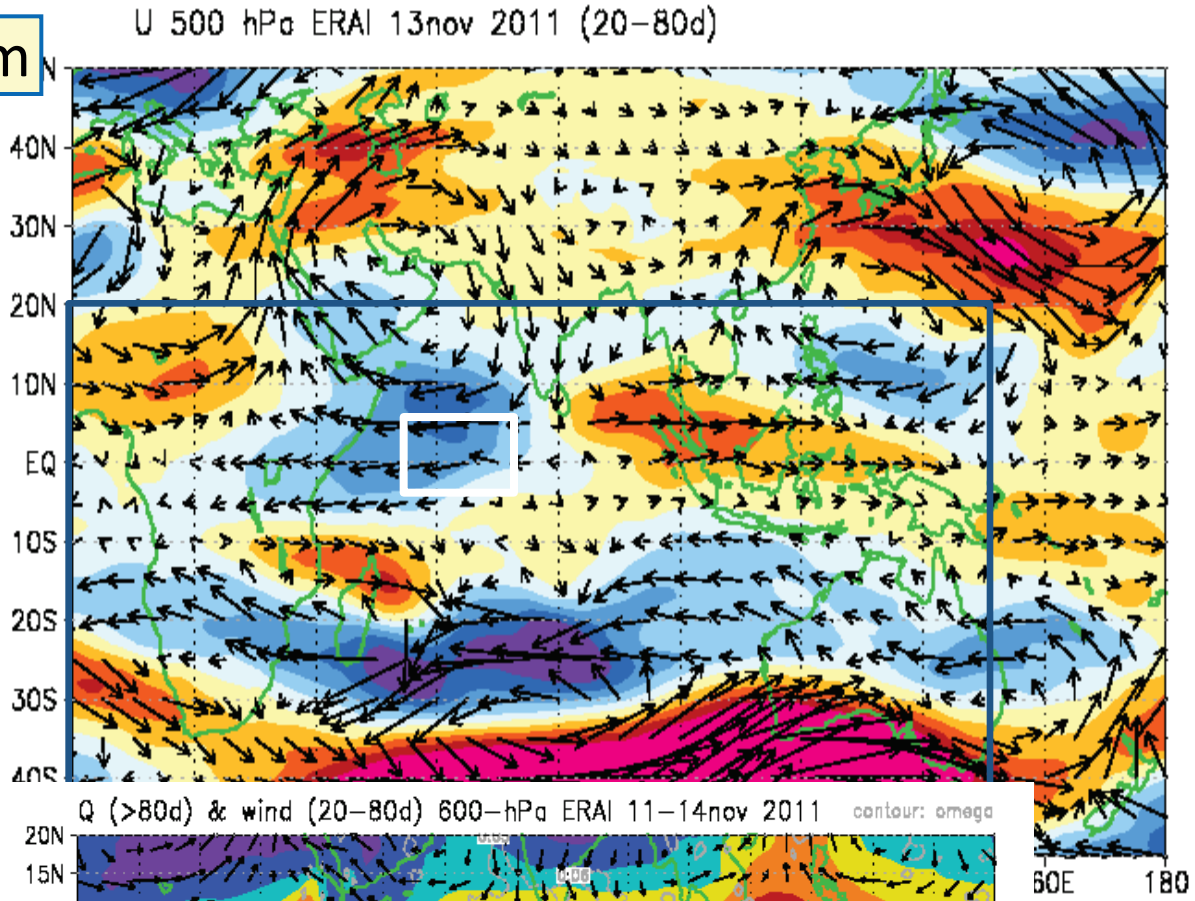

600 hPa
Basic
moisture
(> 80d)
ISO wind
(20-80 d)

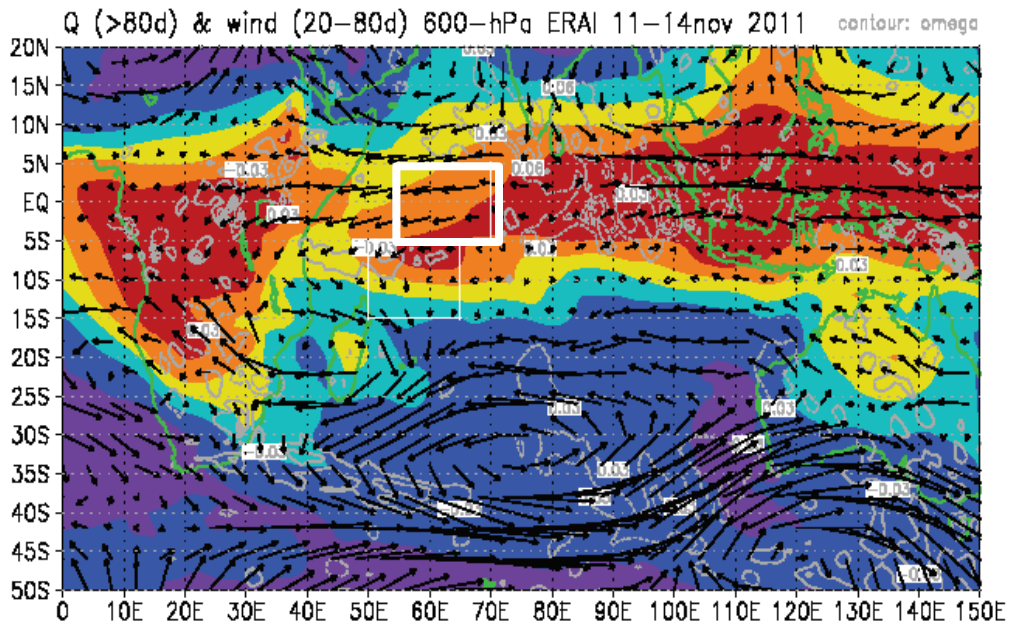

Discussion

20-80 day filtered U (10S-10N)

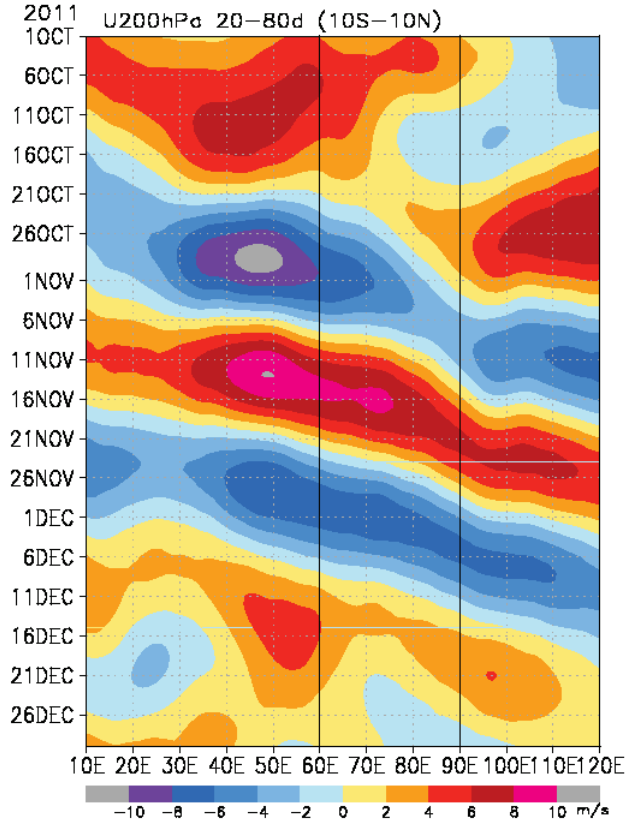

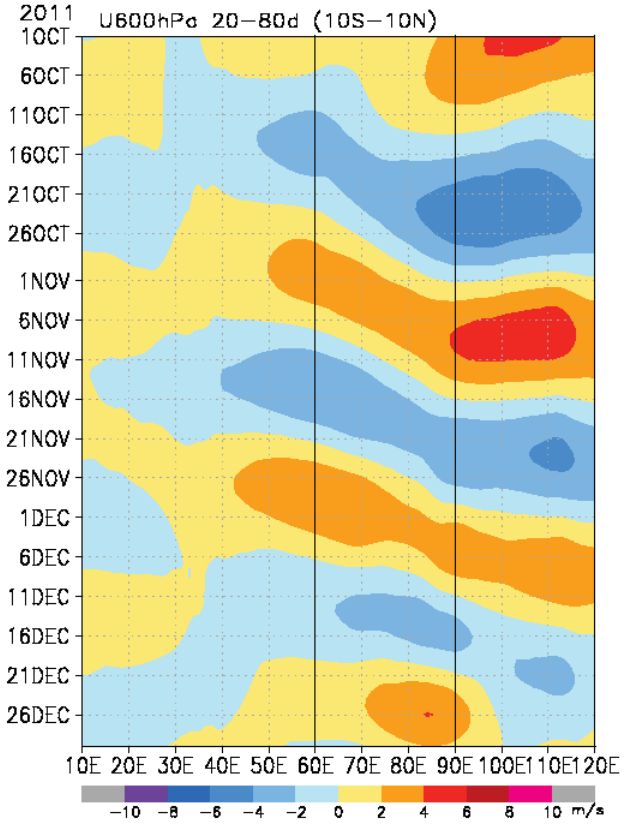

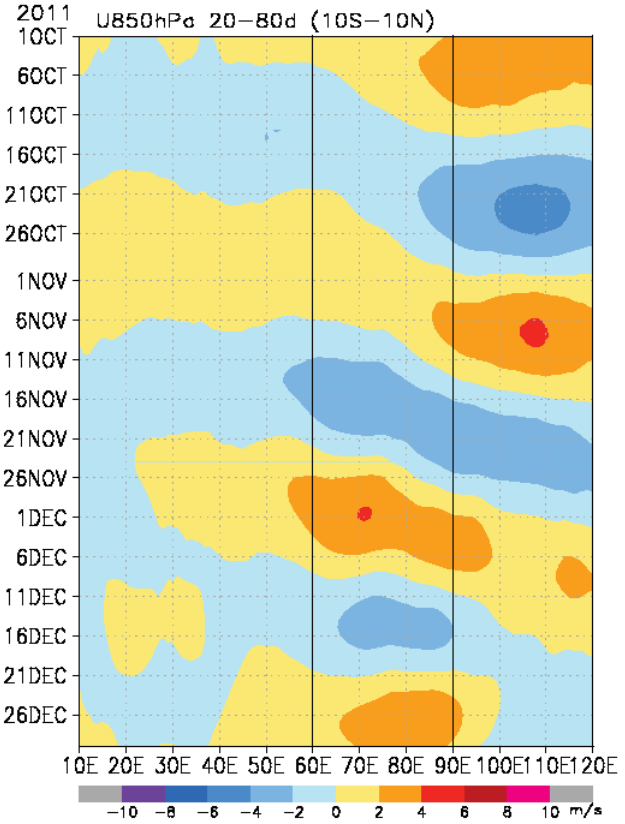

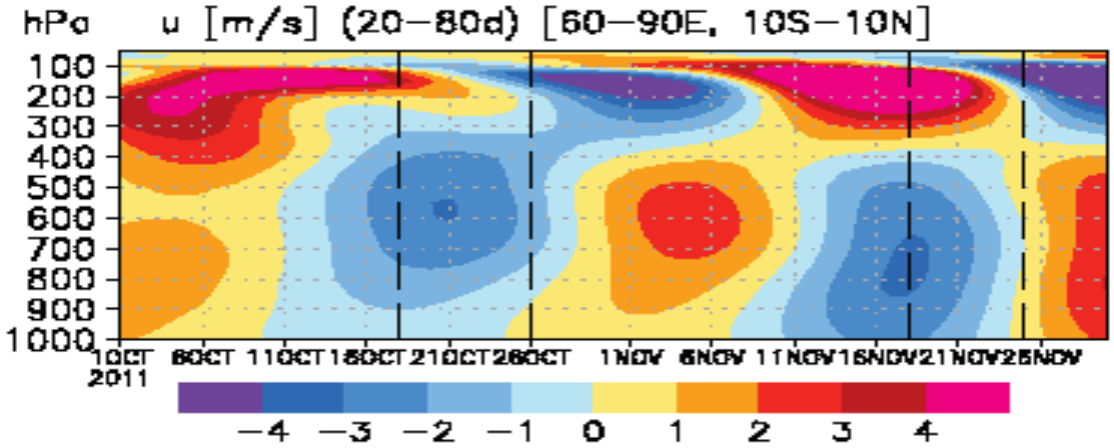
hPa
u [m/s] (20–80d) [60–90E, 10S–10N]
100
200
300
400
500
600
700
800
900
1000
10OCT 2011
60CT 110CT 160CT 210CT 260CT 1NOV 6NOV 11NOV 16NOV 21NOV 26NOV
−4 −3 −2 −1 0 1 2 3 4

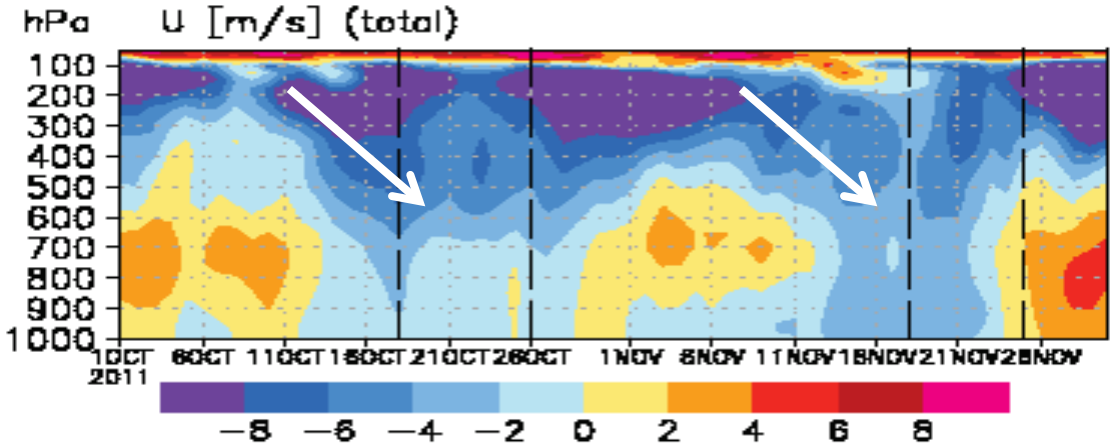
hPa
U [m/s] (total)
100
200
300
400
500
600
700
800
900
1000
10OCT 2011
60CT 110CT 160CT 210CT 260CT 1NOV 6NOV 11NOV 16NOV 21NOV 26NOV
−8 −6 −4 −2 0 2 4 6 8

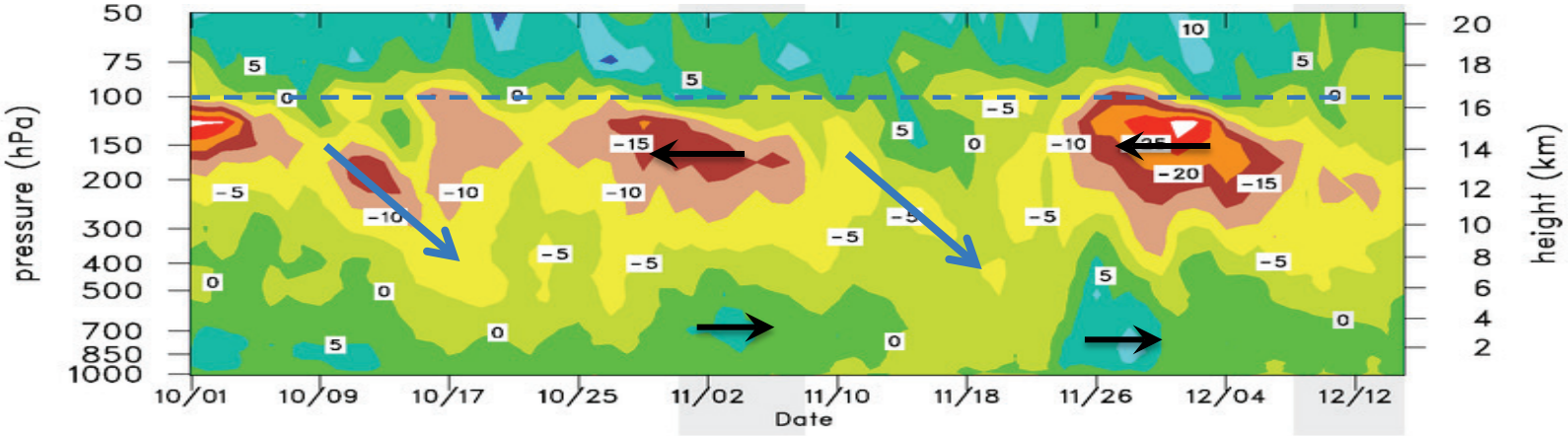
pressure (hPa)
50
75
100
150
200
300
400
500
700
850
1000
10/01
10/09
10/17
10/25
11/02
11/10
11/18
11/26
12/04
12/12
Date
height (km)
20
18
16
14
12
10
8
6
4
2

U (>80d), geopotential height & wind (20-80d)

MJO1 (9-14 oct)

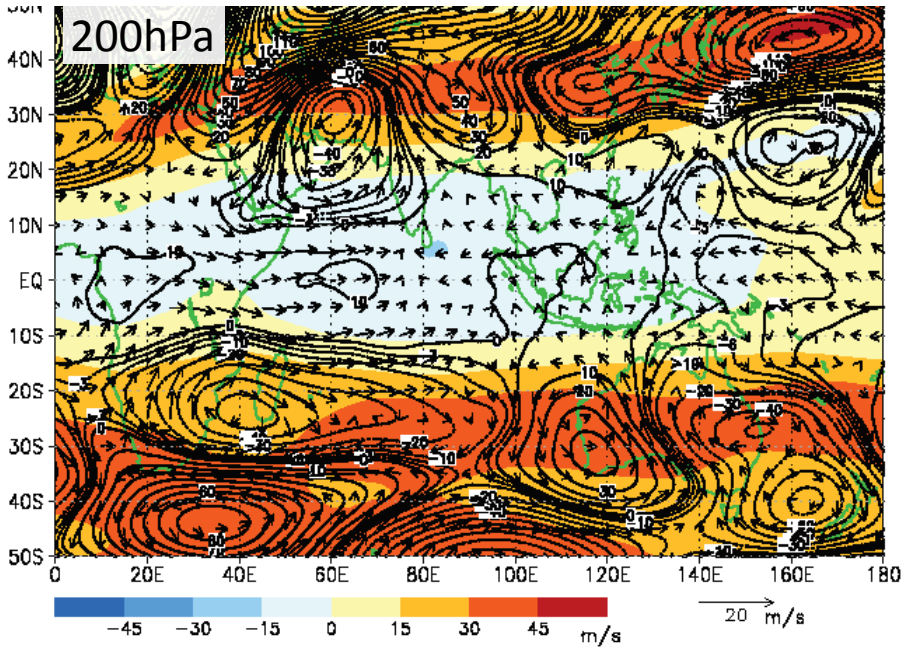

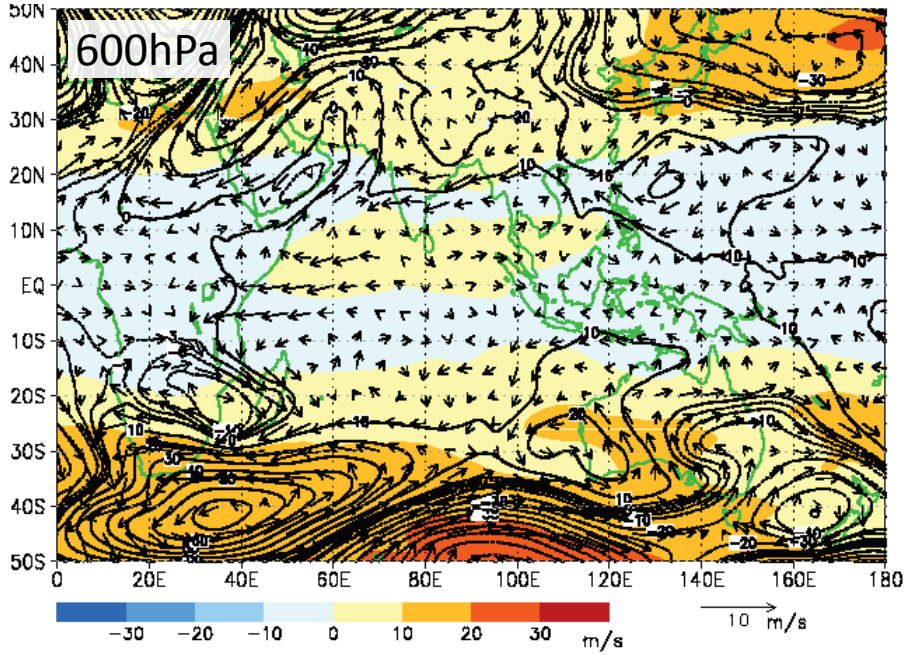

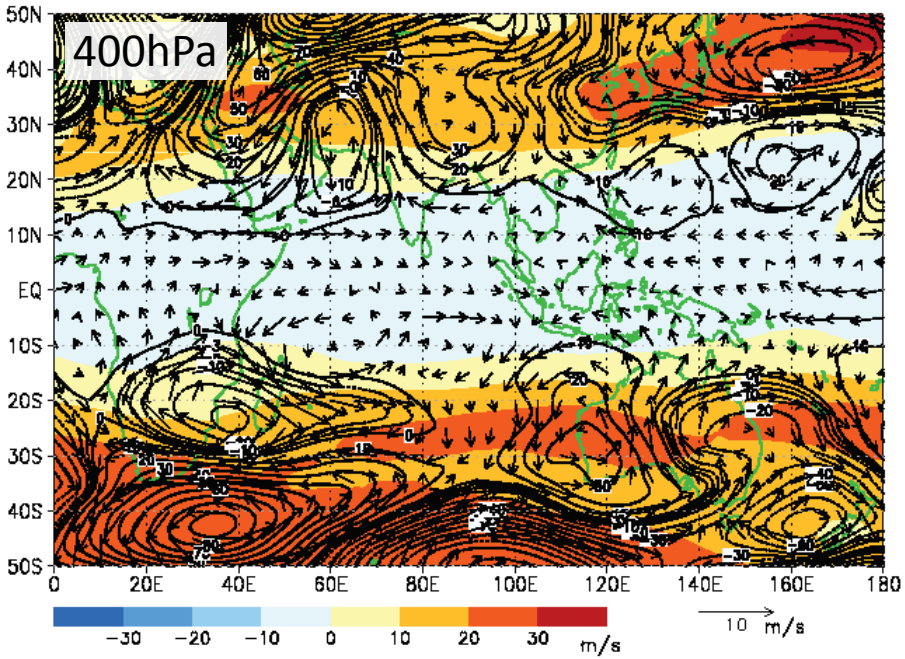

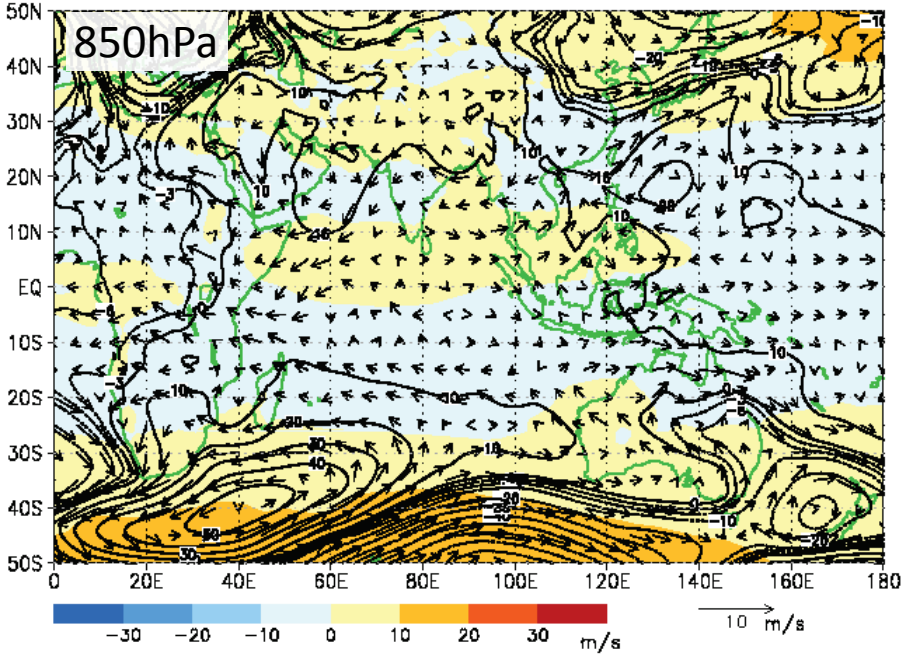

U (>80d), geopotential height & wind (20-80d)

MJO2 (9-14 nov)

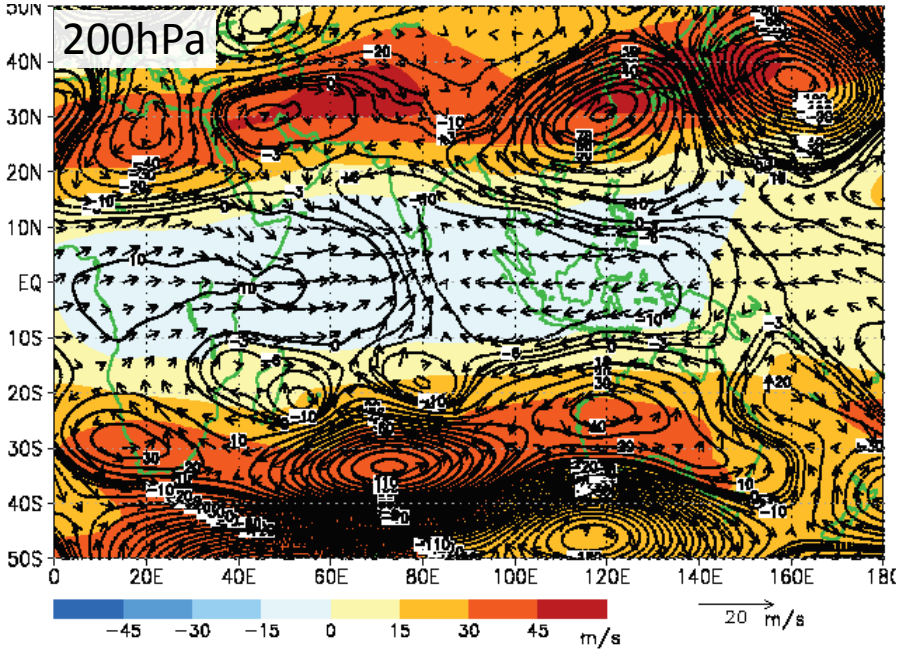

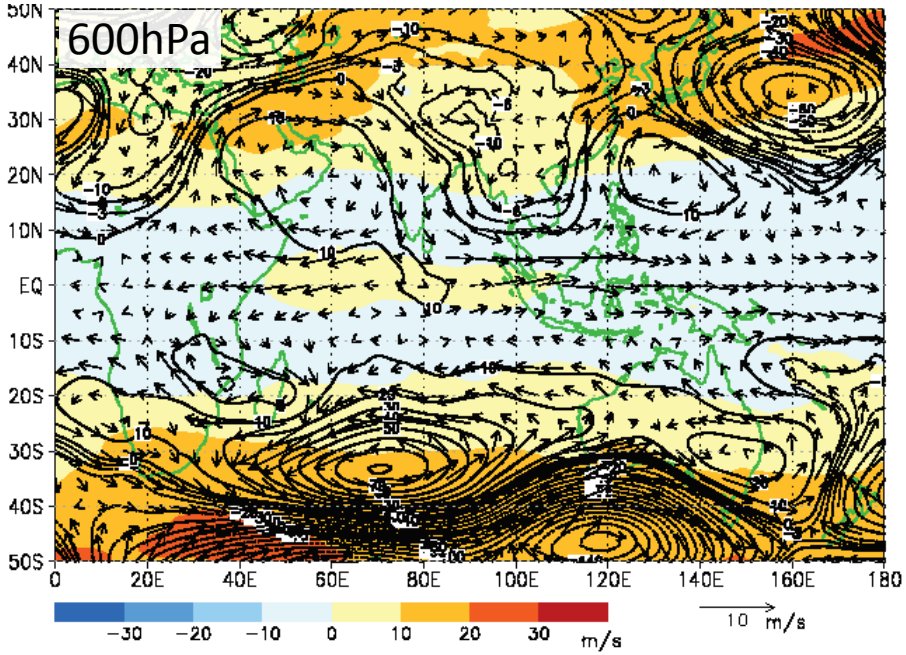

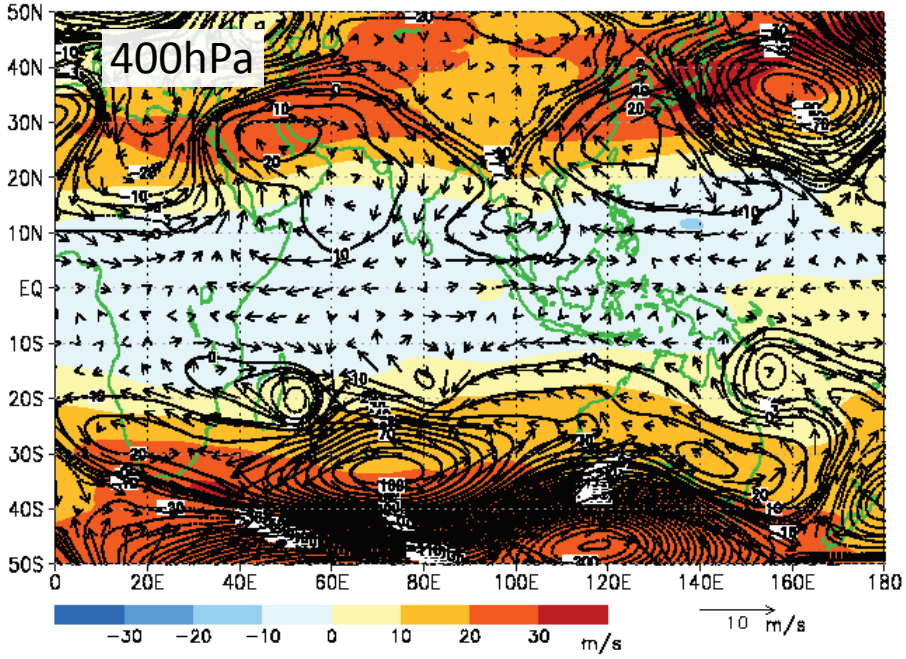

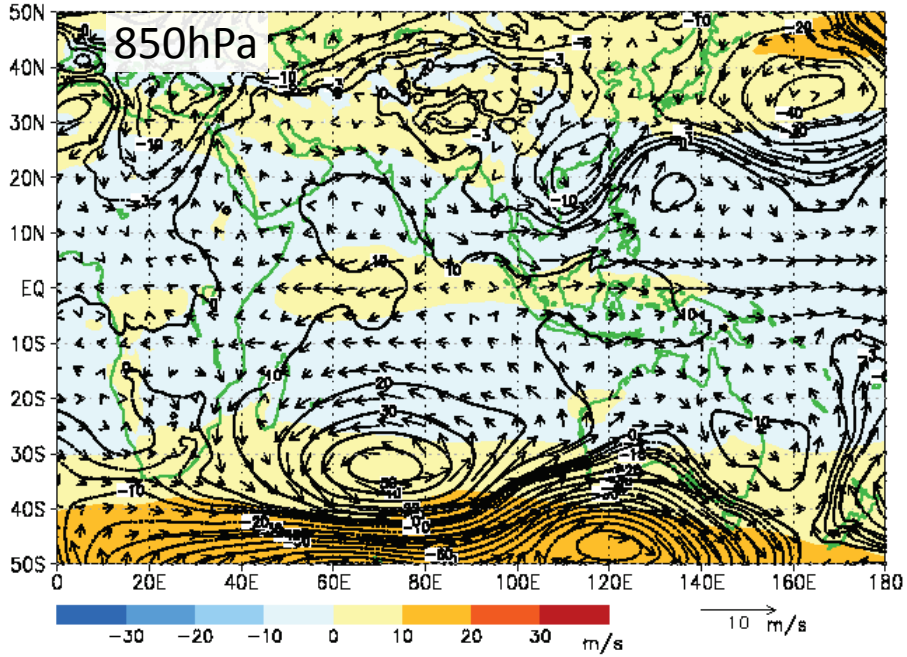

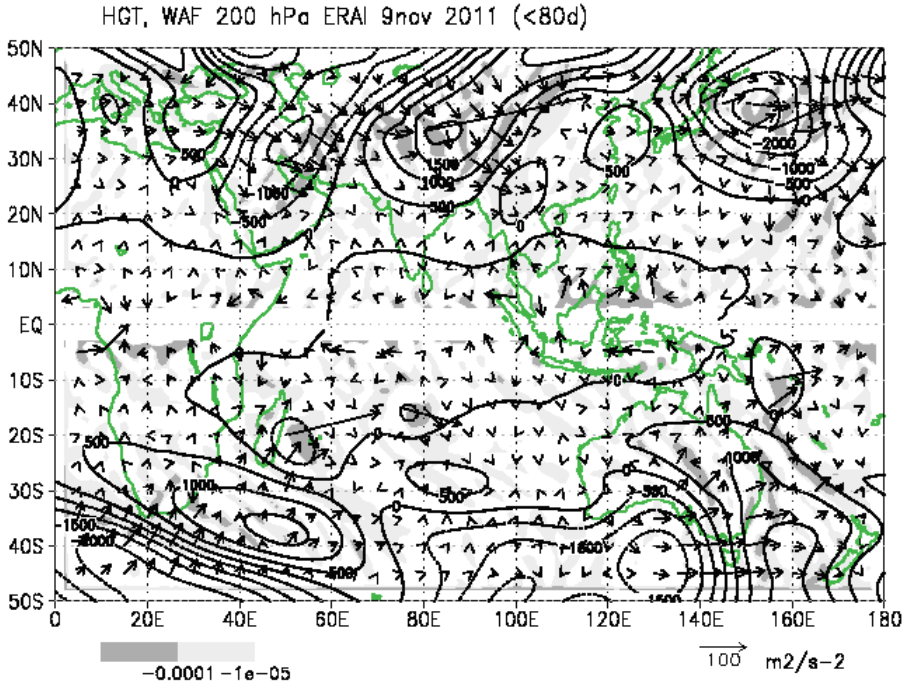
HGT, WAF 200 hPa ERAI 9nov 2011 (<80d)
50N
40N
30N
20N
10N
EQ
10S
20S
30S
40S
50S
0
20E
40E
60E
80E
100E
120E
140E
160E
180
-0.0001 -1e-05
100 m2/s-2

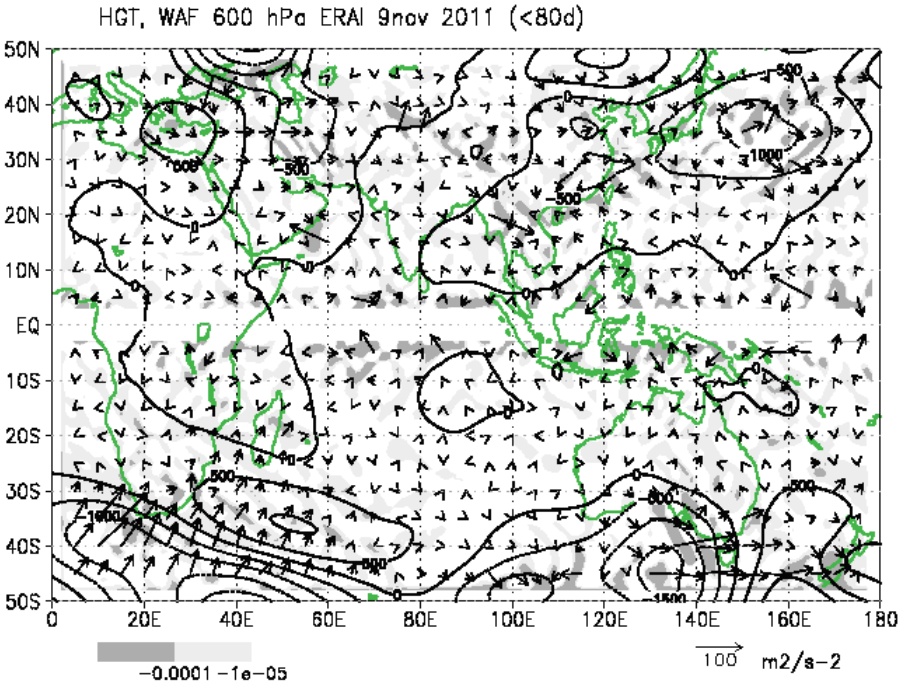
HGT, WAF 600 hPa ERAI 9nov 2011 (<80d)
50N
40N
30N
20N
10N
EQ
10S
20S
30S
40S
50S
0
20E
40E
60E
80E
100E
120E
140E
160E
180
-0.0001 -1e-05
100 m2/s-2

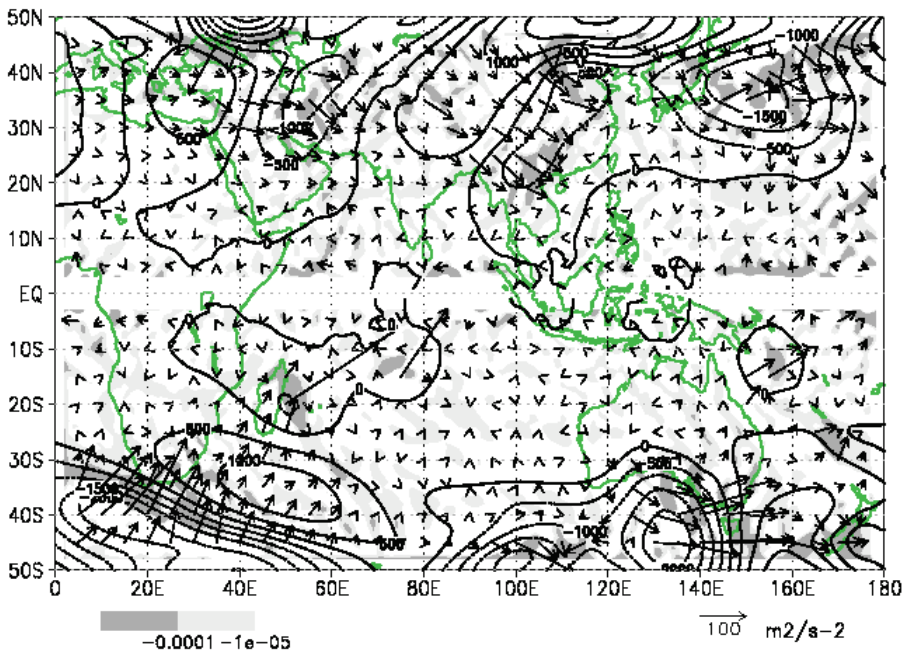
HGT, WAF 400 hPa ERAI 9nov 2011 (<80d)
50N
40N
30N
20N
10N
EQ
10S
20S
30S
40S
50S
0
20E
40E
60E
80E
100E
120E
140E
160E
180
-0.0001 -1e-05
100 m2/s-2

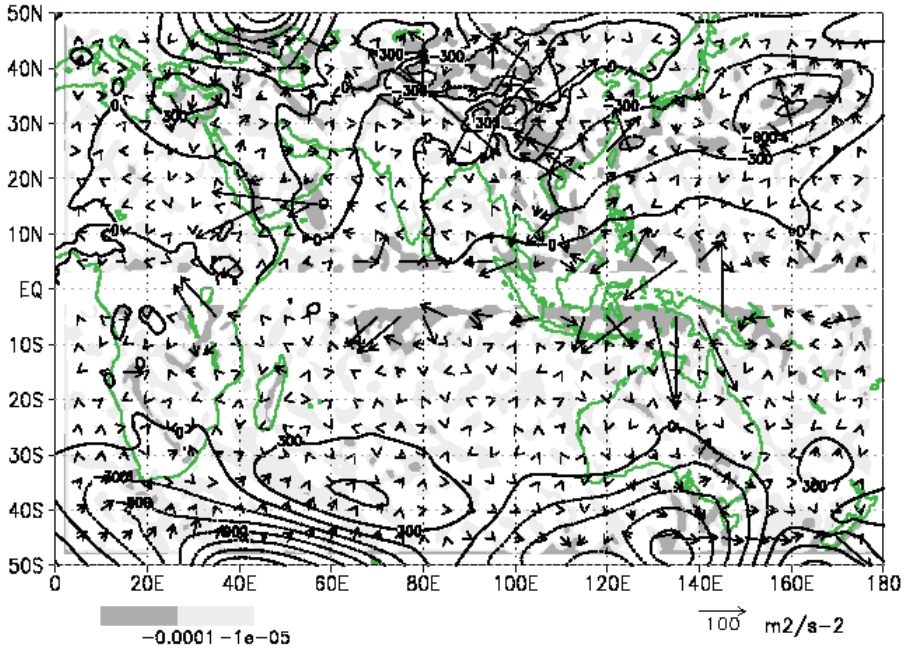
HGT, WAF 850 hPa ERAI 9nov 2011 (<80d)
50N
40N
30N
20N
10N
EQ
10S
20S
30S
40S
50S
0
20E
40E
60E
80E
100E
120E
140E
160E
180
-0.0001 -1e-05
100 m2/s-2

ERA-Interim Moisture advection **ISO + high-freq (<80d)** 60-90E, 10S-10N

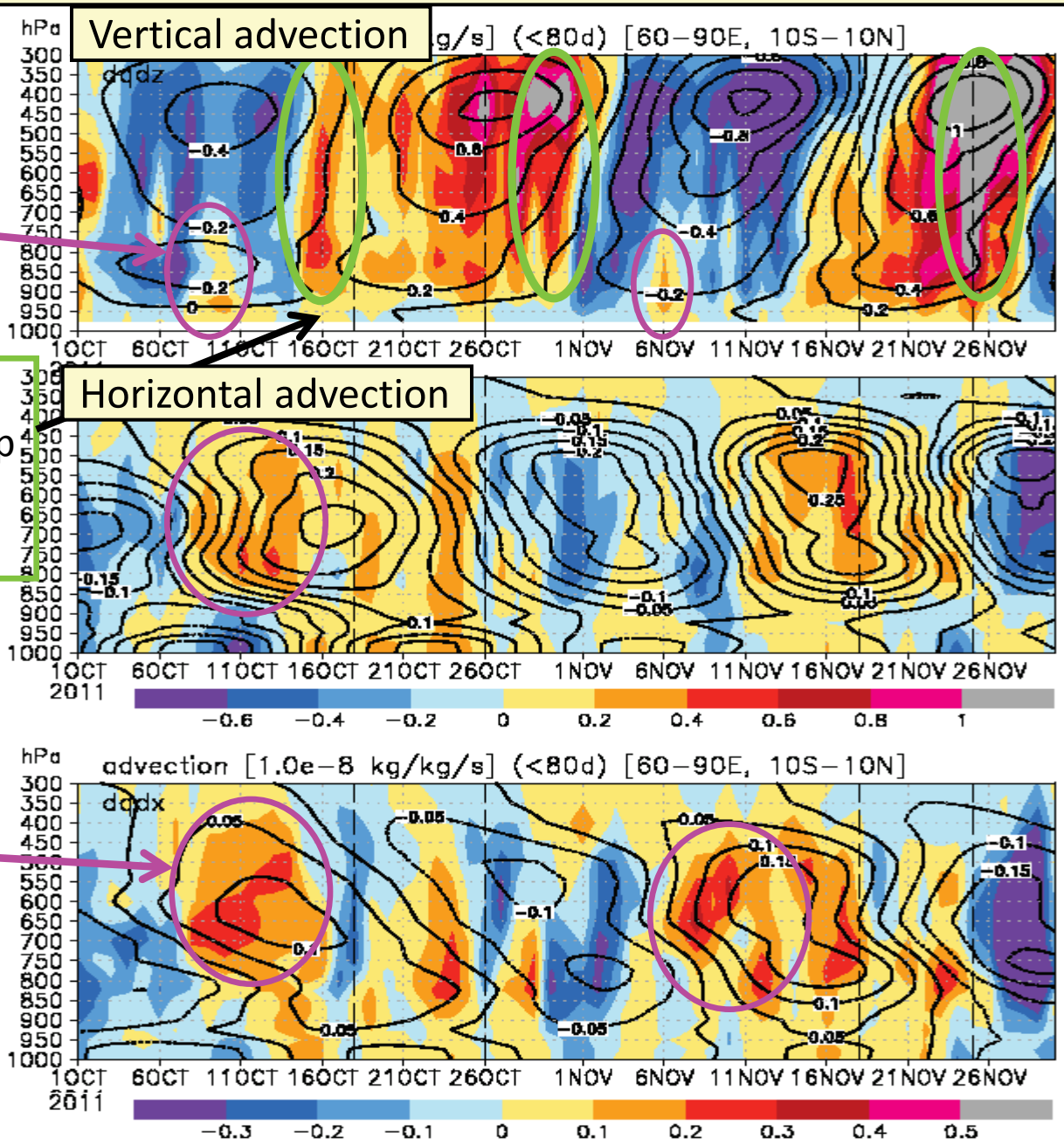

shallow convective events

Synchronization of high-freq deep convection (Kelvin ?)

mid-tropospheric zonal moisture advection

high-freq convection pronounced later stages

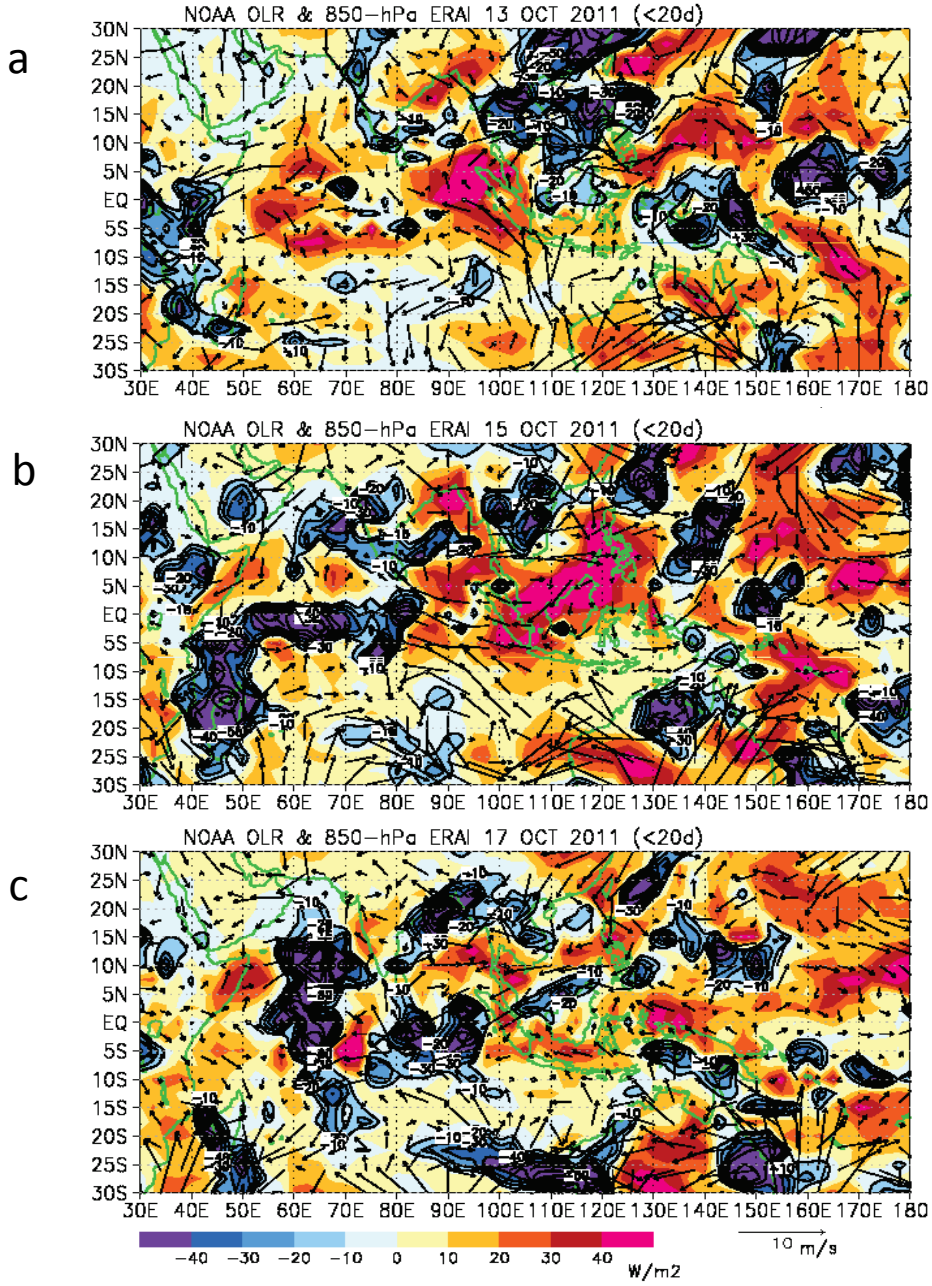

FIG. 18. Same as Fig. 3 except for high-frequency components on (a) 13 (b) 15 and (c) 17 October 2011

Spector analysis of NOAA OLR (15S-15N)

Combined Fourier-Wavelet Transform (CFWT) Kikuchi (2013)

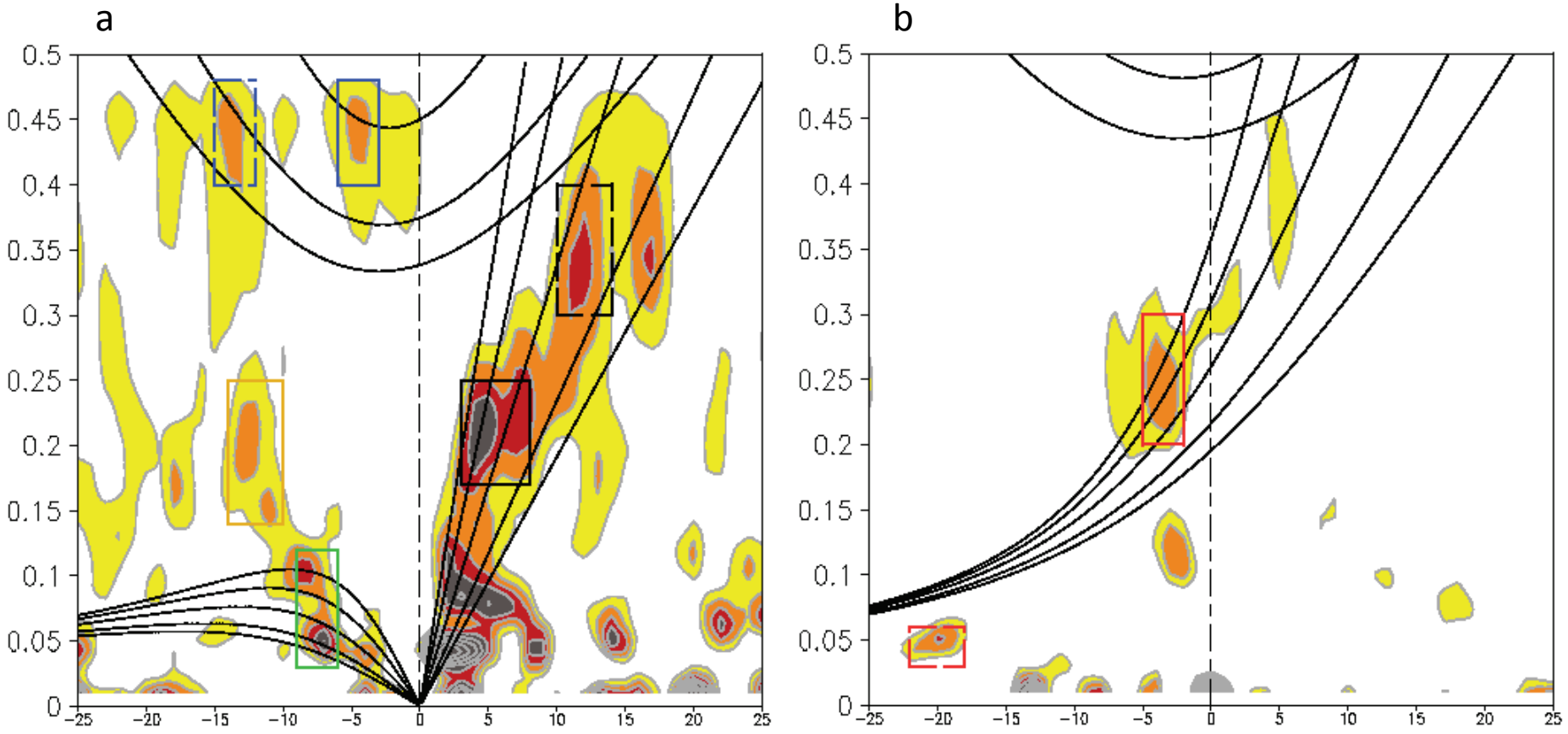

FIG. 19. Zonal wavenumber-frequency power spectrum of NOAA OLR for the equatorially (a) symmetric and (b) asymmetric components based on the CFWT, averaged in 15° S–15° N and normalized by the background spectrum (Kikuchi 2013)

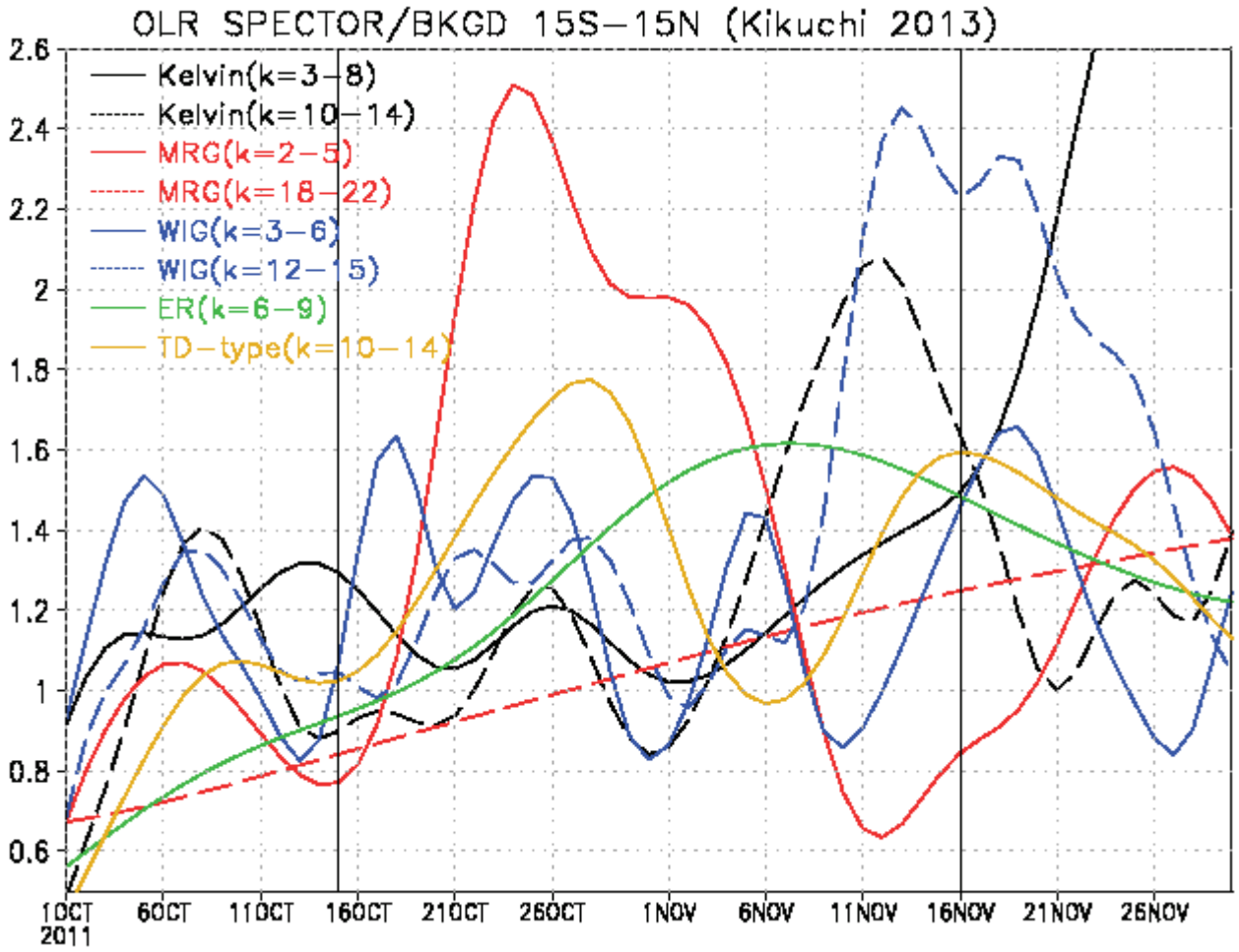

FIG. 20. Time series of the power of NOAA OLR in the specific zonal wavenumber-frequency domains marked in Fig. 19: Equatorial Kelvin waves (black lines), mixed Rossby-gravity wave (red lines), westward inertia-gravity waves (blue lines), equatorial Rossby waves (green line), and tropical repression type waves (yellow line). Solid (dashed) lines indicate lower (higher) zonal wavenumber components.

Decomposition of horizontal moisture advection

Zhao et al. 2013

$$\left(\frac{\partial q}{\partial t}\right)' = \left(-V\nabla q\right)' + \left(-\omega\frac{\partial q}{\partial p}\right)' + \left(-\frac{Q_2}{L}\right)'$$

60-90E, 10S-10N

$$u=\bar{u}+u'+u^* \quad , \quad v=\bar{v}+v'+v^* \quad q=\bar{q}+q'+q^*$$

overbar: >80 day (basic state) prime: 20-80 day (ISO) asterisk: < 20 day (high-freq)

$(-\bar{V}\cdot\nabla\bar{q})'$ 1 $(-\bar{V}\cdot\nabla q')'$ 2 $(-\bar{V}\cdot\nabla q^*)'$ 3 $(-V'\cdot\nabla\bar{q})'$ 4 $(-V'\cdot\nabla q')'$ 5 $(-V'\cdot\nabla q^*)'$ 6 $(-V^*\cdot\nabla\bar{q})'$ 7 $(-V^*\cdot\nabla q')'$ 8 $(-V^*\cdot\nabla q^*)'$ 9

400-750hPa MJO1 750-1000hPa 400-750hPa MJO2 750-1000hPa

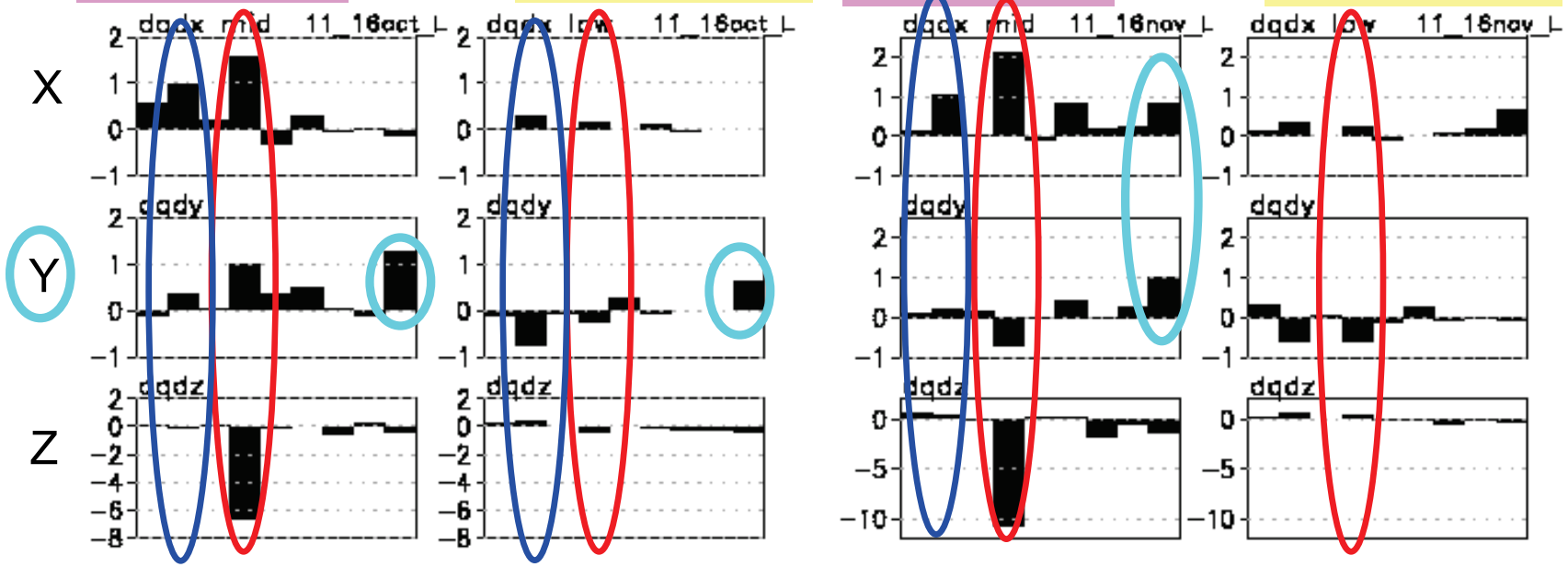

high-freq x high-freq in the meridional component

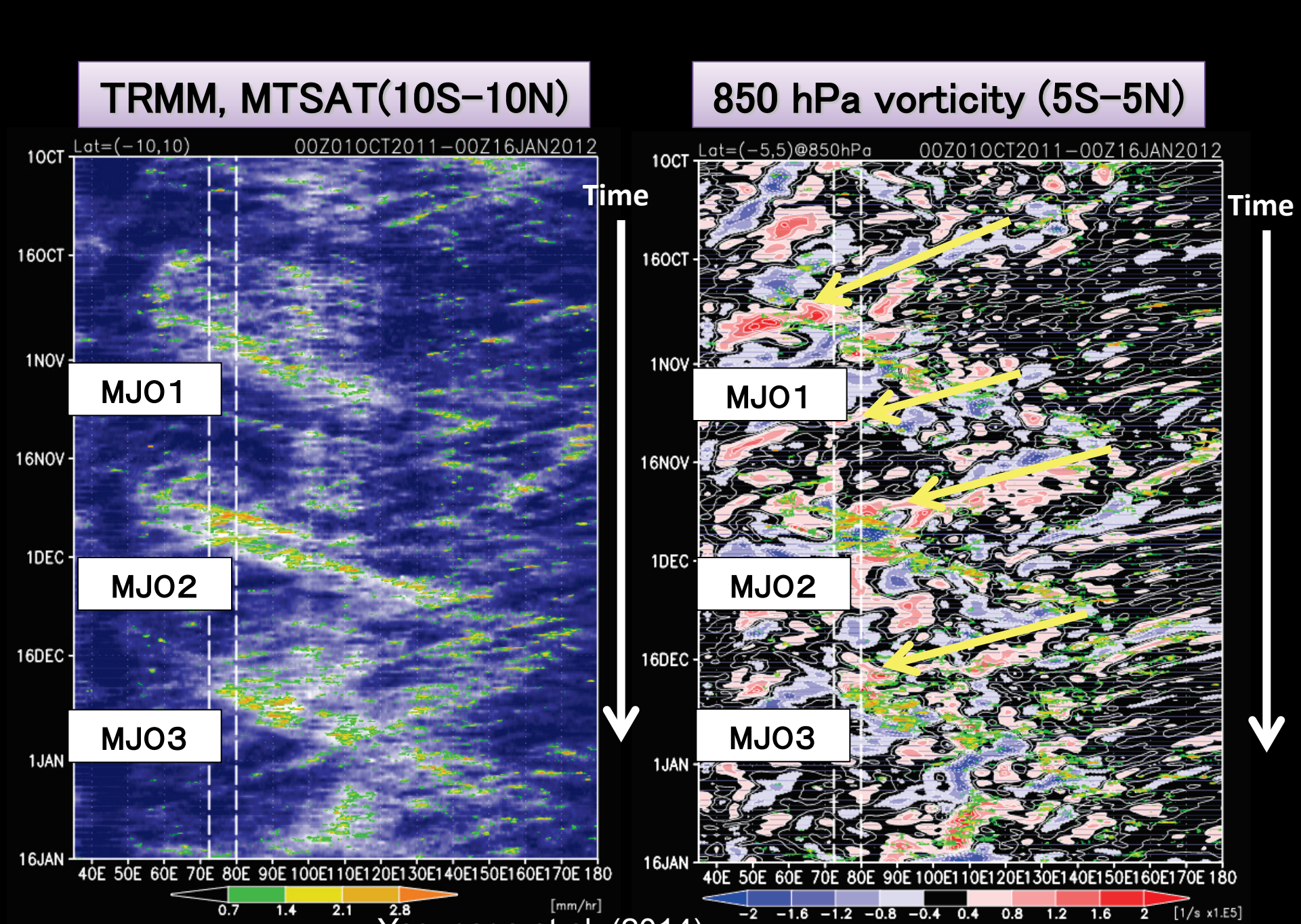

Yasunaga et al. (2014)

Summary and future work

- Horizontal advection of mid-tropospheric moisture by easterly anomalies were detected both in MJO1 and in MJO2.
- The easterly anomalies appear to be associated with extratropical wave trains that intruded into the equatorial region. This suggests contribution of dry dynamics to the moist processes in MJO.
- The different conditions between the two cases (drier condition in MJO1 than in MJO2) may lead to the difference in the vertical evolution (slower in MJO1 than in MJO2) and the contributions from high-frequency disturbances (e.g., equarial waves, transient eddies).
- Evaluation of high-frequency effects (e.g., diabatic heating, CCEWs) using outputs of global cloud-system-resolving simulations is underway.

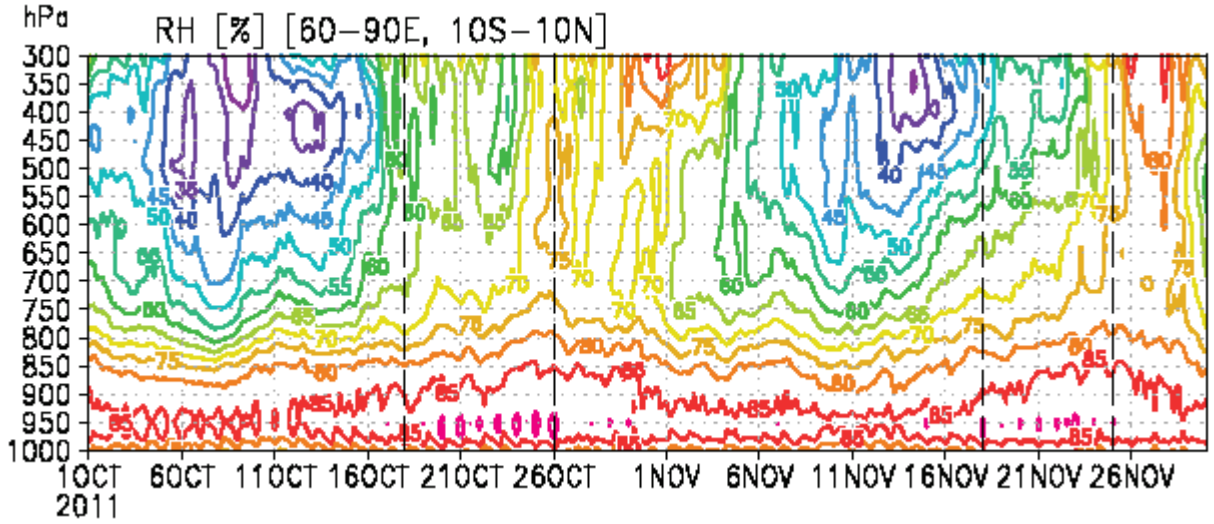

FIG. S2. Time-height sections of relative humidity (ERA-interim) averaged in the 60-90E, 10S-10N domain.

Backup slides

25-90 bandpass filtered fields 15S-15N

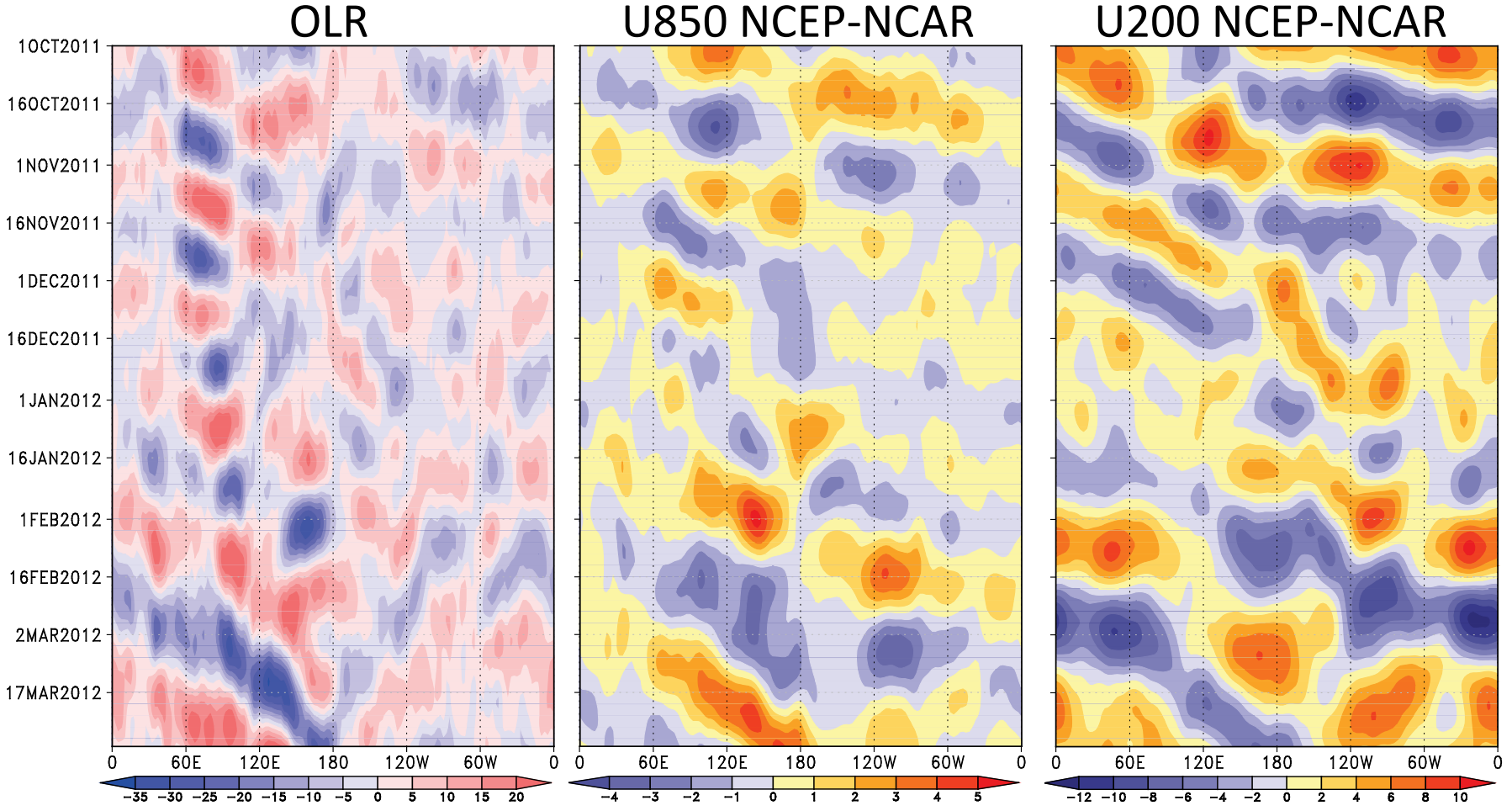

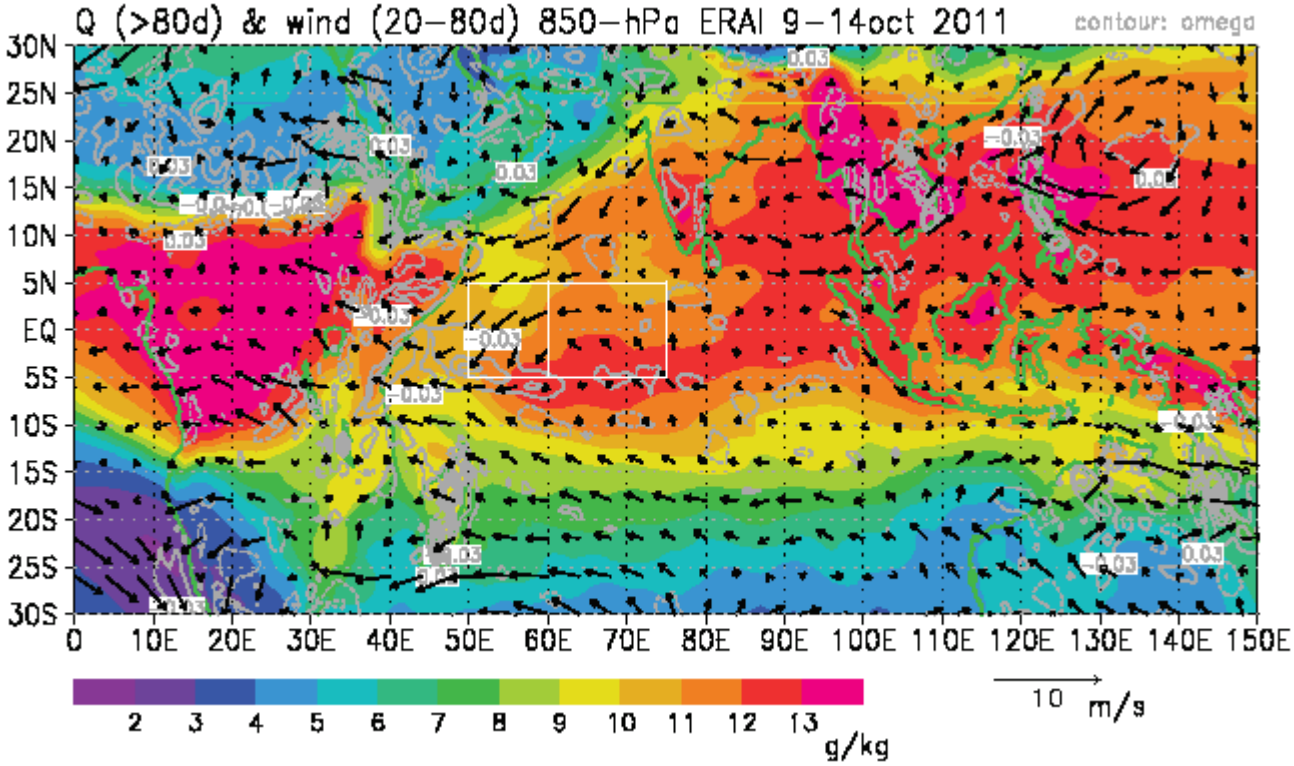

FIG. 12. Horizontal distributions of low-frequency (>80-day) moisture and intraseasonal (20-80 day) wind vectors (a) at 600-hPa in the preconditioning stage and (b) at 850 hPa in the convection initiation period of MJO1. Squares indicate MJO convection initiation region 1.

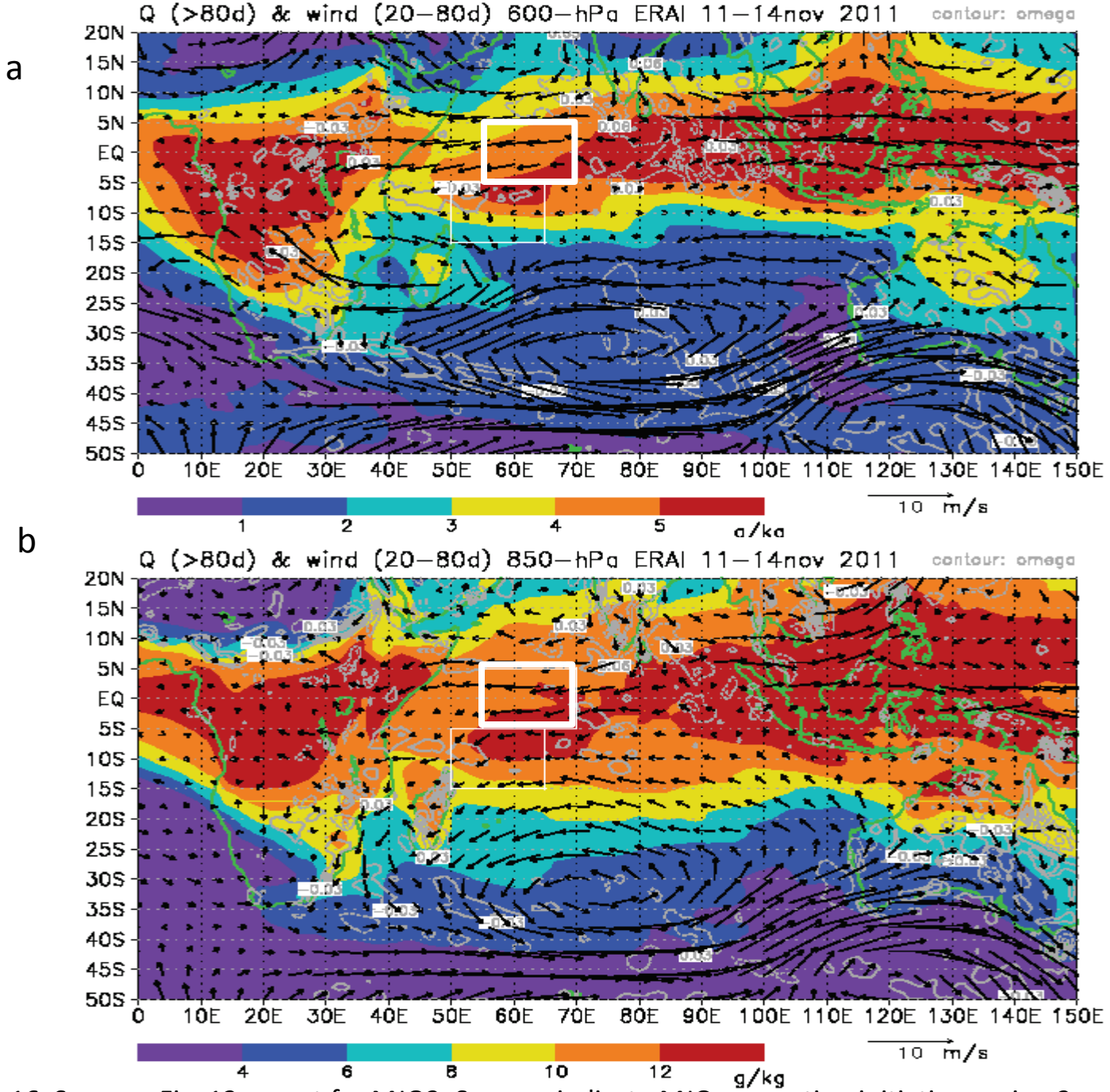

FIG. 16. Same as Fig. 12 except for MJO2. Squares indicate MJO convection initiation region 2.

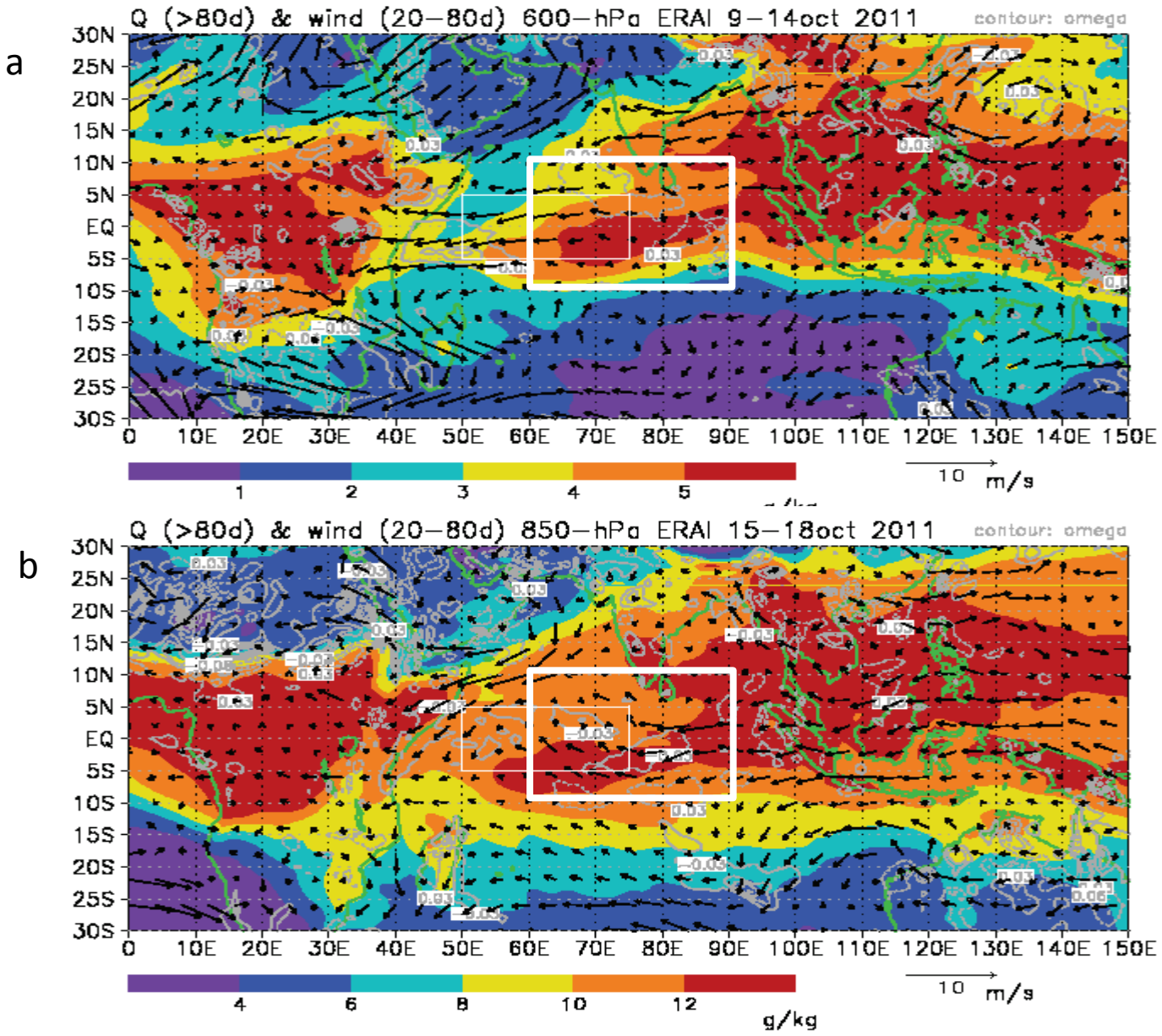

FIG. 12. Horizontal distributions of low-frequency (>80-day) moisture and intraseasonal (20-80 day) wind vectors (a) at 600-hPa in the preconditioning stage and (b) at 850 hPa in the convection initiation period of MJO1. Squares indicate MJO convection initiation region 1.

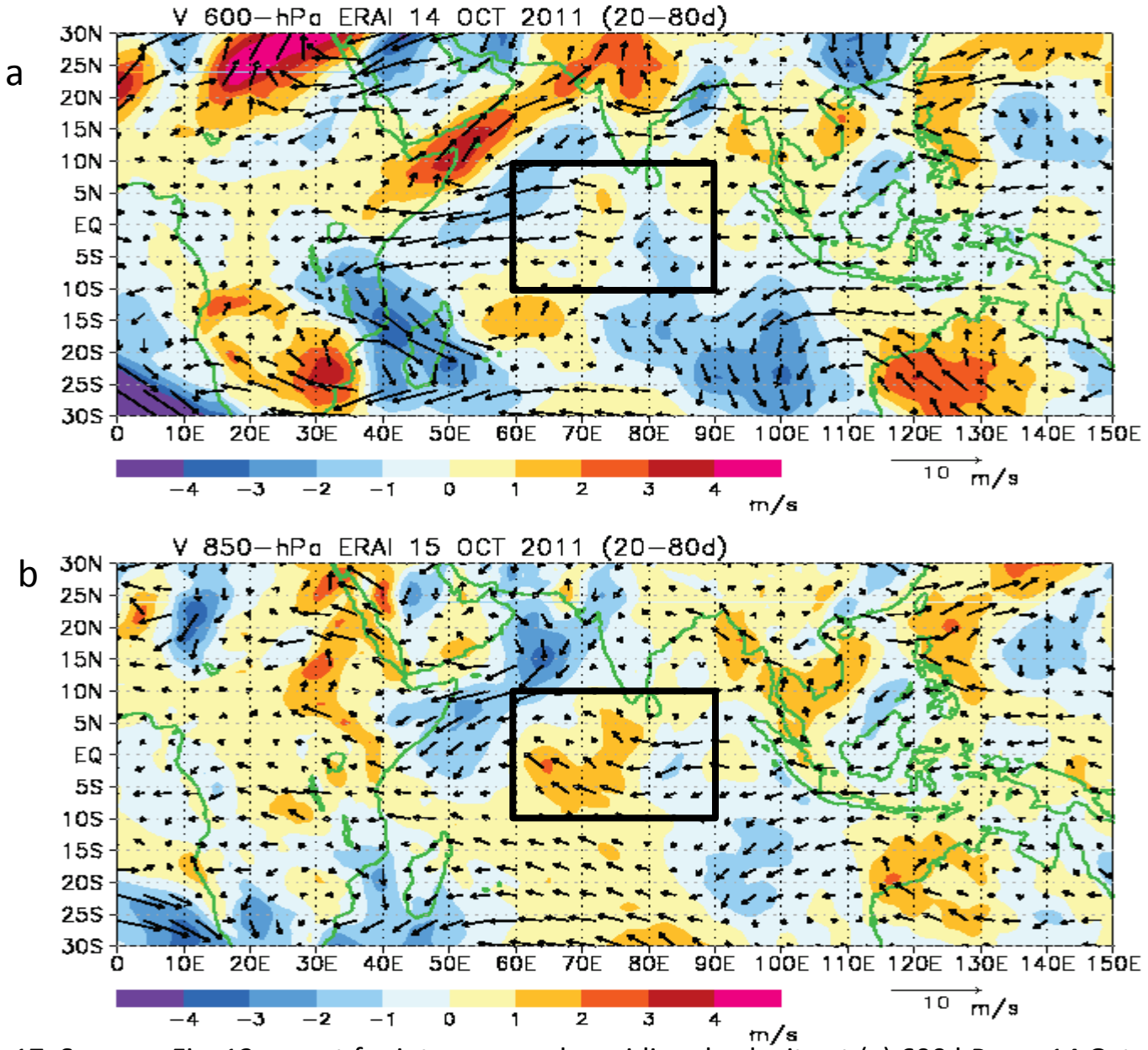

FIG. 17. Same as Fig. 12 except for intraseasonal meridional velocity at (a) 600 hPa on 14 October and (b) 850 hPa on 15 October.

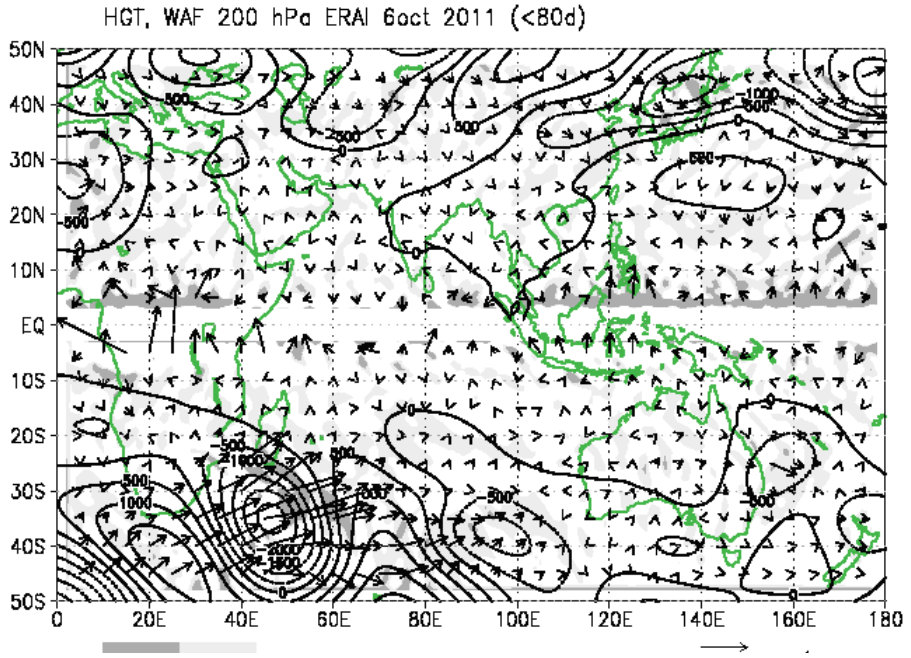
HGT, WAF 200 hPa ERAI 6oct 2011 (<80d)
50N
40N
30N
20N
10N
EQ
10S
20S
30S
40S
50S
0
20E
40E
60E
80E
100E
120E
140E
160E
180

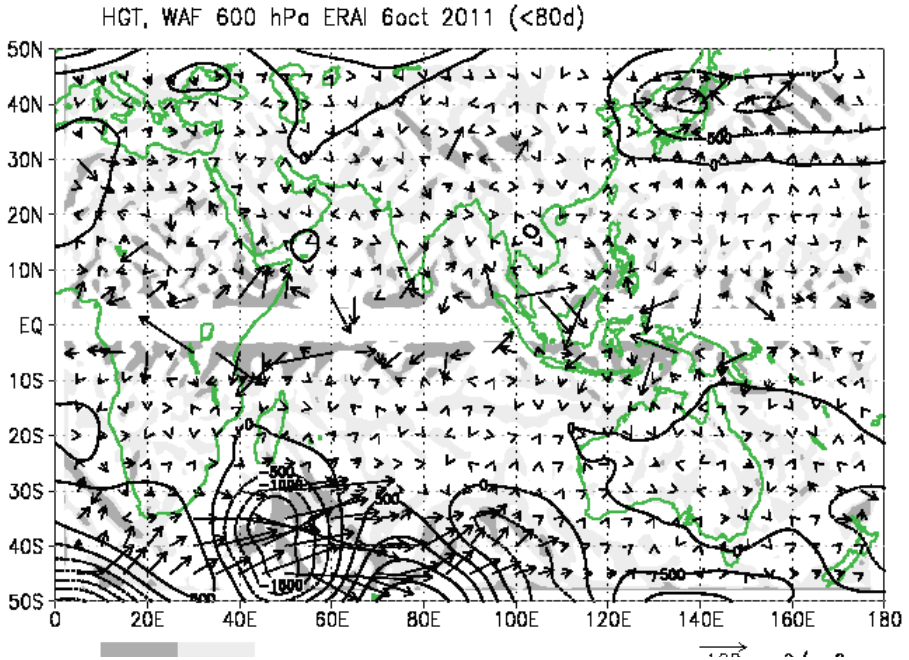
HGT, WAF 600 hPa ERAI 6oct 2011 (<80d)
50N
40N
30N
20N
10N
EQ
10S
20S
30S
40S
50S
0
20E
40E
60E
80E
100E
120E
140E
160E
180

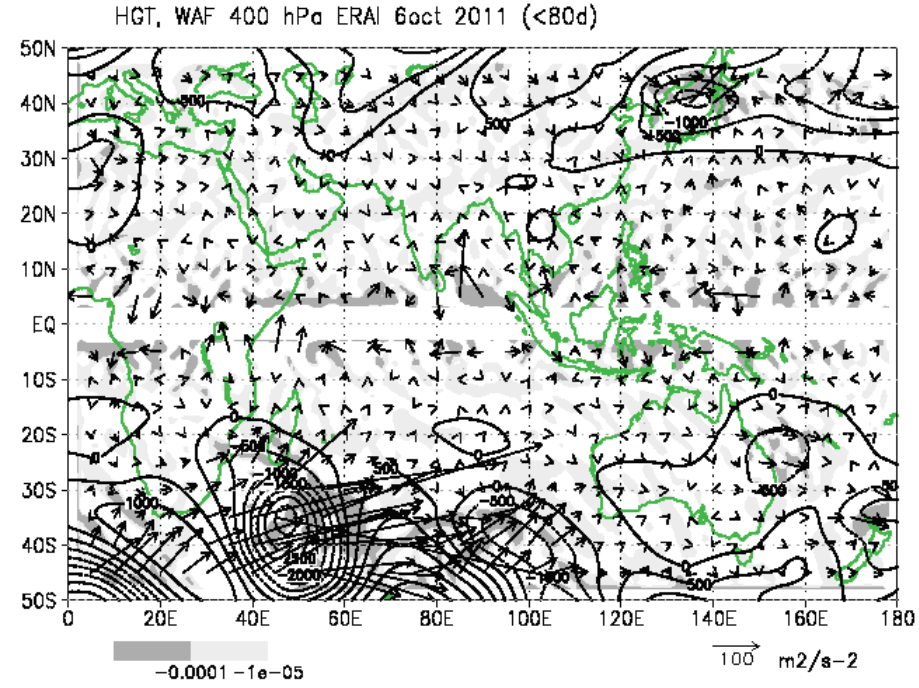
HGT, WAF 400 hPa ERAI 6oct 2011 (<80d)
50N
40N
30N
20N
10N
EQ
10S
20S
30S
40S
50S
0
20E
40E
60E
80E
100E
120E
140E
160E
180
100 m2/s-2
-0.0001 -1e-05

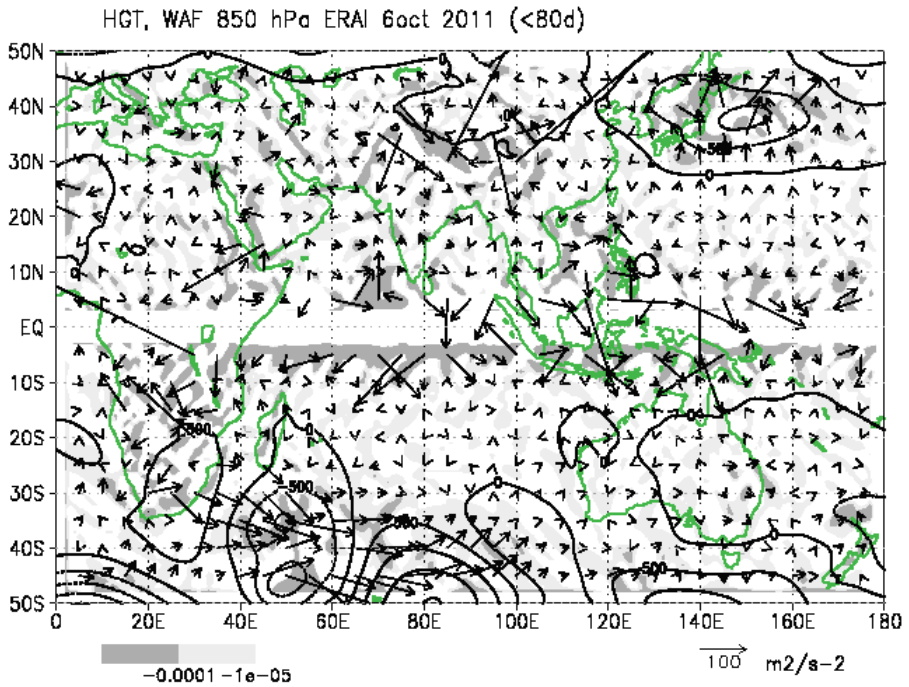
HGT, WAF 850 hPa ERAI 6oct 2011 (<80d)
50N
40N
30N
20N
10N
EQ
10S
20S
30S
40S
50S
0
20E
40E
60E
80E
100E
120E
140E
160E
180
100 m2/s-2
-0.0001 -1e-05

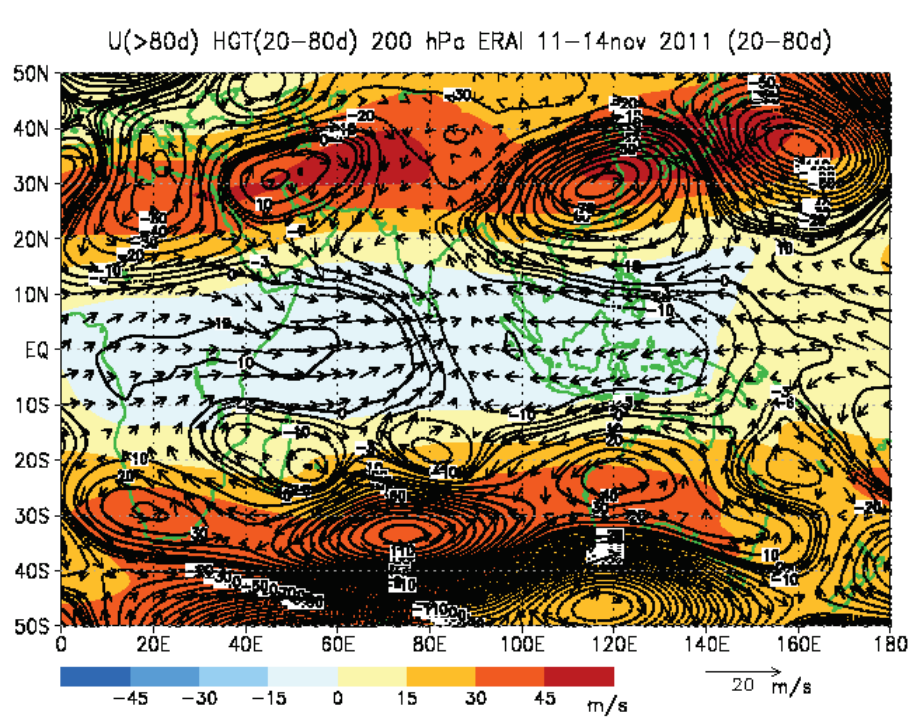
U(>80d) HGT(20-80d) 200 hPa ERAI 11-14nov 2011 (20-80d)
50N
40N
30N
20N
10N
EQ
10S
20S
30S
40S
50S
0
20E
40E
60E
80E
100E
120E
140E
160E
180
-45 -30 -15 0 15 30 45
m/s
20 m/s

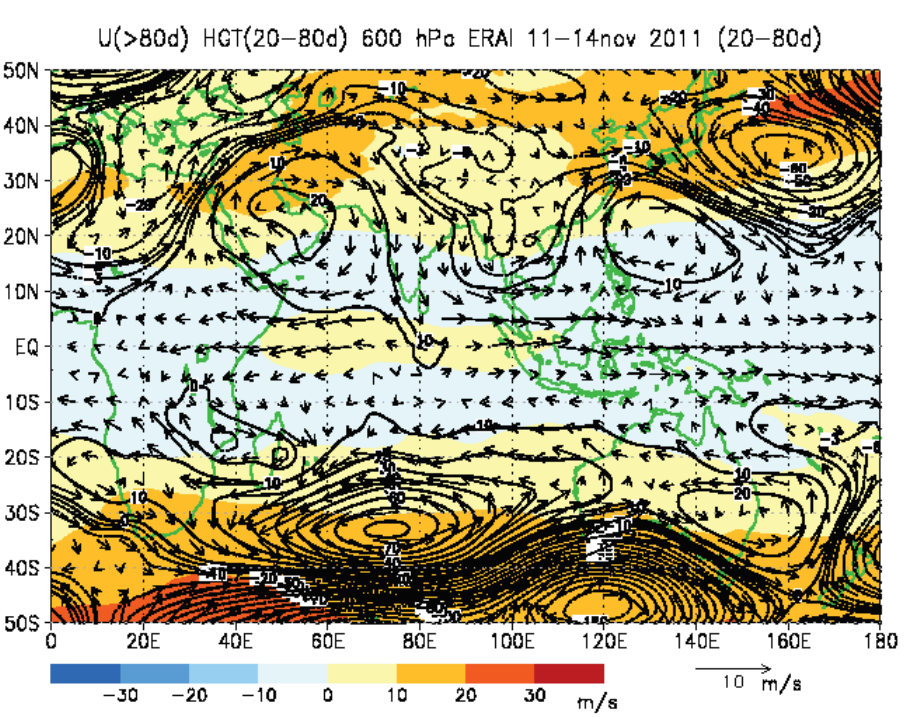
U(>80d) HGT(20-80d) 600 hPa ERAI 11-14nov 2011 (20-80d)
50N
40N
30N
20N
10N
EQ
10S
20S
30S
40S
50S
0
20E
40E
60E
80E
100E
120E
140E
160E
180
-30 -20 -10 0 10 20 30
m/s
10 m/s

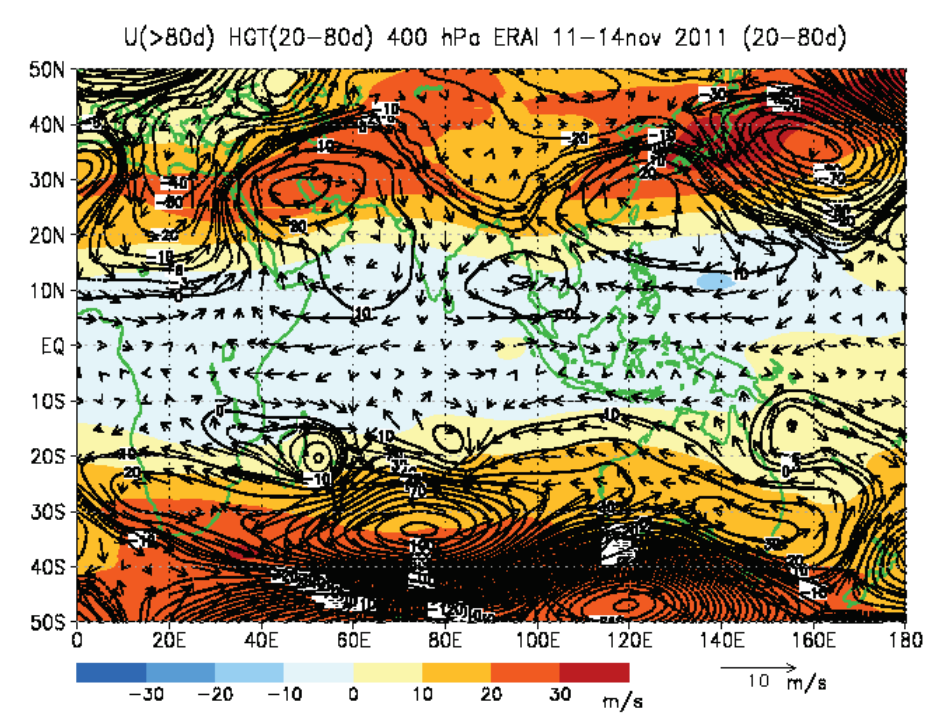
U(>80d) HGT(20-80d) 400 hPa ERAI 11-14nov 2011 (20-80d)
50N
40N
30N
20N
10N
EQ
10S
20S
30S
40S
50S
0
20E
40E
60E
80E
100E
120E
140E
160E
180
-30 -20 -10 0 10 20 30
m/s
10 m/s

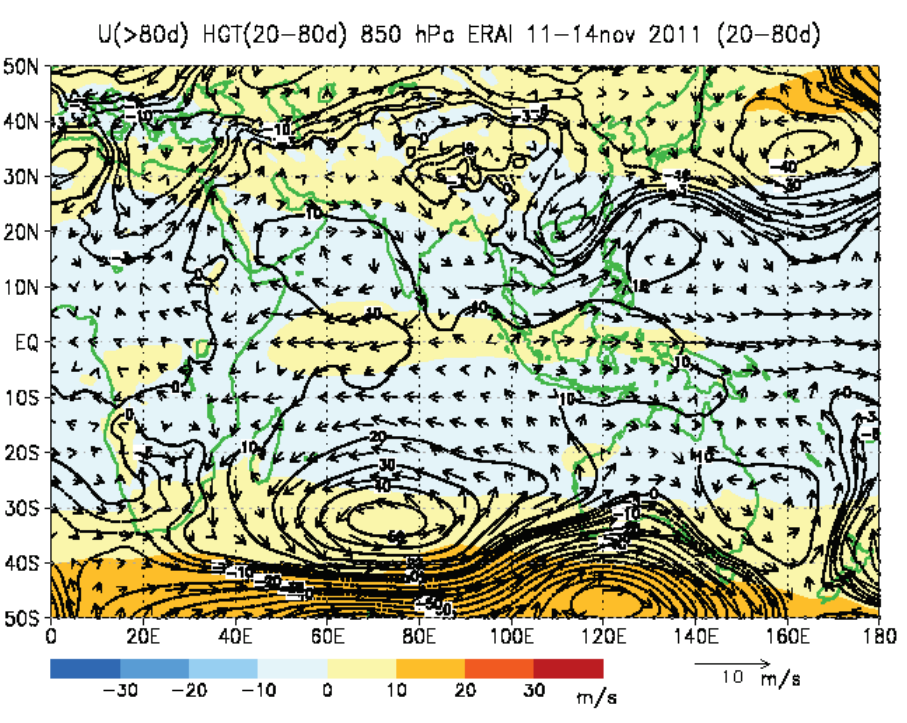
U(>80d) HGT(20-80d) 850 hPa ERAI 11-14nov 2011 (20-80d)
50N
40N
30N
20N
10N
EQ
10S
20S
30S
40S
50S
0
20E
40E
60E
80E
100E
120E
140E
160E
180
-30 -20 -10 0 10 20 30
m/s
10 m/s

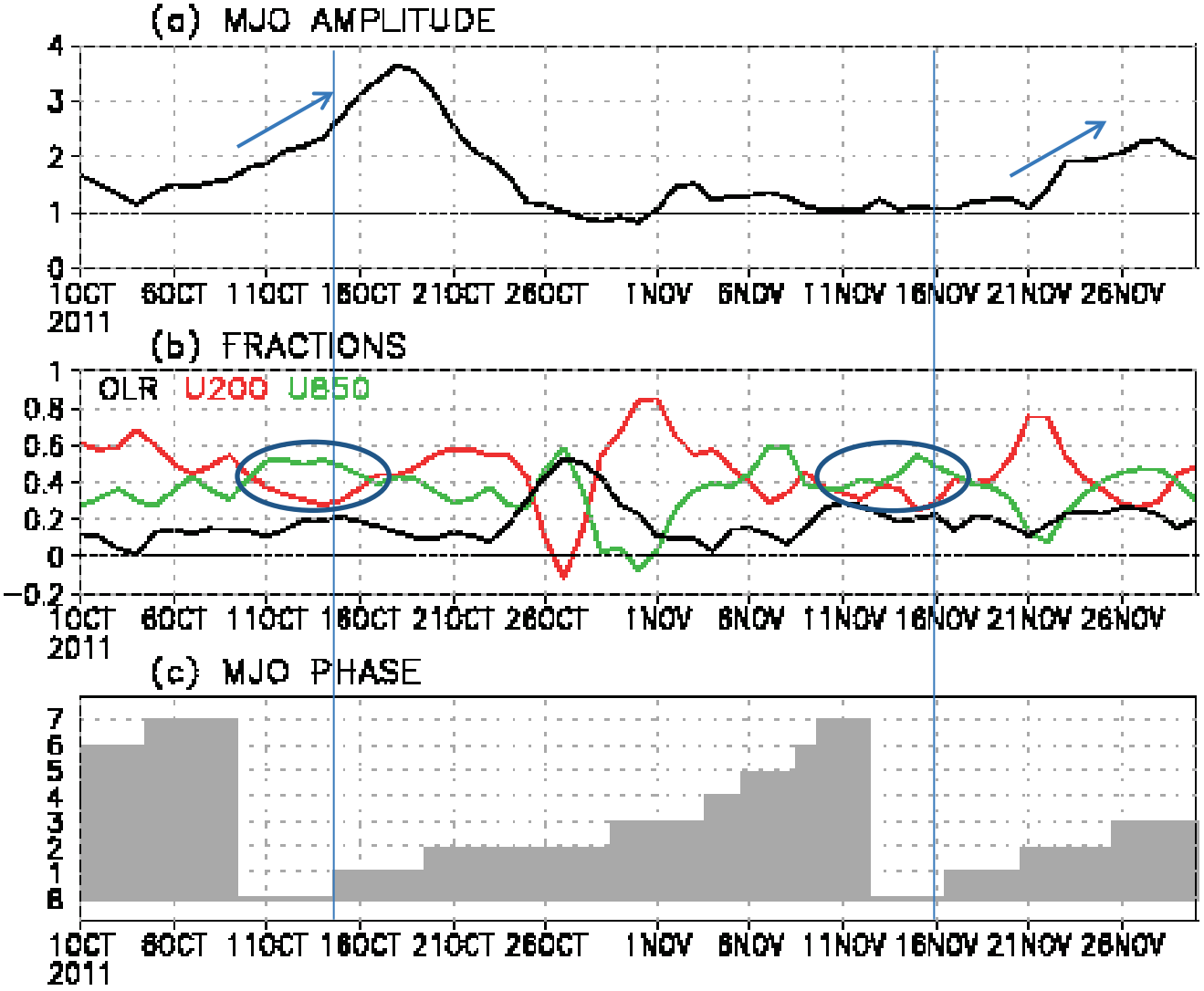

FIG. 2. Time series of (a).MJO amplitude, (b) fractions of OLR (black line), U850 (green line), and U200 (red line), (c) MJO phase based on WH2004. NCEP=NCAR reanalysis data are used. (CAWR web site)

Decomposition of horizontal moisture advection

Zhao et al. 2012

$$u=\bar{u}+u'+u^* \ , \quad v=\bar{v}+v'+v^* \qquad q=\bar{q}+q'+q^*$$

a bar: low-frequency background state (LFBS, > 90 days)

a prime: intraseasonal (20-90-day) component

a star: higher frequency component (< 20 days)

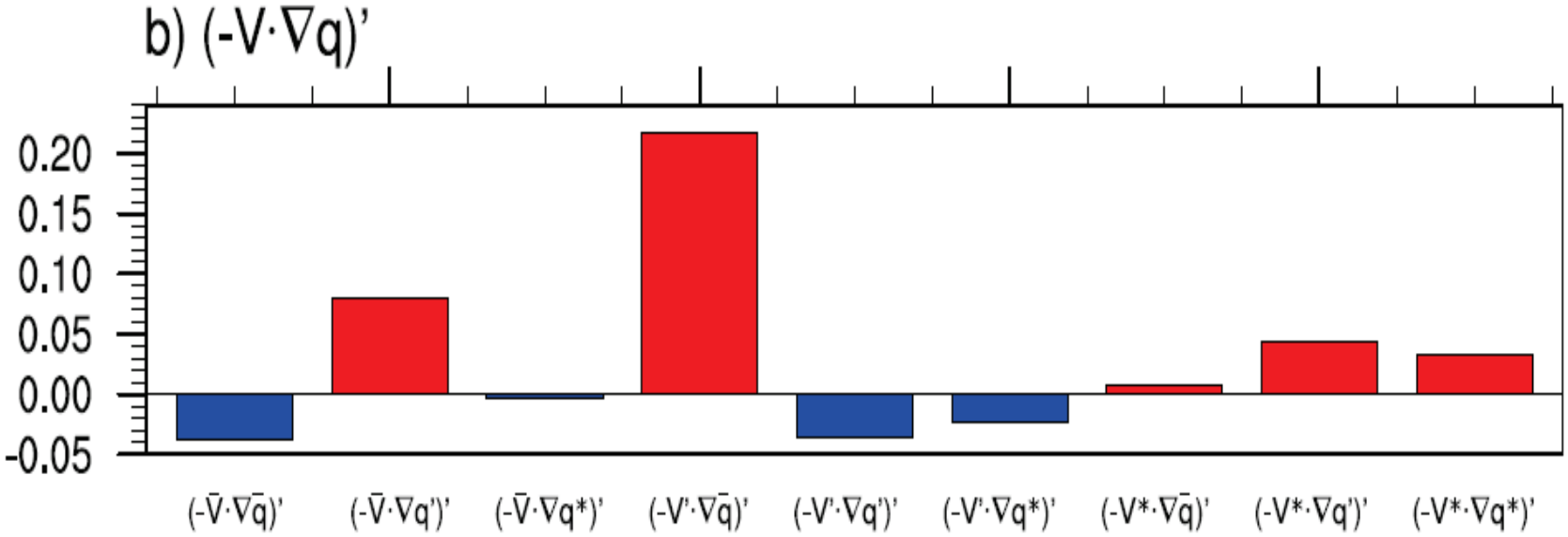

→ The largest terms are the advection of **the mean moisture by the MJO flow** ($-V'\cdot\nabla\bar{q}$) and the advection of **MJO perturbation moisture by the background flow** ($-\bar{V}\cdot\nabla q'$)

Vertically integrated (1000-700hPa) moisture budget analysis

Zhao et al. 2012

$$\left(\frac{\partial q}{\partial t}\right)' = (-V\nabla q)' + (-\omega\frac{\partial q}{\partial p})' + (-\frac{Q_2}{L})'$$

Integrated from **1000 to 700 hPa** **during the initiation period from day -25 to -15** over **50-70E, 20S-EQ**

A prima represents intraseasonal (20-90-day) timescale

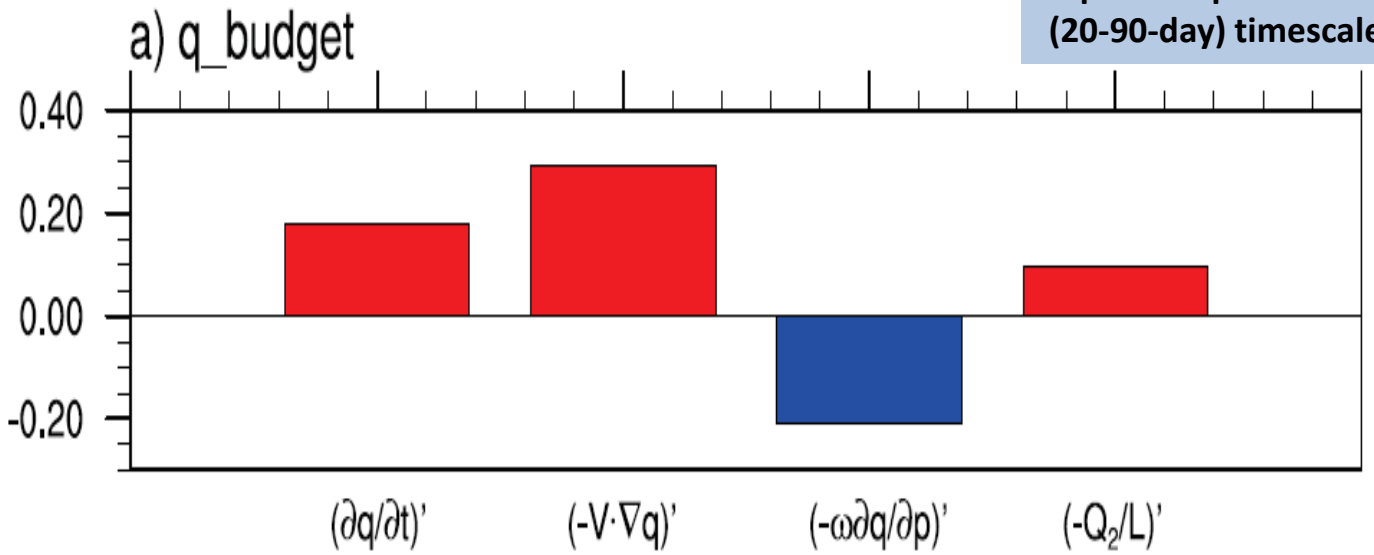

From left to right: **ISO humidity tendency, horizontal advection, vertical advection, apparent moisture source**

anomalous descending motion => **reduces the mean precipitation**

=>**less condensational heating** => **more moisture retained in the atmosphere**

Vertically-integrated heat budget analysis

Zhao et al. 2012

$$(\frac{\partial T}{\partial t})' = (-V\nabla T)' + (\omega\frac{RT}{c_p p} - \omega\frac{\partial T}{\partial p})' + (Q_1/c_p)'$$

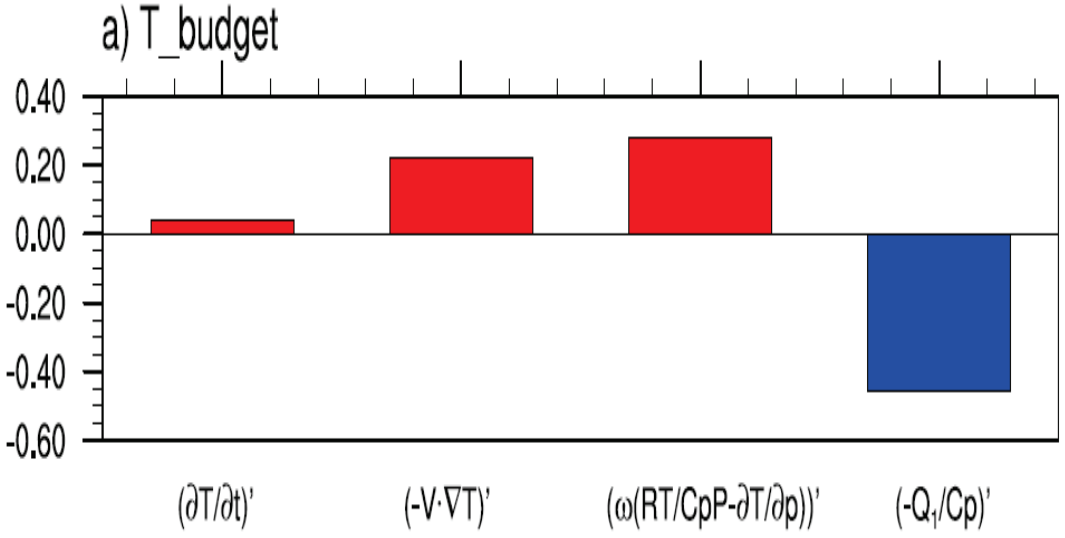

← Descending-induced adiabatic warming is largely offset by diabatic cooling.

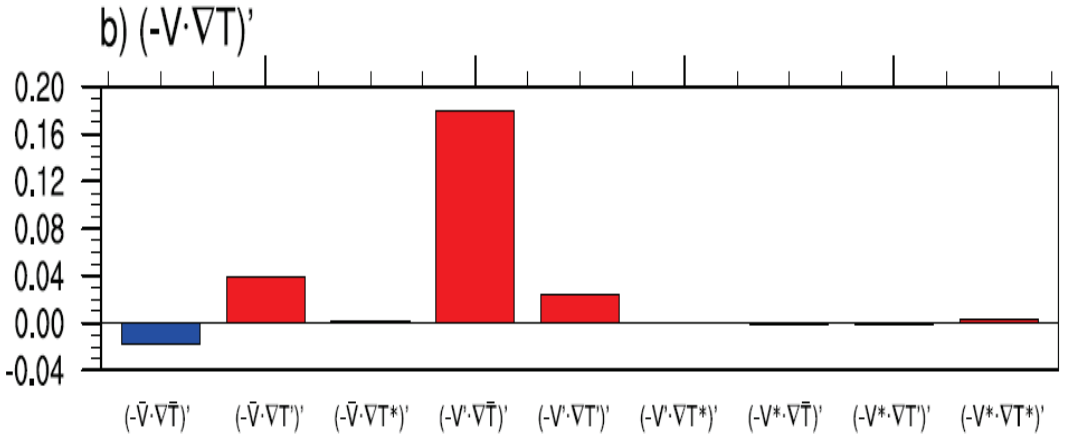

Horizontal advection is primarily attributed to advection of the mean temperature by MJO flow.

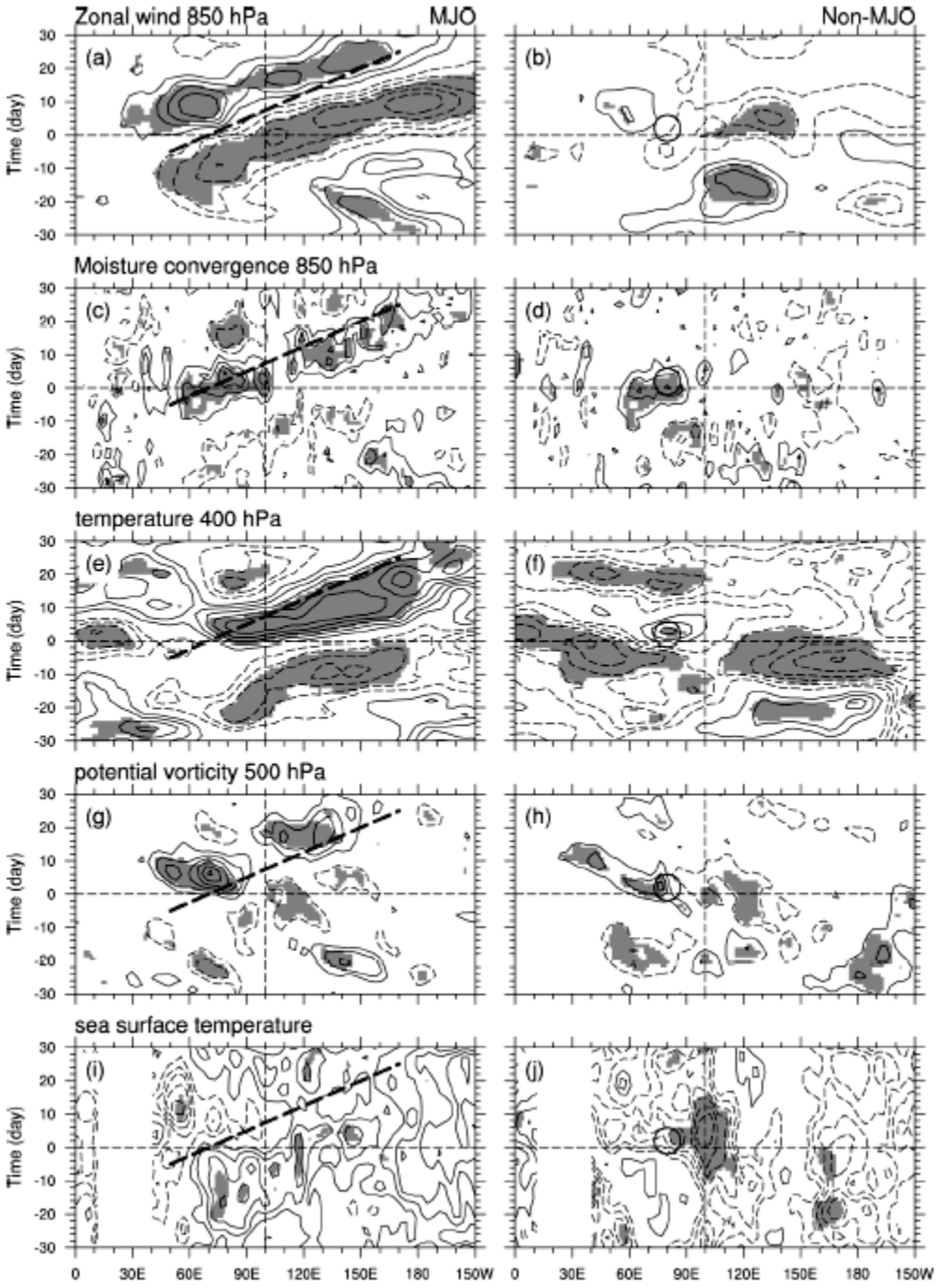

Ling et al (2013)

MJO-1 Sept 30 – Oct 15

MJO-1 Oct 15 – Oct 25

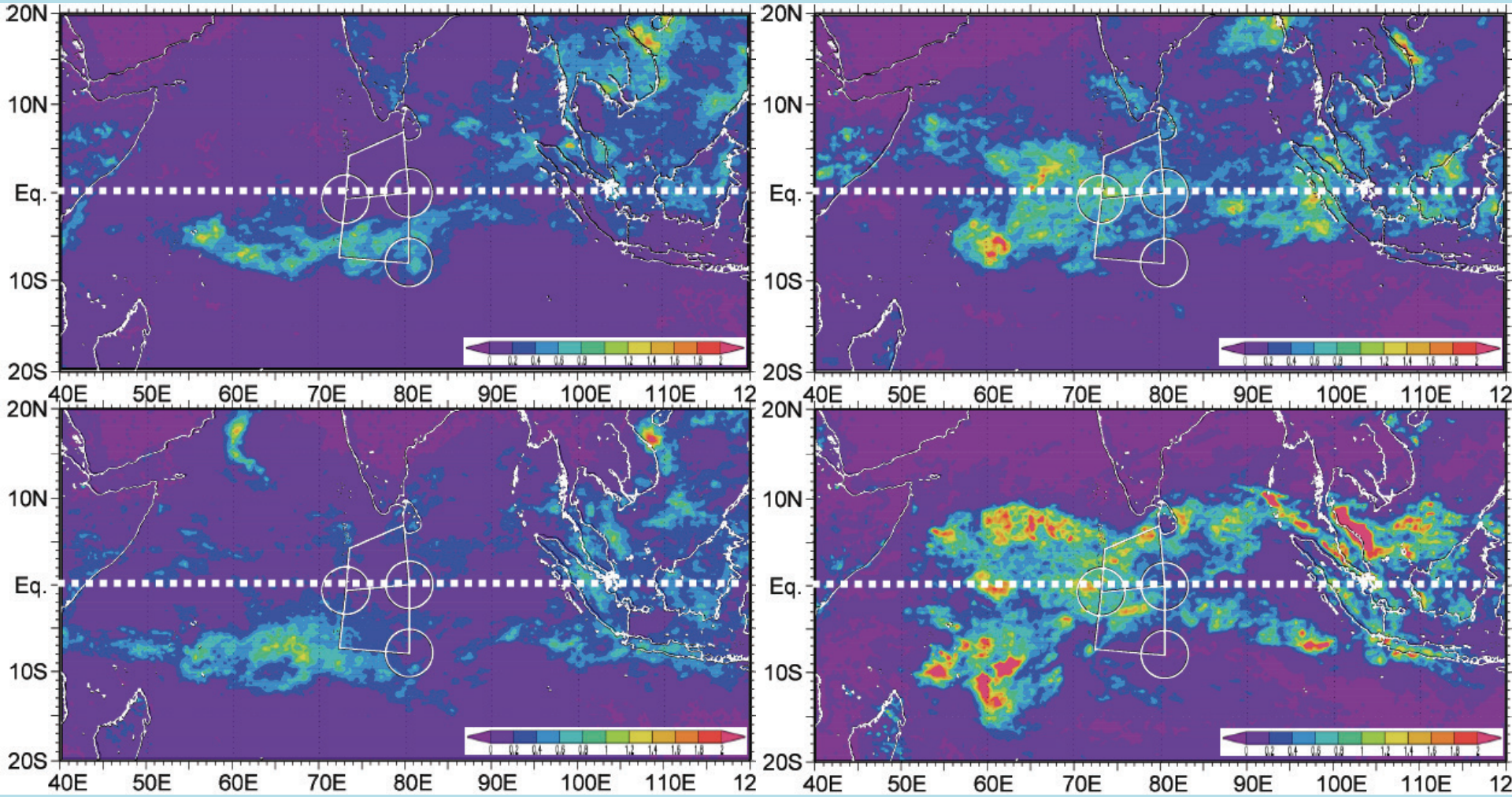

MJO-2 Nov 06 – Nov 20

MJO-2 Nov 20 – Nov 24

Courtesy of Masaki Matsumata

Dynamical drying

Dynamical vs. thermodynamical moistening

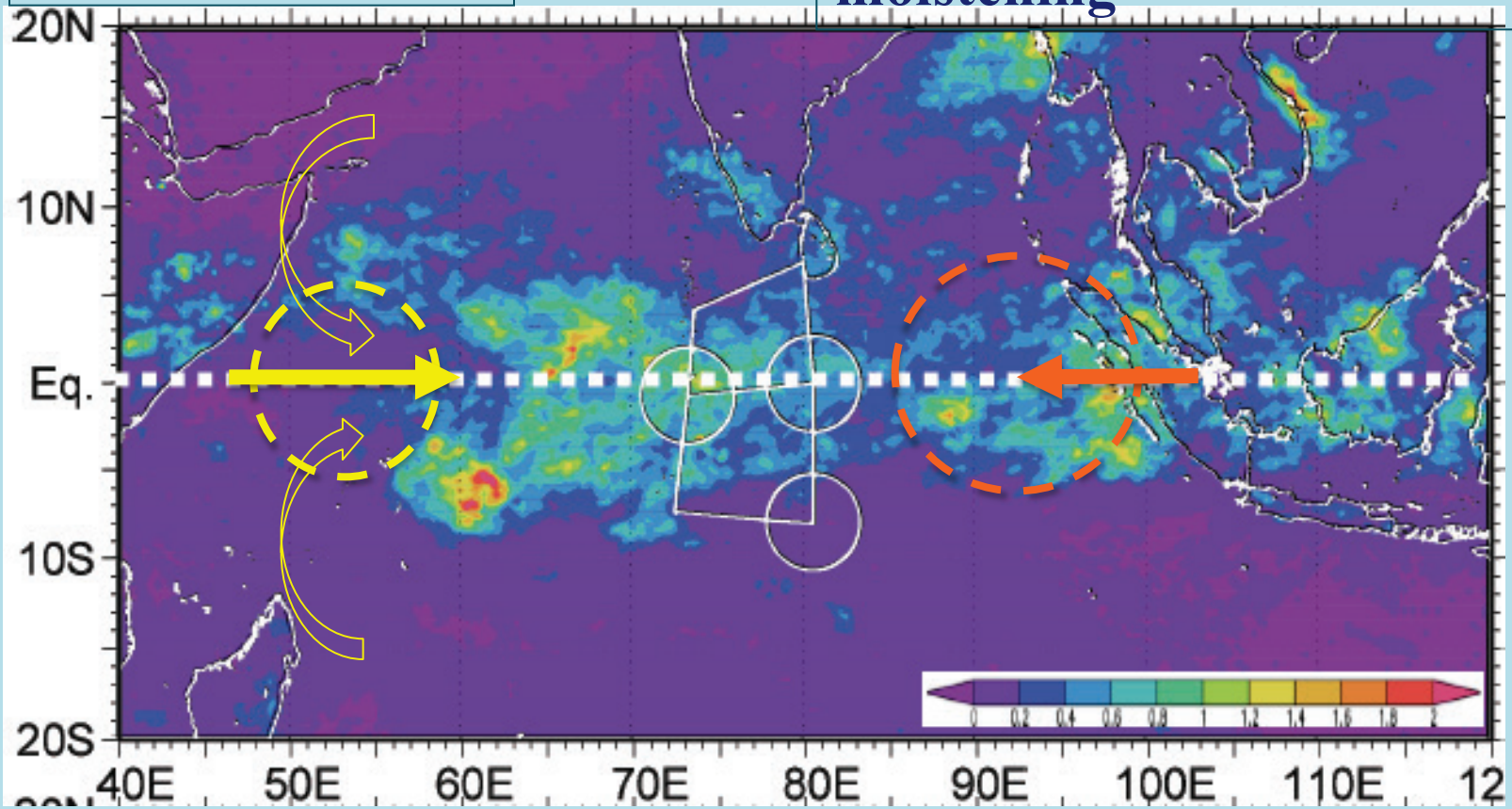

Decomposition of horizontal moisture advection

Zhao et al. (2013)

$$\left(\frac{\partial q}{\partial t}\right)' = (-V\nabla q)' + \left(-\omega\frac{\partial q}{\partial p}\right)' + \left(-\frac{Q_2}{L}\right)'$$

$$u=\bar{u}+u'+u^* \quad , \quad v=\bar{v}+v'+v^* \qquad q=\bar{q}+q'+q^*$$

overbar: >80 day (**basic state**) prime: 20-80 day (ISO) asterisk: < 20 day

$(-\bar{V}\cdot\nabla\bar{q})'$	$(-\bar{V}\cdot\nabla q')'$	$(-\bar{V}\cdot\nabla q^*)'$	$(-V'\cdot\nabla\bar{q})'$	$(-V'\cdot\nabla q')'$	$(-V'\cdot\nabla q^*)'$	$(-V^*\cdot\nabla\bar{q})'$	$(-V^*\cdot\nabla q')'$	$(-V^*\cdot\nabla q^*)'$
1	2	3	4	5	6	7	8	9

Moisture buildup in CINDY2011/DYNAMO Array and 7-km mesh NICAM hindcasts

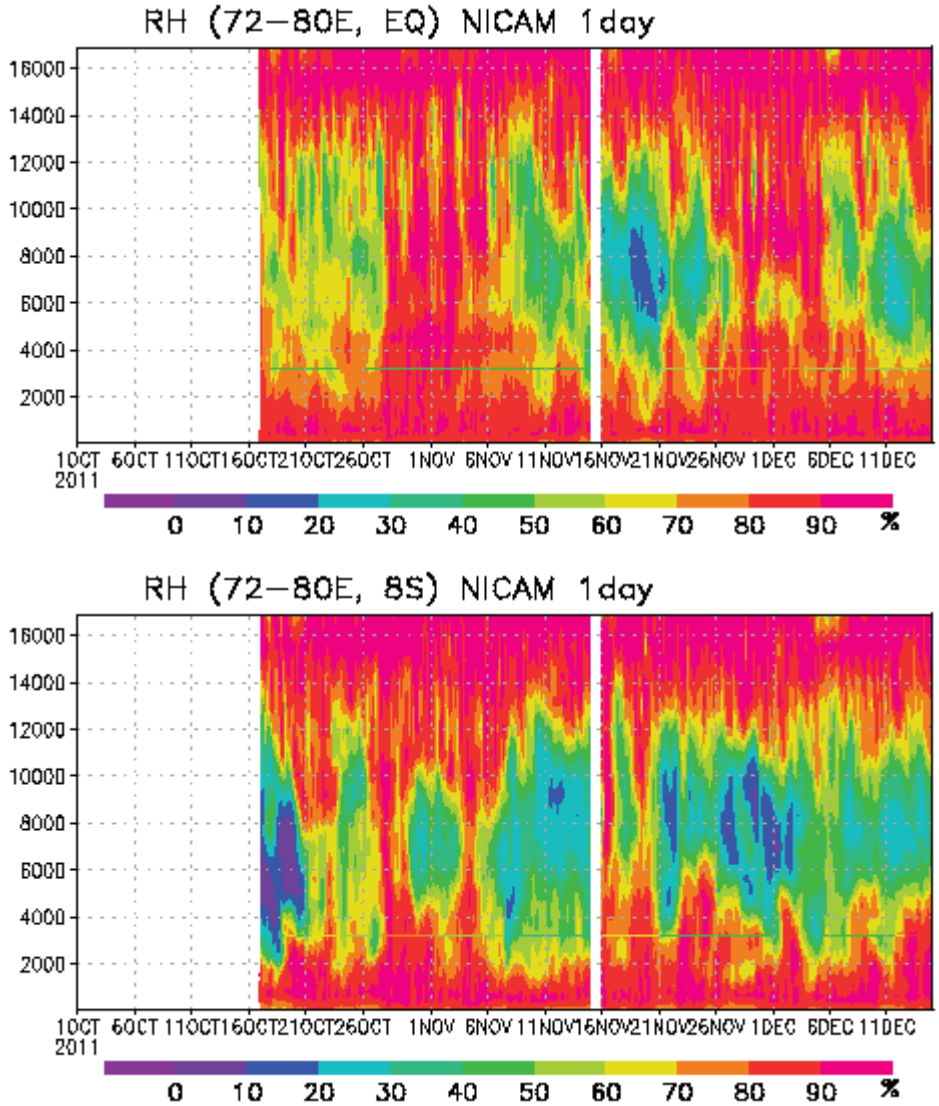

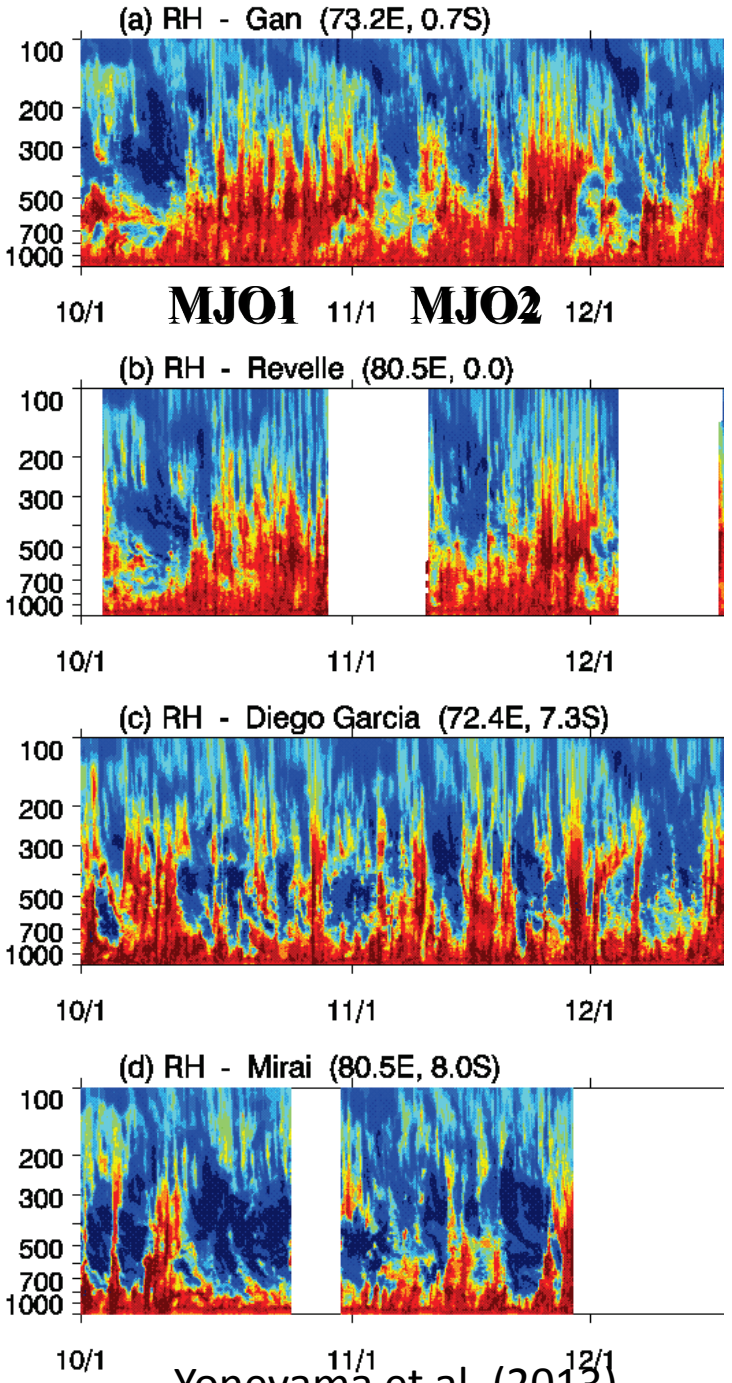

Yoneyama et al. (2013)

Precursor of MJO convective initiation

Precipitable water (5S-5N)

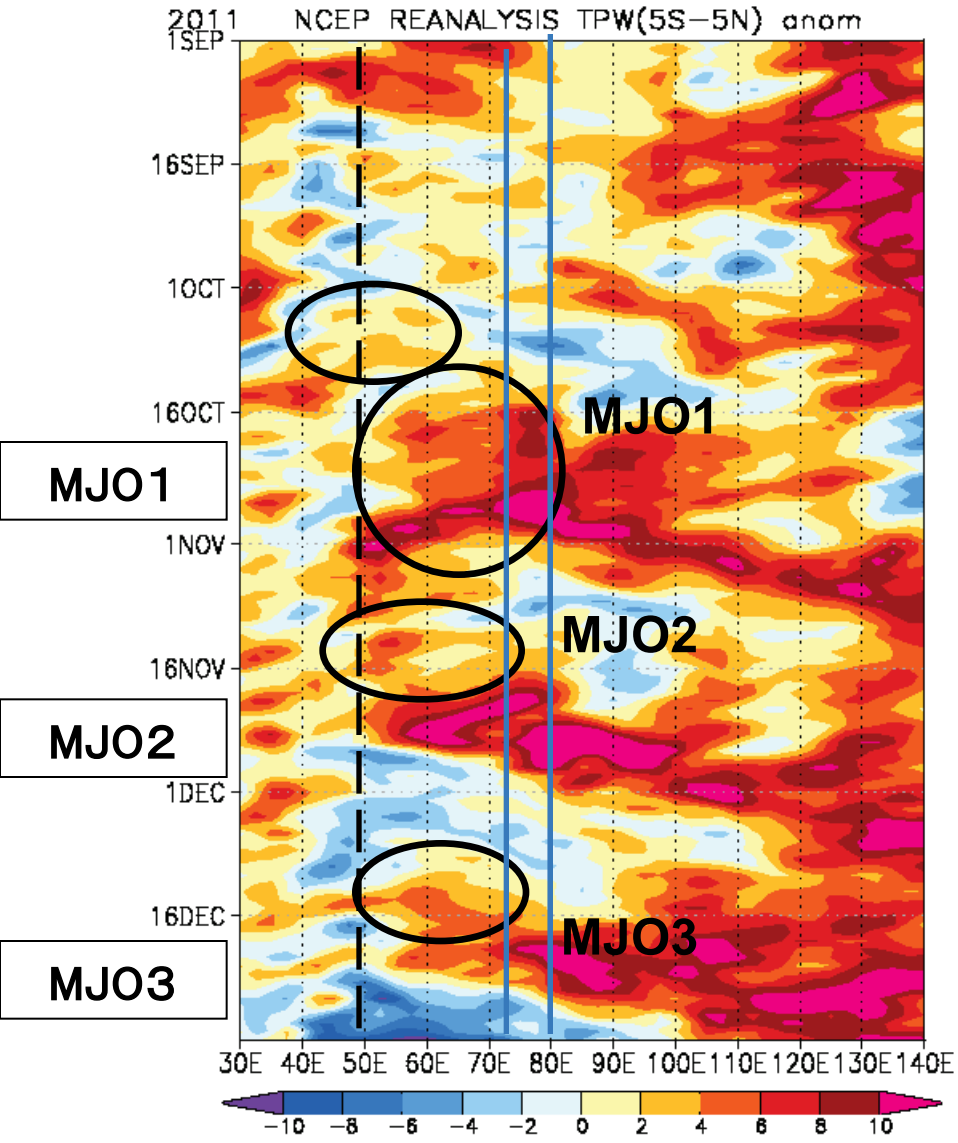

moisture (Zhao et al. 2013)

U850 (5S-5N)

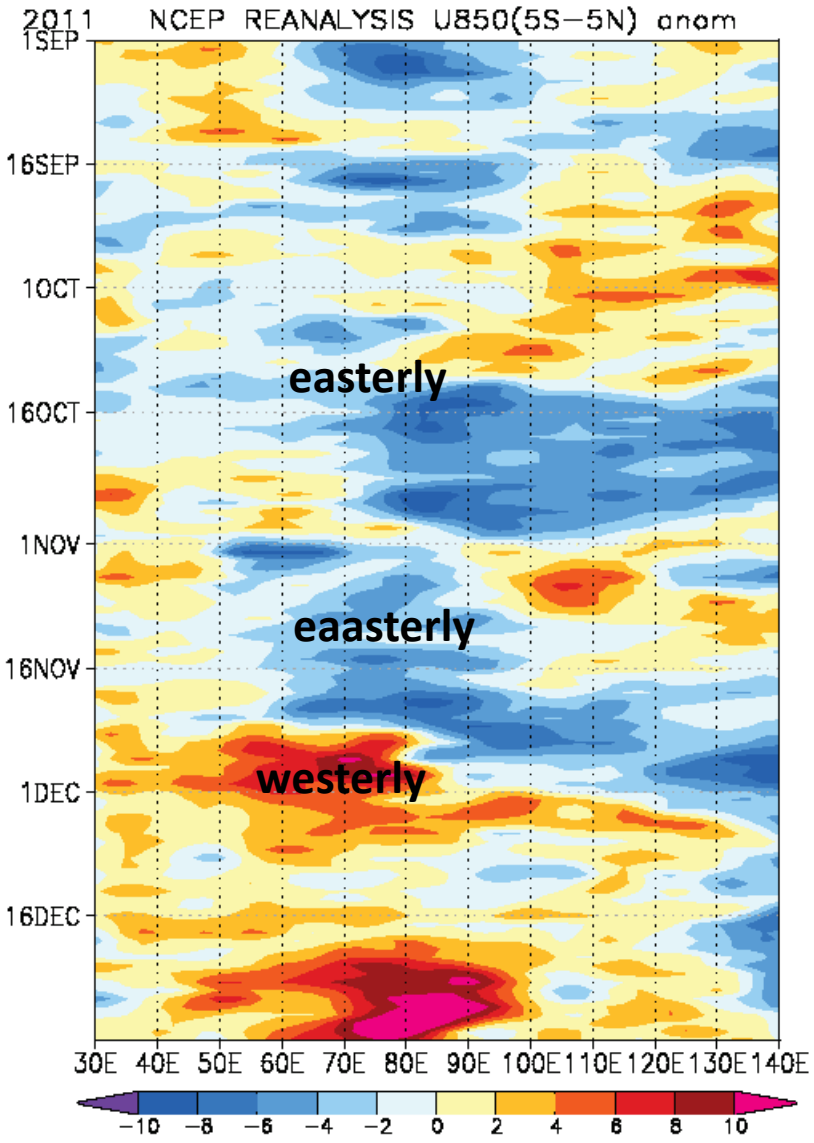

easterly anomalies (Ling et al. 2013)

Averages of the Northern Array

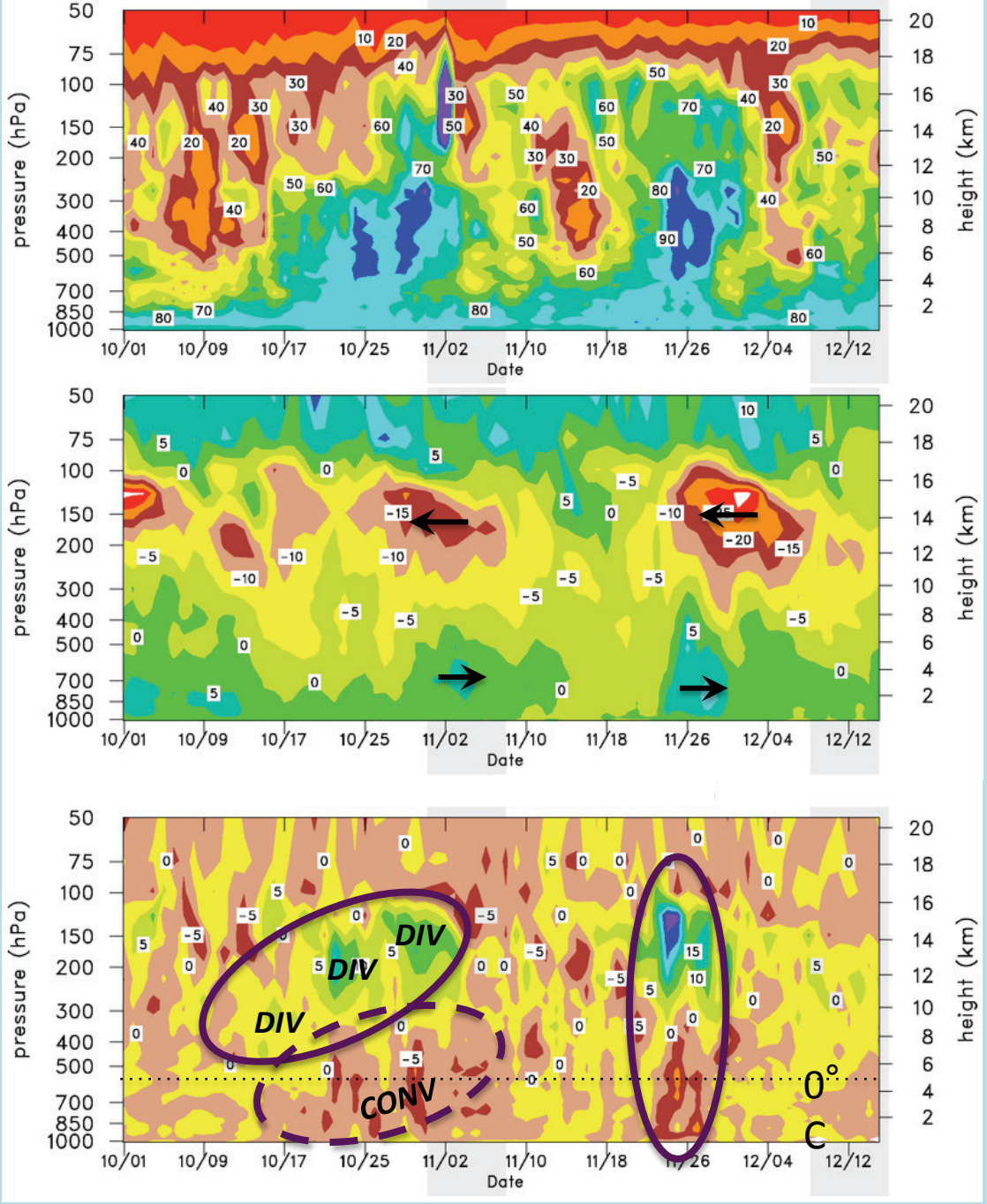

Courtesy of R. Johnson

Hypothesis on MJO initiation

- **Recharge-discharge (Moist Static Energy, moisture)**

Blade and Hartmann (1993); Kemball-Cook and Weare (2001); Maloney and Hartmann (1998); Maloney (2009); Hu and Randall (1994)

★**moisture buildup (observational evidences)**

Kikuchi and Takayabu (2004); Kiladis et al. (2005); Yoneyama et al. (2008, 2013)

"Moisture mode" Raymond (2000); Sobel and Maloney (2013)

- **Circumnavigation (tropical dynamics)**

Knutson and Weickmann 1987; Wang and Li 2004; Matthews 2008; Straub 2013

- **Extratropical forcing (Rossby wave activity; upper troposphere)**

Lau and Peng 1987; Hsu et al. 1990; Ray et al.2009; Ray and Li 2013; Zhao et al. 2013

Precursor of MJO initiation

- Increase in moisture and temperature at low-levels; destabilization (5-10 days before convective initiation) (Zhao et al. 2013)
- Easterly anomalies (low-mid levels), SLP (k=1), and negative T (mid levels) appear 20-day before convective initiation and move eastward (Ling et al. 2013)

★ Importance of **"local "processes to convection initiation** (Straub 2013)

Motivation

Convection initiation of MJO over the western **Indian Ocean (IO)** is one of most difficult tasks in understanding and prediction of MJO. The **CINDY2011/DYNAMO** field program was conducted to tackle this tough problem through October 2011-March 2012 (Yoneyama et al. 2013). Existing theories on MJO dynamics addressed the importance of **buildup of moisture/moist static energy (MSE)** [e.g., Blade and Hartmann 1993; Kemball-Cook and Weare 2001; Maloney 2009] . Zhao et al. (2013) demonstrated that accumulation of moisture in the lower troposphere (−5~−10 day) as a precursor of MJO convection initiation by composite analysis of 20 year boreal winter cases. Here, we discuss the moistening processes in two MJO cases that initialized during the CINDY/DYNAMO period. Our major concern is the roles of dynamical precursors (e.g., extratropical forcing, circumnavigating signals) and high frequency disturbances on the initiation of convection that broke out at a local scale (Straub 2013) in the western IO region.